Stony Brook University

Inhibition of pathological connexin26 hemichannels implicated in keratitis-ichthyosis-deafness syndrome

A Dissertation Presented

by

Noah Alexander Levit

to

The Graduate School

in Partial Fulfillment of the

Requirements

for the Degree of

Doctor of Philosophy

in

Genetics

Stony Brook University

May 2014

Stony Brook University

The Graduate School

Noah Alexander Levit

We, the dissertation committee for the above candidate for the

Doctor of Philosophy degree, hereby recommend

acceptance of this dissertation.

Thomas W. White, PhD – Dissertation Advisor
Professor, Dept. of Physiology and Biophysics

Gerald Thomsen, PhD – Chairperson of Defense
Professor, Dept. of Biochemistry and Structural Biology

Peter R. Brink, PhD
Professor and Chair, Dept. of Physiology and Biophysics

Richard Z. Lin, MD
Professor, Dept. of Physiology and Biophysics

Miduturu Srinivas, PhD
Associate professor, Dept. of Biological Sciences
State University of New York College of Optometry, New York, NY

This dissertation is accepted by the Graduate School

Charles Taber
Dean of the Graduate School

Abstract of the Dissertation

Inhibition of pathological connexin26 hemichannels implicated in keratitis-ichthyosis-deafness syndrome

by

Noah Alexander Levit

Doctor of Philosophy

in

Genetics

Stony Brook University

2014

Connexin (Cx) proteins form intercellular gap junction channels to facilitate the exchange of ions and second messengers between adjacent cells. Mutations in connexins cause several human diseases by interrupting cell-to-cell communication and coupling. Connexins also form functional hemichannels in nonjunctional membranes that have an unclear role in normal physiology but have altered activity in pathological states. Mutations in *GJB2*, the gene encoding connexin26 (Cx26), are linked to sensorineural hearing loss as well as syndromic deafness associated with skin disorders. In contrast to Cx26 mutations causing nonsyndromic deafness, those that also cause skin disease are exclusively gain-of-function single amino acid changes with autosomal dominant inheritance patterns. At least 10 missense mutations clustered toward the N-terminus and first extracellular loop of Cx26 have been linked to keratitis-ichthyosis-deafness (KID) syndrome, which can consist of life threatening skin phenotypes. Functional changes related to hemichannel open probability and/or permeability have been shown for all but one of the tested KID-causing Cx26 mutations by both electrophysiology and dye transfer assays, and in varied expression systems. We, and others, hypothesize that hemichannel overactivity, resulting from mutations

that precipitate failures in Cx26 channel regulation, undermines coordinated keratinocyte proliferation and differentiation in the epidermis. *In vitro* expression of mutant hemichannels causes cellular dysfunction and accelerated death, both in *Xenopus laevis* oocytes and mammalian cell culture, possibly because constitutively active or leaky hemichannels deplete the cells of important metabolites, such as ATP and cAMP. Additionally, imbalances in intracellular-extracellular ionic gradients may disrupt paracrine signaling pathways or cause injurious osmotic pressures.

Pharmacological tools to modulate Cx26 channels are needed to assess the consequences of excessive hemichannel openings on cell viability and tissue integrity. We used two different electrophysiological assays for quantitative evaluation of prospective small molecule inhibitors of mutant Cx26 hemichannels present in KID syndrome, with an extracellular divalent cation, zinc (Zn^{++}), as a positive control for comparison. Mefloquine, and related quinine-family small molecule analogs, emerged as viable candidates, capable of attenuating aberrant Cx26 hemichannel currents at low micromolar doses. Our data revealed differential drug affinities for mutant channels containing distinct biochemical modifications and underscored the need for screening against specific forms present in human disease. In this body of work, we have identified potent Cx26 hemichannel inhibitors with adequate specificity and selectivity properties to appraise the pathogenic culpability of dysregulated hemichannels in KID syndrome. Minimally, our findings support the use of these agents to further structure-function analyses aimed at elucidating the molecular bases of errors in gating and permeation that accompany mutations. Furthermore, we show that select inhibitors are particularly well positioned for testing in an inducible transgenic mouse model of the lethal form of the disease, and may demonstrate therapeutic utility in KID syndrome and other connexin-associated gain-of-function disorders.

Frontispiece

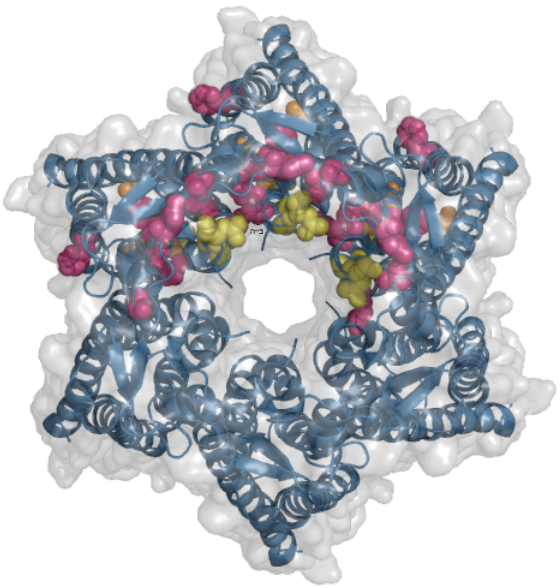

Table of contents

List of Figures

List of Tables

List of Abbreviations

2-APB—2-aminoethoxydiphenyl borate

35delG—Deletion of guanine at position 30, resulting in a frame-shift

167delT—Deletion of thymine at 167, resulting in a frame-shift

235delC—Deletion of cytosine at 235, resulting in a frame-shift

Å—Angstrom

A40V—Missense mutation of alanine at 40 to valine

A88V— Missense mutation of alanine at 88 to valine

ATP—Adenosine triphosphate

BSA—Bovine serum albumin

Ca^{++}—Calcium ion

cAMP—3'-5'-cyclic adenosine monophosphate

CBX—carbenoxolone (3β-Hydroxy-11-oxoolean-12-en-30-oic acid 3-hemisuccinate)

cDNA—Complementary deoxyribonucleic acid

CNS—central nervous system

cRNA—Complemantary ribonucleic acid

Cx—Connexin

Cx26—Connexin26

Cx30—Connexin30

Cx31—Connexin31

Cx36—Connexin36

Cx43—Connexin43

Cx50—Connexin50

D50A—Missense mutation of aspartic acid at 50 to alanine

D50N—Missense mutation of aspartic acid at 50 to glutamine

DAPI—4',6-Diamidino-2-phenylindole nuclear dye

DMSO—Dimethyl sulfoxide

E1—first extracellular loop domain of connexin topology

EDTA—Ethylenedinitrilotetraacetic acid

eGFP—Excitatory green fluorescent protein

EGTA—Ethylene glycol tetraacetic acid

EtBr—Ethidium bromide

EtoH—Ethanol

FFA—Flufenamic acid (N-(α,α,α-Trifluoro-m-tolyl)anthranilic acid, N-(3-[Trifluoromethyl]phenyl)anthranilic acid

γ_j—unitary conductance

G11R—Missense mutation of glycine at 11 to arginine

G12R—Missense mutation of glycine at 12 to arginine

G45E—Missense mutation of glycine at 45 to glutamic acid

GFP—Green fluorescent protein

GJB2—Gap junction beta 2 gene encoding connexin26

GJB3—Gap junction beta 3 gene encoding connexin31

GJB6—Gap junction beta 6 gene encoding connexin30

H1047R—substitution of arginine for histidine at residue 1047

HED—Hidrotic ectodermal dysplasia

HeLa—Transformed (immortal) cell line derived from human cervical cancer

HEPES—4-(2-hydroxyethyl)-1-piperazineethanesulfonic acid

IACUC—Institutional animal care and use committee

I_m—Membrane current or hemichannel current

IRES—Internal ribosome entry site

K14—Keratin14

kDa—kiloDalton

KID—Keratitis-ichthyosis-deafness syndrome

KO- knockout

LY—Lucifer yellow

µA—microAmpere

MB—Modified Barth's medium

Mg^{++}—Magnesium ion

MFQ—Mefloquine HCl ([R*,S*]-[2,8-Bis-trifluoromethyl-quinolin-4-yl]-piperidin-2-yl-methanol hydrochloride)

µM—microMolar

mM—milliMolar

mRNA—Messenger ribonucleic acid

mV—milliVolt

MW—Molecular weight

N14K—Missense mutation of asparagine at 14 to lysine

N14Y—Missense mutation of asparagine at 14 to tyrosine

N2A—Mouse neuroblastoma cell line

nA—nanoAmpere

NAD^{++}—Nicotinamide adenine dinucleotide

NPPB—5-nitro-2-(3-phenylpropylamino)-benzoate

NSAID—non-steroidal anti-inflammatory

NT—amino terminal domain of connexin topology

N-terminus—Amino terminus of protein

OMIM—Online mendelian inheritance in man

pA—picoAmpere

PBS—Phosphate buffered saline

PCR—Polymerase chain reaction

pF—picoFarad

PI3K—phosphatidylinositol-4,5-bisphosphate 3-kinase

PPK—Palmoplantar keratoderma

pS—picoseimens

QU020—[2,8-Bis-trifluoromethyl-quinolin-4-yl]-pyridin-2-yl-methanone

QU021—2,8-Bis[trifluoromethyl]-4-quinolyl[1-oxypyrid-2-yl] methane

QU022—4-Chloro-2-trichloromethyl-quinoline

QU026—[2,8-Bis-trifluoromethyl-quinolin-4-yl]-pyridin-2-yl-methanol

R42P—Missense mutation of arginine at 42 to proline

rtTA—Reverse tetracycline transactivator

S17F—Missense mutation of Serine at 17 to Phenylalanine

SCAM—Substituted cysteine accessibility method

SD—Standard deviation

SDS—Sodium dodecyl sulfate

SE—Standard drror

siRNA—Small interference ribonucleic acid

SKH1—Euthymic and immunecompetent mouse strain

SNHL—Sensorineural hearing loss

TBS—Tris-buffered saline

TM1—first transmembrane domain of connexin topology

TM2—second transmembrane domain of connexin topology

TRE—Tetracycline response element

TRP—transient receptor potential family of cation channels

V37E—Missense mutation of valine at 37 to glutamic acid

V84L—Missense mutation of valine at 84 to leucine

V_m—Membrane voltage

WT—Wild-type

Zn^{++}—Zinc ion

Acknowledgments

I wish to extend my sincere gratitude to my advisor, Dr. Thomas W. White, for welcoming a wandering engineer with a then uncertain career trajectory into the fold of basic biological science. He has provided for me a formidable example of how to strategically confront questions and challenges, both inside of the scientific arena and out. His attentiveness to the unique needs of each of his trainees and deliberate approach to our professional development made for a personal and rewarding experience.

Thank you to Drs. Caterina Sellitto and Helen Li for their ardent commitment to the efficient running and steady productivity of the lab. Caterina, thank you for enriching my laboratory experience through your insistence on logical thinking and sensible experimental design as well as your categorical objections to chaos and waste. Helen, the versatility of your talents will continue to baffle me. Thank you both for your patience and meticulousness in teaching routine and complex techniques alike.

To my labmates, Zunaira Shuja and Jennifer Martinez, thank you for promoting a day-to-day environment of collaborative camaraderie. More specifically, thank you for supplying well over 75% of my buffers and reagents.

I would like to thank the members of my dissertation committee, Drs. Jerry Thomsen, Peter Brink, Richard Lin, and Miduturu Srinivas, for their earnest assessments of my progress and influential questions and suggestions. I am grateful, too, for having made yourselves so accessible and for your efforts to accommodate the MSTP and school of medicine timelines.

Thank you to the Brink lab, and specifically to Dr. Hong-Zhan Wang, for sharing his expertise in conducting patch clamp electrophysiology experiments.

Finally, to my family, any attempt to acknowledge the extent of your investment in my education and wellbeing here would be a thesis unto itself.

Chapter 1. Introduction to connexin-mediated skin disease

Intercellular communication is a hallmark of multicellular organisms. In chordate animals, the connexin family of structural proteins form intercellular membrane channels called gap junctions (Goodenough, 1974). Connexin (Cx) proteins have been studied for nearly five decades in the context of these intercellular gap junction channels that facilitate electrical and biochemical coupling of adjacent vertebrate cells (Harris, 2001; Revel and Karnovsky, 1967; Robertson, 1963; Wei *et al.*, 2004). Gap junctions are well characterized with regard to their role in maintaining tissue homeostasis by enabling exchange of ions, second messengers, and metabolites (Bevans *et al.*, 1998; Kanno and Loewenstein, 1964; Lawrence *et al.*, 1978; Veenstra, 1996). Connexins are now known to also be capable of forming functional hemichannels in nonjunctional membranes, linking the cytoplasm of a cell with its extracellular microenvironment (Bennett *et al.*, 2003; Evans *et al.*, 2006; Goodenough and Paul, 2003; Saez *et al.*, 2005; Saez *et al.*, 2010). Hemichannels are thought to participate in paracrine functions and there is evidence to indicate that hemichannels mediate calcium signaling through ATP release (Stout *et al.*, 2004; Stout *et al.*, 2002). Hemichannels presently have an unclear role in normal physiology, but there is accumulating evidence showing that their activity can be altered under certain pathological conditions (Schalper *et al.*, 2009).

Mutations of connexin-encoding genes contribute to the etiology of a variety of human genetic diseases, including, but not limited to, skin disorders, congenital cataract, peripheral neuropathies, and non-syndromic sensorineural deafness (Anand and Hackam, 2005; Liang *et al.*, 2005; Mese *et al.*, 2007; Wei *et al.*, 2004; White and Paul, 1999). New mutations are continually discovered due to improved availability and affordability of DNA sequencing technology at academic medical centers and the high frequency of mutations in some human connexins, like connexin26 (Cx26). These findings establish a genetic basis for clinical illness, but provide little insight regarding pathophysiological mechanistic details. Connexin proteins are key players in a diverse

set of fundamental cellular processes, leaving numerous possible targets for pathological interference that may include hemichannels. Filling in the gaps between connexin mutations and phenotypic consequences will help inform efforts to develop targeted therapies. Here, we consider pathological hemichannel activation that may lead to disturbances in the normal patterns of keratinocyte proliferation and differentiation in the skin and have been implicated as a gap junction-independent mechanism of disease in the context of keratitis-ichthyosis-deafness (KID) syndrome. Cx26, the most frequently mutated connexin in the epidermis, is the primary focus of this dissertation, although hypotheses may be relevant to other forms of connexin-driven disease.

CONNEXIN HEMICHANNELS

Connexins are 4-transmembrane domain proteins that oligomerize to form hexameric structures that have been termed connexons or hemichannels (Goodenough and Paul, 2003). Gap junctions are assembled when hemichannels in the membranes of two adjacent cells become aligned at their extracellular surfaces (Harris, 2001). Hemichannels may be assembled from 6 of the same connexin to form so-called homomeric structures, or may be constituted by a combination of different connexins, producing heteromers. The connexin composition of hemichannels is dependent on cell-type and may affect channel properties, including permeability to second messengers and other solutes (Mese *et al.*, 2007; Sun *et al.*, 2005).

Evidence for active hemichannels was first observed *in vivo* by whole-cell voltage clamp studies of solitary horizontal cells isolated from the catfish and skate retina (DeVries and Schwartz, 1992; Malchow *et al.*, 1993). A time- and voltage-dependent outwardly rectifying membrane current was identified with behaviors consistent with half of a gap junction channel (DeVries and Schwartz, 1992). The existence of active

hemichannels was initially suggested by *in vitro* expression of cloned connexins in single *Xenopus* oocytes, which resulted in increased membrane currents and permeability to fluorescent probes (Paul *et al.*, 1991). Single-channel conductances have now been shown by various mammalian cell-expression systems to substantiate these findings (Beahm and Hall, 2002; Valiunas, 2002; White *et al.*, 1999).

Hemichannels are thought to rest in a predominantly closed state *in vivo*, with transient openings in response to a wide range of stimuli (Saez *et al.*, 2010). Interestingly, hemichannel conductance is modulated by transmembrane voltage, calcium concentration, and intracellular pH as well as other variables known to regulate gap junction permeability (Bukauskas and Verselis, 2004; DeVries and Schwartz, 1989; Verselis and Srinivas, 2008). Post-translational covalent modifications of connexin carboxy-terminal amino acids may also influence hemichannel open probability (Giepmans *et al.*, 2001; Locke *et al.*, 2006; Retamal *et al.*, 2006; Solan and Lampe, 2009). Finally, increased activity of hemichannels may also result from pathological mutations in connexin proteins. Although insights have been gained into the mechanisms of hemichannel gating, the impact of hemichannel activity on tissue homeostasis remains poorly understood at this time, making it difficult to evaluate possible physiological roles for normal hemichannel activity.

Disease-causing connexin mutations are largely single amino acid deletions or substitutions that have the potential to modify the topological and biochemical characteristics of the proteins and subsequently impact the function of the channels they form. Preliminary experimental work has suggested that mutations in connexin genes can functionally alter hemichannel properties with potentially deleterious consequences for the cell (Gerido *et al.*, 2007; Lee *et al.*, 2009; Montgomery *et al.*, 2004; Stong *et al.*, 2006). Constitutively active, or dysregulated ‘leaky’ hemichannels may deplete the cytoplasm of essential small molecules, depolarize the plasma membrane by permitting uncontrolled uptake of molecules, or cause lysis via osmotic

pressures (Essenfelder *et al.*, 2004). To date, there have been no conclusive findings showing aberrant hemichannel fluxes as causative of clinical phenotypes.

CONNEXIN26 IN EPIDERMAL PATHOLOGY

At least 9 of the known 21 human connexin isoforms are found in skin. Connexins have overlapping expression patterns in the three inner layers of the epidermis and are thought to mediate the continuous process of keratinocyte renewal (Di *et al.*, 2001a; Kelsell *et al.*, 2000; Mese *et al.*, 2007). Dye-transfer studies have confirmed the presence of gap junctional communication in human and mouse skin (Kam *et al.*, 1986; Salomon *et al.*, 1988). Connexin proteins have dynamic spatial and temporal expression patterns and are most notably upregulated in states of increased keratinocyte proliferation and differentiation. For example, Cx26 is highly overexpressed in hyperproliferative psoriatic plaques (Labarthe *et al.*, 1998; Rivas *et al.*, 1997) as well as neoplastic papilloma lesions (Sawey *et al.*, 1996). Experimentally induced wounds result in differential changes in connexin expression: upregulation in the wound proper and downregulation at the wound periphery (Goliger and Paul, 1995; Lucke *et al.*, 1999). Finally, in patients with skin disorders linked to Cx26 mutations, expression of the mutant protein is greatly increased in the diseased epidermis (Rouan *et al.*, 2001). At face value, these observations could be taken to imply an important role for Cx26 proteins in keratinocyte regulation.

Cx26 is found in keratinocytes of the stratum basale and stratum granulosum as well as other organ systems (Di *et al.*, 2001a; Lee and White, 2009b; Lucke *et al.*, 1999; Salomon *et al.*, 1988). Mutations in *GJB2*, the gene encoding Cx26, are linked to congenital sensorineural deafness as well as syndromic hearing loss associated with skin disorders (Petit, 2006). Cx26 mutations are known to be the leading cause of autosomal recessive hearing loss, predominantly through a loss-of-function mechanism.

The most common Cx26 mutation leading to non-syndromic deafness in Caucasian families is the single nucleotide deletion 35delG (Petit *et al.*, 2001), which produces a frame shift that truncates the protein after encoding only a short segment of the amino-terminus, rendering it entirely non-functional. Similarly, the most prevalent Cx26 mutations leading to deafness in eastern Asian populations and Ashkenazi Jewish populations are 235delC and 167delT respectively, both of which also cause premature termination of the protein (Lerer *et al.*, 2000; Martinez *et al.*, 2009). Testing of other mutations has shown that loss of channel function ranges from partial-to-complete and may result from impaired trafficking of proteins to the plasma membrane and improper open-channel assembly. It is important to note that inherited deafness is genetically diverse and, though less common, cases are also linked to mutations in Cx26 that yield channels retaining some level of function. However, such mutations commonly produce channels with distinctly altered gating and permeability properties; it is often the case that they become impermeable to molecules regularly passed by wild-type channels (Mese *et al.*, 2008; Wang *et al.*, 2003). For example, the V84L mutation found in recessive non-syndromic deafness forms channels with similar gross unitary channel conductance to wild-type Cx26 gap junctions but with deficient permeability to inositol 1,4,5-trisphosphate (Beltramello *et al.*, 2005; Zhang *et al.*, 2005). Thus, total or partial loss-of-function mutations are responsible for non-syndromic deafness and these patients do not suffer from defective cutaneous wound healing or skin abnormalities (Bruzzone *et al.*, 2003; Zhao *et al.*, 2006), other than anecdotal reports of increased epidermal thickness (D'Adamo *et al.*, 2009; Meyer *et al.*, 2002).

In contrast to the numerous Cx26 mutations causing non-syndromic deafness, those that also cause skin disease are all single amino acid changes with autosomal dominant inheritance patterns that confer either some type of pathological gain- or alteration-of-function (Gerido and White, 2004; Lai-Cheong *et al.*, 2007; Richard, 2005). These missense mutations are clustered in the amino-terminus and first extracellular loop of the protein and lead to a broad spectrum of dermatologic presentations (Lee and White, 2009b). Two main hypotheses follow: 1) Cx26 mutations that cause skin

disorders do so by a novel gain- or alteration-of-function and 2) overexpression of mutated forms of Cx26 linked to KID syndrome in the epidermis in response to tissue injury (Labarthe *et al.*, 1998; Rivas *et al.*, 1997; Sawey *et al.*, 1996) may in fact be harmful if active hemichannels are formed.

Single-cell voltage clamp experiments in *Xenopus* oocytes initially identified a Cx26 mutant linked to deafness and skin disease exhibiting aberrant hemichannel activity (Montgomery *et al.*, 2004). Subsequently, hemichannel activity was evaluated for additional mutations in syndromic deafness, and has currently been shown to be a common feature of the Cx26-G45E, -A40V, -N14K, -D50N, -G12R, -A88V and -D50A

Table 1-1. Biophysical evidence of increased Cx26 hemichannel activity in *GJB2* mutations causing KID syndrome via single-cell electrophysiology

Mutation	Oocyte voltage clamp	Mammalian cell patch clamp	Refs
A40V	Yes	Yes	(Gerido *et al.*, 2007; Griffith *et al.*, 2006; Montgomery *et al.*, 2004) (Figure 1-2)
G45E	Yes	Yes	(Gerido *et al.*, 2007; Griffith *et al.*, 2006; Stong *et al.*, 2006) (Figure 1-2)
D50N	Yes	?	(Lee *et al.*, 2009)
N14K	Yes	?	(Lee *et al.*, 2009)
G12R	Yes	?	(Lee *et al.*, 2009)
A88V	Yes	Yes	(Mhaske *et al.*, 2013)
D50A	Yes	Yes	(Mhaske *et al.*, 2013)
S17F	No	?	(Lee *et al.*, 2009)

mutations causing keratitis-ichthyosis-deafness (KID) syndrome (OMIM 148210) (Table 1-1) (Arita *et al.*, 2006; Janecke *et al.*, 2005; Jonard *et al.*, 2008; Lee *et al.*, 2009; Mazereeuw-Hautier *et al.*, 2007; Mhaske *et al.*, 2013; Montgomery *et al.*, 2004; Richard *et al.*, 2002; Stong *et al.*, 2006). Palmoplantar Keratoderma (PPK) with Deafness (OMIM 148350) is a clinically distinct Cx26 congenital syndrome with no known role for hemichannel activity (Richard *et al.*, 1998; Rouan *et al.*, 2001). The skin pathology in PPK is thought to proceed from Cx26 mutations via *trans*-dominant inhibition of other connexins residing in the epidermis, such as connexin43 or connexin30 (Bakirtzis *et al.*, 2003; Rouan *et al.*, 2001). Notably, visualization of a three-dimensional Cx26 hemichannel (Maeda *et al.*, 2009) shows mutations in KID to be spatially oriented near pore-lining residues while those in PPK are more evenly distributed throughout the channel wall (Figure 1-1), underscoring the potential of the former group to have direct implications on pore conformation and gating. There are also rare KID mutations that are not associated with hemichannel dysfunction, such as S17F (Lee *et al.*, 2009). In addition, several KID mutations have not yet been tested. It has been hypothesized that those lacking hemichannel activity may lead to distinct dermatologic phenotypes, but this has been difficult to conclusively establish due to the small number of cases and heterogeneous nature of the disorders (de Zwart-Storm *et al.*, 2011).

CONNEXIN26 HEMICHANNEL PROPERTIES

The biophysical properties of hemichannels formed by two KID mutations, Cx26-G45E and Cx26-A40V (Janecke *et al.*, 2005; Jonard *et al.*, 2008; Montgomery *et al.*, 2004), have been examined in the greatest detail. Cx26-G45E in particular is linked to high patient mortality within the first year of life (Griffith *et al.*, 2006; Janecke *et al.*, 2005; Jonard *et al.*, 2008; Sbidian *et al.*, 2010). Both show uniquely large hemichannel currents when expressed in single cells, surpassing any recorded wild-type connexin hemichannel currents that may contribute to normal homeostatic maintenance (Gerido *et al.*, 2007; Montgomery *et al.*, 2004; Stong *et al.*, 2006). This finding is consistent in

data derived from oocyte voltage clamp experiments as well as patch clamp recordings from transfected mammalian cells (Figure 1-2). Furthermore, both mutations lead to rapid oocyte lysis and death in culture. Membrane depolarization and decreases in extracellular calcium have been shown to cause exaggerated activation of mutant hemichannels (Gerido *et al.*, 2007; Lee *et al.*, 2009; Montgomery *et al.*, 2004; Stong *et al.*, 2006). Conversely, hyperpolarization and high concentrations of divalent cations in the extracellular milieu stabilize the cell membrane and delay cell death (Figure 1-3) (Ebihara and Steiner, 1993; Lee *et al.*, 2009). Increased extracellular calcium positively shifts the activation voltage of hemichannels, leading to tighter gating and mitigation of excessive hemichannel currents.

A recent study sought to quantify hemichannel regulation by extracellular calcium for wild-type Cx26 as well as the Cx26-G45E and Cx26-A40V mutants (Sanchez *et al.*, 2010). Connexins were exogenously expressed in *Xenopus* ooctyes and macroscopic hemichannel currents were recorded by two-electrode voltage clamp during sequential perfusion with increasing concentrations of calcium. For wild-type Cx26 hemichannels held at voltages approximating normal keratinocyte membrane potentials, low extracellular calcium resulted in detectable currents that were progressively reduced as extracellular calcium was increased. The Cx26-A40V mutant hemichannel showed larger currents with a shifted response curve, suggesting reduced regulation by calcium. In contrast, the Cx26-G45E mutation showed increased permeability to calcium, compared to wild-type Cx26, and follow up experiments with the substituted cysteine accessibility method (SCAM) demonstrated that Cx26-G45E is a pore-lining residue, implying a tentative role in channel gating and permeability (Sanchez *et al.*, 2010).

Residues 40 and 45 localize to the proximal portion of the Cx26 first extracellular domain, and mutations of either result in severe forms of KID syndrome (Lee and White, 2009b). However, the development of aberrant hemichannel currents may proceed via distinct functional alterations of channel properties related to three-dimensional

structure and electrochemical interactions dictated by the specific amino acid substitutions. The specificity of amino acid substitution is underscored by the apparent discrepancy in clinical phenotypes for two mutations of the same asparagine residue, Cx26-N14K and Cx26-N14Y. Each is associated with KID syndrome, but the skin pathologies are divergent (Arita *et al.*, 2006; de Zwart-Storm *et al.*, 2011). Moreover, Cx26-N14K produces aberrant hemichannel currents whereas Cx26-N14Y does not (Lee and White, 2009a).

Whether excessive hemichannel currents are sufficient to cause reduced cell viability and epidermal pathology remains to be definitively shown. *Xenopus* oocyte expression systems show a consistent correlation between large single-cell transmembrane currents and accelerated cell death (Gerido *et al.*, 2007; Montgomery *et al.*, 2004). The cellular lethality of Cx26-G45E hemichannels was independently validated in transfected HEK-293 cells (Stong *et al.*, 2006). Recently, HeLa cell culture following transfection of the hemichannel-forming Cx26-N14K construct also showed increased cell death (de Zwart-Storm *et al.*, 2011). Mammalian cells are cultured in serum-containing media that is rich in growth factors and signaling molecules that may influence hemichannel patency and permeability. Studies suggesting that discrepancies exist in data derived from oocyte assays and data obtained from transfected mammalian cells should be cautious about drawing conclusions from subjective dye permeation assays (de Zwart-Storm *et al.*, 2011), as the more quantitative biophysical methods of evaluating hemichannel activity through direct measurement of membrane current have been in good agreement (Figure 1-2). Still, *in vivo* work with transgenic animals is needed to follow up hypotheses developed from *in vitro* findings to conclusively define a role for hemichannel-mediated pathology in differentiating keratinocytes.

The experimental use of pharmacological channel inhibitors may help elucidate the degree to which gained hemichannel function contributes to disease pathogenesis.

The search for connexin-efficacious blockers among chemical agents known to function on other proteins involved in membrane transport has produced candidate blocker molecules such as 2-Aminoethoxydiphenyl borate (2-APB), 5-nitro-2-(3-phenylpropylamino)-benzoate (NPPB), or flufenamic acid (FFA) (Bai *et al.*, 2006; Eskandari *et al.*, 2002; Spray *et al.*, 2002; Srinivas and Spray, 2003; Tao and Harris, 2007). As is the case with extracellular divalent cations (Ca^{++}, Zn^{++}, Mg^{++}) (Verselis and Srinivas, 2008), hemichannels formed from different mutant subunits may show differing sensitivities to drugs. FFA achieves rapid and reversible suppression of hemichannel currents in wild-type Cx26 as well as mutants (Figure 1-4). FFA was previously shown to effectively repress the propagation of calcium waves and ATP release through connexin hemichannels in astrocytes (Stout *et al.*, 2002). It is important to note that the mechanisms of blockade are not well defined and may be indirect, with ancillary effects on unknown targets. Identifying or developing small molecule inhibitors of higher specificity and potency is limited by the requirement for testing of connexin mutants individually. However, this may be a worthwhile avenue to explore given the topical accessibility of connexin-expressing keratinocytes in the epidermis.

Further support for a generalizable role of aberrant hemichannels in epidermal pathology can be drawn from studies of mutations in *GJB6*, the gene that encodes Cx30. Mutations in Cx30 are linked to hidrotic ectodermal dysplasia (HED). Two mutant proteins, Cx30-G11R and Cx30-A88V, were reported to cause cell death when expressed in *Xenopus* oocytes by microinjection of the connexin mRNA (Essenfelder *et al.*, 2004). Additionally, large voltage-activated currents were detected in mutant cells that were absent in wild-type controls. Transfection of HeLa cells with the Cx30 mutants resulted in increased ATP leakage into the extracellular medium (Essenfelder *et al.*, 2004). Excessive release of metabolites may not only be injurious to individual cells, but could also constitute a paracrine message to propagate untoward effects throughout the tissue.

In summary, skin disease-associated mutations of connexin proteins can cause functional disturbances in hemichannel activity that may, or may not, be accompanied by changes in gap junctional intercellular conductance. It is likely that multiple disease mechanisms, including alteration of hemichannel activity, are involved across the wide spectrum of hereditary diseases involving connexin proteins. Indeed, mechanisms may even vary within individual clinical classifications, but further characterization is necessary. Experimental paradigms combining specific small molecule inhibitors with animal models will be a powerful next step toward confirming, or eliminating, the proposed role of hemichannel openings in skin disease. As an additional benefit, novel therapeutic strategies to rescue tissue integrity may emerge in the process.

SPECIFIC AIMS

Connexin (Cx) proteins form intercellular gap junction channels to facilitate the exchange of ions and small molecules (<1kD) between adjacent cells. Mutations in connexins cause several human diseases by interrupting normal cell-to-cell communication. Connexins also form functional hemichannels in nonjunctional membranes that have an unclear role in normal physiology but have altered activity in pathological states. Mutations in *GJB2*, the gene encoding connexin26 (Cx26), are linked to sensorineural hearing loss as well as syndromic deafness associated with skin disorders. In contrast to Cx26 mutations causing nonsyndromic deafness, those that also cause skin disease are exclusively gain-of-function single amino acid substitutions with autosomal dominant inheritance patterns. Keratitis-ichthyosis-deafness (KID) syndrome is a congenital ectodermal disorder of varied clinical presentation caused by (at least) 10 distinct point mutations of Cx26. The definitive pathophysiologic mechanism(s) leading to the skin phenotype(s) in KID syndrome are presently unknown. Functional studies have now demonstrated aberrant hemichannel activity compared to wild-type (WT) Cx26 for 7 KID-causing mutant variants. We hypothesize that gained functional abnormalities of normally quiescent hemichannels account for the

dermatologic manifestations of KID syndrome. The objective of this dissertation was to identify potent small molecule inhibitors of Cx26 with attention to isoform-selectivity and affinity for mutant channel forms implicated in KID syndrome. Inhibitory efficacy was assayed by electrophysiological methods capable of quantitating drug-mediated reduction of Cx26 hemichannel currents. Newly characterized inhibitors will have utility both in probing for physiological functions of hemichannels and establishing dysregulated unapposed channels as a specific pharmacological target in connexin-associated gain-of-function disorders. Furthermore, we have performed preliminary experiments to inform future thorough testing of therapeutic strategies in a transgenic mouse model of KID syndrome. Topical delivery of appropriate Cx26 hemichannel inhibitors, selected by rigorous *in vitro* testing, will ultimately provide unambiguous evidence for, or against, hypotheses connecting leaky hemichannels to the loss of epidermal homeostasis in KID syndrome.

Specific Aim 1a: Screening of 5 quinine analogs for Cx26-G45E and Cx26-D50N hemichannel current suppression in single *Xenopus laevis* oocytes by two-electrode voltage clamp electrophysiology. Cx26-G45E causes a lethal form of KID syndrome and displays marked hemichannel overactivity. Cx26-G45E is regarded as the archetypal KID mutation due to its clinical urgency and because it typifies the 'functional phenotype' common among the majority of KID mutations. Cx26-D50N is the most commonly reported mutation in KID syndrome. We performed a screen of mefloquine and 4 related derivatives previously used for blockade of connexin36 and connexin50 gap junctions by expressing Cx26-G45E and Cx26-D50N in *Xenopus* oocytes. Whole-cell membrane currents, a measure of global hemichannel activity, were recorded in the absence and presence of candidate inhibitors at low micromolar (therapeutic range) concentration.

Specific Aim 1b: Testing mefloquine responses across the set of 7 KID-causing and hemichannel-forming Cx26 mutations. Individual missense mutations linked to

KID syndrome may interrupt the normal gating and/or permeability of connexin26 hemichannels through distinct failures of regulation. Moreover, specific biochemical modifications may render mutant channels insensitive to certain modes of pharmacological inhibition. Using the *Xenopus* oocyte expression system, we examined the susceptibility of Cx26-G45E, -D50N, -A40V, -D50A, -G12R, -N14K, and -A88V to inhibition by mefloquine and characterized the concentration dependence of each effect to probe for unique mutant hemichannel behaviors.

Specific Aim 2: Isolating primary keratinocytes from a transgenic mouse model of KID syndrome to measure macroscopic membrane current responses to mefloquine perfusion. Mice expressing human Cx26-G45E in basal keratinocytes develop skin abnormalities and reduced viability mirroring the human disease described for this mutation. The double transgenic design enables reverse tetracycline transactivator (rtTA) inducible expression of a bicistronic element encoding Cx26-G45E and eGFP in cells of the stratum basale. Hyperkeratotic plaques consistent with erythrokeratoderma were excised for isolation of basal keratinocytes. Keratinocyte transgene expression, as evidenced by eGFP fluorescence, was retained in tissue culture for several hours *ex vivo*. Patch clamp electrophysiology was performed to detect amplified hemichannel activity and the extent to which mefloquine attenuated membrane currents.

Specific Aim 3: Examining the effects of broad-acting and clinically utilized gap-junction inhibitor compounds on hemichannels formed by lethal KID mutations Cx26-G45E and Cx26-A88V. The Cx26-G45E and Cx26-A88V mutations have been reported in pediatric patients with life threatening KID syndrome. Dermatologic defects included extensive ichthyosiform erythroderma and resultant mucocutaneous infections, leading to septicemia and death in early childhood. Given the immediate need for drugs capable of controlling rapidly escalating hyperkeratosis, we studied two gap-junction inhibitors with a history of safe use in clinical practice as prospective blockers of Cx26-

G45E and Cx26-A88V hemichannels. Flufenamic acid (FFA) is a non-steroidal anti-inflammatory agent with broad membrane channel blocking activities. Carbenoxolone (CBX) disodium salt is a synthetic derivative of a licorice root extract appreciated to inhibit pannexins and connexins and licensed in the United Kingdom for treatment of esophageal ulcer. Patch clamp and voltage clamp electrophysiological techniques were used with transiently transfected HeLa cells and cRNA-injected *Xenopus* oocytes, respectively, to assess the putative applicability of FFA and CBX to Cx26-G45E- and Cx26-A88V-driven KID syndrome.

Specific Aim 4: Initiating a paradigm for *in vivo* testing of hemichannel inhibitors by topical administration in a transgenic mouse model of KID syndrome. The inducible expression of Cx26-G45E in mouse epidermis recapitulates the gross and histopathological features of KID syndrome. Moreover, transgenic Cx26-G45E keratinocytes exhibit increased hemichannel activity that is in close agreement with *in vitro* functional analyses. The skin disease onset kinetics and the reversibility properties of the system upon removal of the induction agent were characterized prior to *in vivo* trials to pharmacologically prevent or interrupt the loss of epidermal homeostasis in the mouse model. Additionally, a solvent vehicle capable of prompt absorption and proper delivery to the sub-granular epidermal layers was validated. Finally, preliminary experiments are being performed with inhibitors showing robust activity in cell-based studies to generate early indicators of potential for future use as adjunct therapies in KID syndrome.

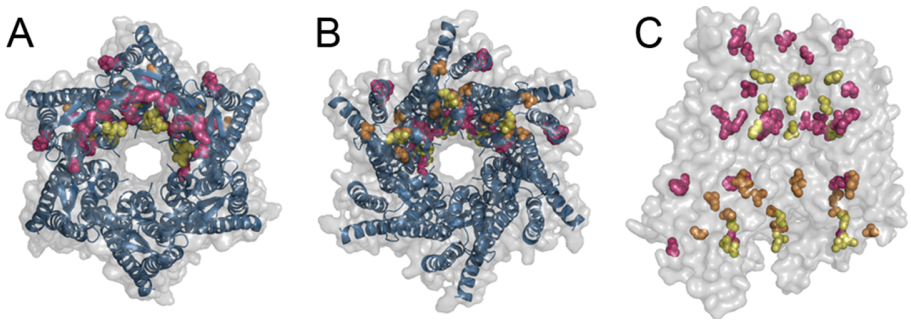

Figure 1-1 (Levit *et al.*, 2012). Three-dimensional structure of a Cx26 hemichannel. Mutated residues linked to keratitis-ichthyosis-deafness syndrome (yellow and orange) and palmoplantar keratoderma with deafness (pink) are mapped onto three of the six subunits of the reported Cx26 crystal structure (Maeda *et al.*, 2009). The blue protein backbone illustrates the topology of Cx26, which consists of 4 transmembrane domains, 2 extracellular loops, and 1 cytoplasmic loop. (A) View of the extracellular portion of the channel. (B) View of the cytoplasmic side of the channel, including both the amino and carboxy-termini. (C) Lateral view of the channel with 3-subunits and the protein backbone removed to simplify visualization of mutations. The yellow residues have been associated with aberrant hemichannel activity when mutated and are spatially confined to pore-lining domains.

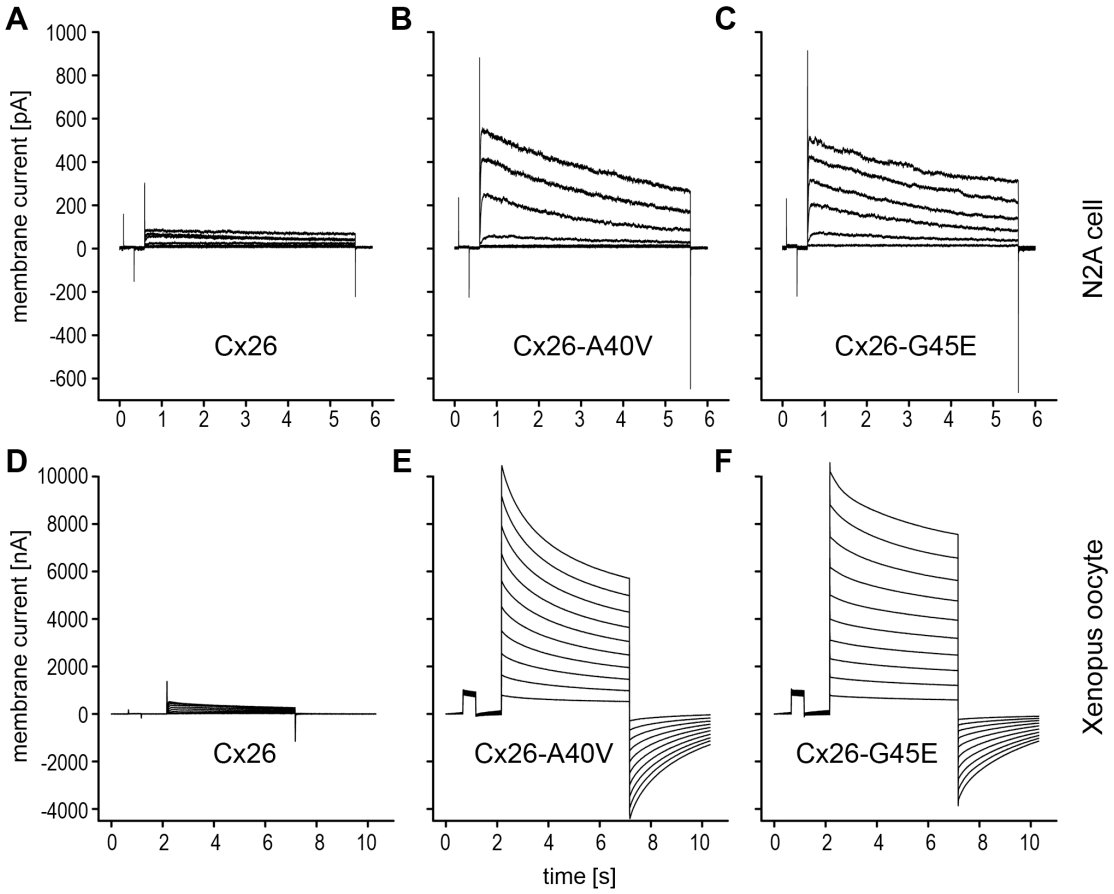

Figure 1-2 (Levit *et al.*, 2012). Membrane current recordings in *Xenopus* oocytes (A-C) and N2A cells expressing wild-type connexin26 (A, D) as well as Cx26-A40V (B, E) and Cx26-G45E (C, F). Oocyte expression assay is accomplished by microinjection of cloned human Cx26 mRNA. Single-cell voltage clamp (A-C) is performed with a holding potential of -40mV and voltages ranging from -30 to +60mV are tested with 5 second pulses. Mammalian cell expression system involves transfection with plasmid vectors containing the human Cx26 coding region. Whole-cell patch clamp data corresponds to voltages ranging from -90 to +90mV. Cx26-G45E and Cx26-A40V show elevated hemichannel currents relative to wild-type in both *Xenopus* oocytes and N2A cells.

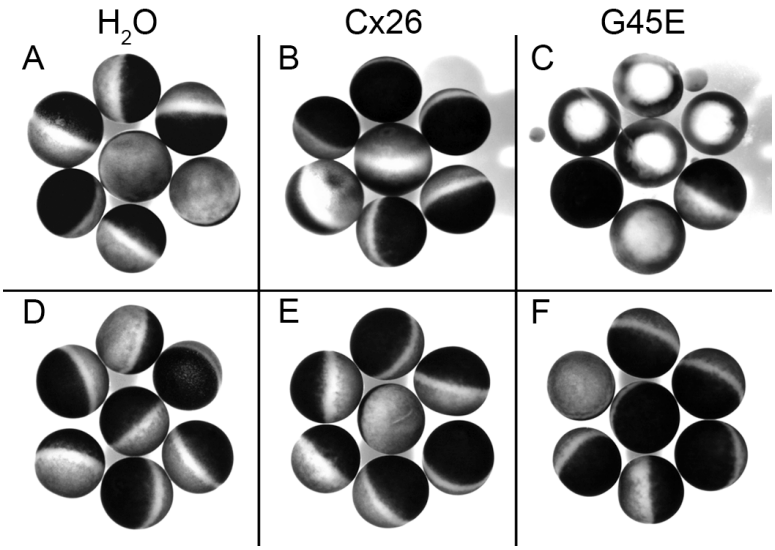

Figure 1-3 (Levit *et al.*, 2012). The Cx26-G45E mutant leads to accelerated cell death when expressed in *Xenopus* oocytes which can be rescued by culture in elevated Ca^{++}. H2O-injected (left), wild-type Cx26-injected (middle), and Cx26-G45E-injected (right) cells were incubated in 0mM (A-C) or 4mM extracellular Ca^{++} (D-F) for 40 hours. Cells expressing the Cx26-G45E mutant exhibit pigment disorganization, blebbing, and/or lysis in the low calcium condition but resembled the healthy negative and positive control cells in the high calcium condition.

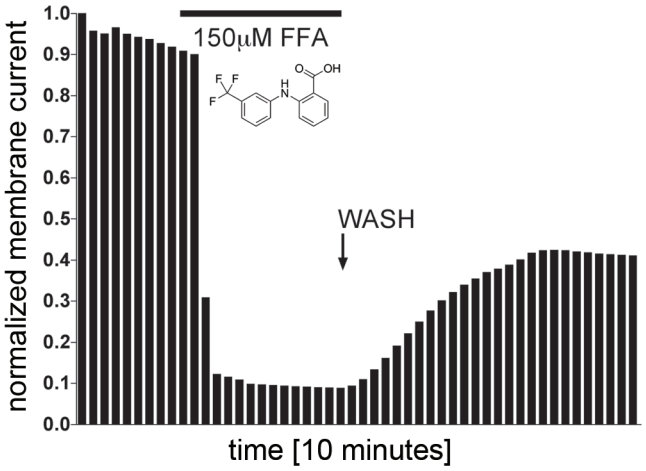

Figure 1-4 (Levit *et al.*, 2012). Hemichannel current suppression by flufenamic acid. A single Cx26-G45E-expressing oocyte was held at -40mV and pulsed successively at 100mV for 10 minutes. Bars correspond to the average instantaneous membrane current recorded during each voltage pulse. 2 minutes were allowed for membrane stabilization before perfusion with 150μM FFA for 3 minutes. Hemichannel currents shown are normalized to the initial value to monitor fractional change. >80% hemichannel current inhibition is achieved with 150μM FFA that is partially reversed by 5 minutes of washout with the drug-free culture medium.

Chapter 2. Inhibition of Cx26 hemichannel forms present in KID syndrome by quinine analogs and ionic zinc

ABSTRACT

Keratitis-ichthyosis-deafness (KID) syndrome is an ectodermal dysplasia caused by dominant mutations of connexin26 (Cx26). Loss of Cx26 function causes non-syndromic sensorineural deafness, without consequence in the epidermis. Functional analyses have revealed that a majority of KID-causing mutations confer a novel expansion of hemichannel activity, mediated by connexin channels in a non-junctional configuration. Inappropriate Cx26 hemichannel opening is hypothesized to compromise keratinocyte integrity and epidermal homeostasis. Pharmacological modulators of Cx26 are needed to assess the pathomechanistic involvement of hemichannels in the development of hyperkeratosis in KID syndrome. We have used electrophysiological assays to evaluate small molecule analogs of quinine for suppressive effects on aberrant hemichannel currents elicited by KID mutations. Here, we show that mefloquine inhibits several mutant hemichannel forms implicated in KID syndrome with high affinity when expressed in *Xenopus* laevis oocytes (IC_{50}≈16μM), using an extracellular divalent cation, zinc (Zn^{++}), as a non-specific positive control for comparison (IC_{50}≈3μM). Furthermore, we used freshly isolated transgenic keratinocytes to show that micromolar concentrations of mefloquine attenuated increased macroscopic membrane currents in primary mouse keratinocytes expressing human Cx26-G45E, a mutation linked to a lethal form of KID syndrome.

INTRODUCTION

Connexin-encoding genes contribute the structural subunits of gap junctions, which establish a direct signaling pathway between virtually all contacting cell-types (Goodenough and Paul, 2009). Gap junction plaques are an assemblage of intercellular channels that enable diffusional exchange of ions, second messengers, and small metabolites to mediate coordinated functions within tissues (Bruzzone *et al.*, 1996). Connexins are tetraspan integral membrane proteins that form highly specialized hexameric oligomers, termed 'hemichannels,' which dock in pairs to couple adjacent cells. Several connexins are now appreciated to produce functioning hemichannels in the nonjunctional configuration with yet uncertain physiological relevance (DeVries and Schwartz, 1992; Ebihara and Steiner, 1993; Malchow *et al.*, 1993).

Connexin mutations occur with high frequency and account for a multitude of human hereditary diseases (Pfenniger *et al.*, 2011). Mutations in connexin26 (Cx26 or *GJB2*) are a major cause of nonsyndromic sensorineural deafness as well as syndromic hearing loss that presents in conjunction with skin disorders, such as keratitis-ichthyosis-deafness (KID) syndrome (Scott and Kelsell, 2011). Cx26 is found to be either partially or completely nonfunctional for a vast proportion of autosomal recessive mutations leading to nonsyndromic deafness (Zhao *et al.*, 2006). Conversely, clinical scenarios involving skin pathology are transmitted through dominant Cx26 mutations that are suspected to confer novel channel activities (Richard, 2005).

KID syndrome is a rare disorder characterized by profound hearing loss, vascularizing keratitis, and extensive erythrokeratoderma (Richard *et al.*, 2002; Skinner *et al.*, 1981). KID patients suffer recurrent mucocutaneous infections that can precipitate lethal septicemia (Haruna *et al.*, 2010; Sbidian *et al.*, 2010). Additional features include reports of the follicular occlusion triad (dissecting folliculitis, hidradenitis suppurativa, and cystic acne) and malignant transformation of hyperkeratotic plaques to squamous

cell carcinoma (Mazereeuw-Hautier *et al.*, 2007; Montgomery *et al.*, 2004). 10 distinct Cx26 missense mutations are associated with KID syndrome, although genotype-phenotype correlations have been difficult to establish due to a small number of cases and heterogeneous nature of the disorder. Electrophysiological analysis, completed for 8 KID-causing Cx26 mutations at the time of writing, has exposed a pattern of aberrant hemichannel behavior shared by all but one. Specifically, Cx26-G45E, -D50N, -A40V, -N14K, -G12R, -A88V, and -D50A induce significantly greater hemichannel activity than wild-type channels under the same experimental conditions (Donnelly *et al.*, 2012; Gerido *et al.*, 2007; Lee *et al.*, 2009; Mhaske *et al.*, 2013; Montgomery *et al.*, 2004; Sanchez *et al.*, 2010; Stong *et al.*, 2006). Constitutively active or 'leaky' hemichannels are predicted to cause ionic imbalances and disrupt signal transduction in differentiating keratinocytes with injurious consequences for the epidermis.

A pathogenic role for dysregulated hemichannels in KID syndrome awaits definitive demonstration. Pharmacological tools to modulate Cx26 channels are needed to assess the impact of excessive hemichannel openings on cell viability and tissue integrity. Systematic searches for highly specific inhibitors are lacking due to challenges in adapting connexin functional assays to high-throughput screening. Several approaches have implemented dye transfer methods with automated fluorescence microscopy imaging to identify candidate compounds (Li *et al.*, 2003; Picoli *et al.*, 2012). However, these studies were unable to discriminate between direct and indirect inhibitor actions. Moreoever, these approaches fail to account for the possibility of differential drug affinities for mutant channel forms important in human disease. Using two different electrophysiological assays, we show quantitative evaluation of prospective small molecule inhibitors of mutant Cx26 hemichannels present in KID syndrome, and include an extracellular divalent cation, zinc (Zn^{++}), for comparison. Mefloquine emerged as a leading candidate among 5 tested compounds selected for affinity to connexin targets. Compounds showed varying activities across mutant channel forms containing distinct biochemical modifications. Our results indicate that micromolar doses of mefloquine potently attenuate Cx26 hemichannel currents associated with the majority of KID

mutations and show that it is particularly well positioned for testing in a transgenic mouse model of the lethal form of the disease.

RESULTS AND DISCUSSION

Increased hemichannel activity associated with KID-causing Cx26 mutations

Previous reports have described alterations in gap-junction-independent functionality of hemichannels to be a common feature shared by Cx26 mutations linked to KID syndrome with few exceptions (Donnelly *et al.*, 2012; Gerido *et al.*, 2007; Lee *et al.*, 2009; Mhaske *et al.*, 2013; Montgomery *et al.*, 2004; Sanchez *et al.*, 2010; Stong *et al.*, 2006). As a prerequisite to pursuing inhibitor studies, we quantified membrane currents in single *Xenopus* oocytes expressing Cx26-G45E, -D50N, -A40V, -N14K, -G12R, -D50A, and -A88V, with Cx26-WT- and water-injected cells serving as reference. The above set of *GJB2* mutations result from single amino-acid substitutions that structurally localize to the Cx26 N-terminus and first extracellular loop, with the exception of A88V, which appears in the second transmembrane domain. All mutants are associated with KID syndrome. To assay membrane current, single cells were voltage clamped at -40mV and subjected to a series of depolarizing transmembrane voltage pulses (Figure 2-1a). Negligible membrane current was recorded from oocytes injected with H_2O for voltages ranging -30 to +60mV. Wild-type Cx26 hemichannels favored a low open-probability resting state with outward current induced by membrane depolarization and an approximately linear current-voltage relationship as previously demonstrated (Gonzalez *et al.*, 2006; Ripps *et al.*, 2004). The Cx26-G45E, -D50N, -A40V, -N14K, -G12R, -D50A, and -A88V mutants displayed increased outward currents, to varying extents, relative to H_2O or Cx26-WT-injected cells for the same set of depolarizing stimuli. At the largest voltage tested, Cx26-WT hemichannels passed maximal currents of 0.5-1.5μA and conductance was recorded to be 10.5-, 7.5-, 8-, 8-,

4.5-, 4-, and 8-fold higher in Cx26-G45E, -D50N, -A40V, -N14K, -G12R, -D50A, and -A88V respectively. The apparent increase in membrane permeability associated with the mutant forms of Cx26 implies a reduction in membrane resistance and suggests the presence of aberrantly active hemichannels. Western blotting of cell lysates for total Cx26 content eliminated the possibility that the markedly different magnitudes of membrane current arose from unequal levels of protein expression by individual cells (Figure 2-1b). The Cx26 band intensity was approximately consistent across the 7 mutant groups, which all closely mimicked the result for Cx26-WT.

In vitro screening of quinine-analogs for inhibitory efficacy on Cx26-G45E and Cx26-D50N hemichannels

At least two organic molecules therapeutically classified as antimalarial agents have been recognized to rapidly suppress hemichannel currents by direct action on connexin subunits (Cruikshank *et al.*, 2004; Rubinos *et al.*, 2012). Partial-selectivity properties are conferred to these compounds by differences in affinities for connexin subtypes (Cruikshank *et al.*, 2004; Srinivas *et al.*, 2001). At present, evidence for direct-binding sites and mechanisms of action are lacking for mefloquine, the most potent connexin channel inhibitor identified to date. Inhibitor studies involving mefloquine have most extensively focused on connexin50 and connexin36, in the context of their roles as gap junction proteins that couple lens epithelial cells and neurons, respectively (Cruikshank *et al.*, 2004). An ability of mefloquine to modulate connexin26 channel activity had received only cursory examination and only with regard to wild-type junctional communication. We screened mefloquine and four related derivatives (QU020, QU021, QU022, and QU026) for inhibitory capacity against dysregulated hemichannels resulting from two connexin26 mutations associated with KID syndrome. Cx26-G45E causes a lethal form of KID syndrome (Griffith *et al.*, 2006; Janecke *et al.*, 2005; Jonard *et al.*, 2008) and is characterized by robust hemichannel activity that represents the most significant deviation from wild-type channel behavior (Gerido *et al.*,

2007). Cx26-D50N is the most commonly reported mutation in cases of KID syndrome. Drug screening was performed by perfusion of candidate inhibitors during voltage clamp recording of Cx26-G45E (Figure 2-2a) and Cx26-D50N (Figure 2-2b) hemichannel currents in single *Xenopus* oocytes. Sequential depolarizing +50mV pulses were able to stimulate repeated channel opening and consistent bursts of whole-cell membrane current. Inhibitor effects were evaluated by exchange of the bathing media for a segment of each recording (Figure 2-2, left). At a drug concentration of 30μM, QU022 displayed unimpressive inhibition of membrane currents (<20% reduction) for both Cx26-G45E and Cx26-D50N. QU022 lacks the aliphatic piperidine ring present in mefloquine and also substitutes a $–CCl_3$ group for the $–CF_3$ found on the quinolone ring, representing the most dissimilar molecule to mefloquine included in the study. QU020 also failed to produce any dramatic suppression of Cx26-G45E hemichannels (25±14%) but was twice as effective when tested on Cx26-D50N hemichannels (49±7.3%). QU021 performed at a similar level, approximately halving membrane currents passed by both mutant channels (52±7.8% and 43±12% for Cx26-G45E and -D50N respectively). Mefloquine and QU026 elicited the most striking diminution in membrane currents recorded from single cells expressing either Cx26-G45E (70±17% for 30μM MFQ; 59±13% for 30μM QU026) (Figure 2-2a, right) or Cx26-D50N (69±15% for 30μM MFQ; 73±11% for 30μM QU026) (Figure 2-2b, right). QU026 replaces the piperidine ring in mefloquine with a third aromatic ring but includes no other structural deviation, possibly accounting for the parallel results. Two $-CF_3$ groups appear on the quinolone backbone of mefloquine, QU020, QU021, and QU026—a feature that enhances the lipophilicity of these molecules. For this reason, it is possible that lipid-rich yolk granules abundant in stage V-VI oocytes may sequester a portion of the drug, effectively reducing the delivered dose and causing underreporting of potency in this system. Lipophilicity is, however, an appealing property of any drug considered for targeting epidermal proteins via topical delivery strategies. Given the status of mefloquine as an FDA approved drug with a history of safety and pharmacokinetic data, it was selected for further characterization (Schlagenhauf *et al.*, 2011).

Mefloquine rapidly attenuated hemichannel currents produced by 5 of 7 KID-causing Cx26 mutations with concentration-dependence and partial reversibility

We assessed the utility of mefloquine for inhibiting the entire set of Cx26 mutations linked to KID syndrome and resulting in aberrantly high hemichannel activity. Three low micromolar concentrations were evaluated to probe for differences in sensitivity that may arise from unique biochemical or structural characteristics imparted by amino-acid substitutions. Mefloquine showed concentration-dependent reduction of Cx26-G45E hemichannel activity, with maximal suppression nearing total ablation of membrane currents (95.2% reduction at 100μM). Raw recordings from three single cells tested at 10, 30, and 100μM are shown to illustrate the instantaneous response of Cx26-G45E hemichannels to drug exposure and slow recovery of currents upon drug washout (Figure 2-3a). The magnitude of inhibition after 1.5min of 10, 30, and 100μM mefloquine was 43±8.0% (N=5), 71±7.9% (N=5), and 89±2.0% (N=5), respectively (extrapolated IC_{50}≈16μM). Recovery of currents remained incomplete after 2.5min of drug washout, ranging from 54±5.0% (N=5) to 84±3.5% (N=10) of initial current with an inverse correlation to concentration. Equivalent experiments were completed for Cx26-D50N, -A40V, -N14K, -G12R, -A88V, and -D50A and summary data is provided for the average residual current in the presence of 10, 30, and 100μM mefloquine as a percentage of the pre-perfusion value (Figure 2-3c). None of the other mutants showed sensitivity comparable to Cx26-G45E, although Cx26-D50N, -A40V, -G12R, and -D50A hemichannel currents were all suppressed by 50% or better at 30μM. In particular, Cx26-D50N and Cx26-G12R channels were >70% inactivated. Cx26-A88V and Cx26-N14K were refractory to inhibition by mefloquine.

A limited number of studies have examined the biophysical effects of connexin inhibitors with sufficient resolution to visualize single-channel gating events (Bukauskas and Peracchia, 1997; Srinivas and Spray, 2003; Weingart and Bukauskas, 1998). A consensus in findings suggests that quinine-analogs and mefloquine affect channel

activity by stimulating slow closure transitions that resemble loop gating (Rubinos *et al.*, 2012; Srinivas *et al.*, 2001; Verselis and Srinivas, 2013). Structural components of the loop gating machinery are provided by domains within the connexin N-terminus and first extracellular loop that form the hemichannel pore (Kronengold *et al.*, 2012; Kronengold *et al.*, 2003; Maeda *et al.*, 2009; Tang *et al.*, 2009; Verselis *et al.*, 1994; Verselis *et al.*, 2009). As mentioned earlier, there is conspicuous clustering of nearly all identified KID-causing Cx26 mutations to the protein N-terminus and first extracellular loop. It is possible that mutations leading to increased hemichannel activity may corrupt the intrinsic voltage-sensitive activation of slow gating or mechanically impede movement of the loop. Mefloquine may function to restore loop gating and thereby prevent leaking of unapposed hemichannels. The inability of mefloquine to inhibit currents associated with Cx26-N14K may suggest a binding site in the vicinity of this residue in the cytoplasmic end of the channel pore. Though we present no direct evidence for this hypothesis, it is in agreement with previous mechanistic descriptions of connexin50 inhibition by a quaternary derivative of quinine, N-benzylquininium (Rubinos *et al.*, 2012). The absence of mefloquine activity on Cx26-A88V, taken together with its atypical spatial appearance in the second transmembrane domain, may imply that divergent triggers of aberrant hemichannel behavior exist. In the case of Cx26-A88V, an inhibitor capable of complete pore block may be necessary to reduce channel open dwell times. Due to the size of the hemichannel pore (15~40Å) (Maeda *et al.*, 2009), this strategy would require a larger molecule.

Extracellular Zn^{++} suppressed abnormal hemichannel activities for 7 KID-causing Cx26 mutants

A foreseeable limitation of quinine-family connexin inhibitors is their failure to distinguish between junctional and nonjunctional channel configurations. As such, dissecting apart a specific role for hemichannels in normal physiology and/or as putative mediators of disease processes will prove challenging. Divalent cations, with Ca^{++} the

classical example, inhibit connexin channels and have been shown to act at the extracellular aspect of the pore to promote loop gating (Verselis and Srinivas, 2008). Robust gap junctional conductances are routinely measured from cell pairs in the presence of extracellular Ca^{++}, indicating that binding of ions likely occurs at sites only accessible in undocked hemichannels. We recorded hemichannel currents from single *Xenopus* oocytes expressing Cx26-G45E in the presence and absence of 1, 10, and 100μM extracellular Zn^{++}. Oocytes injected with H_2O passed negligible current, again providing a negative control. Those expressing Cx26-G45E showed large fluxes, as previously documented. Addition of Zn^{++} to the extracellular milieu caused membrane currents to diminish in a dose-dependent manner (Figure 2-4a). Mean instantaneous currents were plotted as a function of membrane potential for each recording condition to facilitate comparison of current-voltage relationships (Figure 2-4b). Massive outward currents associated with Cx26-G45E were progressively reduced with 1, 10, and 100μM Zn^{++} at all tested voltages, -30 to +60mV. The degree of inhibition was quantified by perfusion of single cells during a paradigm of serial +100mV pulses. For cells expressing Cx26-G45E, 73±2.6% (N=5), 29±2.1% (N=5), and 12±3.9% (N=5) of the initial current persisted after 1.5min of 1, 10, and 100μM Zn^{++}, respectively (extrapolated IC_{50}≈3μM, Figure 2-4c).

Zinc inhibitory testing was repeated at 10 and 100μM for Cx26-D50N, -A40V, -N14K, -G12R, -A88V, and -D50A (Figure 2-4c). Hemichannel activity was largely preserved despite the application of 10μM Zn^{++}; only Cx26-G12R channels were >50% inhibited. Conversely, all mutant forms displayed >50% mean suppression at 10-fold higher Zn^{++} concentration. Notably, as with Cx26-G45E, 100μM Zn^{++} abolished membrane current associated with Cx26-A40V, -G12R, and -N14K by >80%. Together these data support the use of Zn^{++} as a suitable inhibitor to appraise the pathogenic culpability of hemichannels in KID syndrome.

Mefloquine inhibited elevated Cx26-G45E hemichannel currents in isolated primary murine keratinocytes

A mouse model of KID syndrome has previously been developed by inducible epidermal expression of a transgene containing the human Cx26-G45E coding sequence (Mese *et al.*, 2011). Animals harboring Cx26-G45E experience epidermal pathology consistent with clinical reports describing human KID syndrome patients (Koppelhus *et al.*, 2011; Mese *et al.*, 2011; Sbidian *et al.*, 2010). Specifically, the phenotype manifests as diffuse erythrokeratoderma with profound epidermal thickening and scaling (Figure 2-5b). The design strategy featured bicistronic inclusion of the excitatory green fluorescent protein (eGFP) in the founder construct and backcrossing into a hairless strain (Figure 2-5c) to allow for visualization of affected tissue by *in vivo* fluorescence imaging (Figure 2-5d). Keratinocytes isolated from excised lesions retained transgene expression, as evidenced by eGFP signal, for several hours *ex vivo* (Figure 2-5e). We sought to substantiate the effectiveness of mefloquine at suppressing Cx26-G45E membrane currents by whole-cell patch clamp analysis of freshly isolated transgenic keratinocytes. G45E-Cx26 keratinocytes, identified by eGFP signature, showed markedly high macroscopic membrane currents that were suppressed by 100μM mefloquine at both hyperpolarizing and depolarizing membrane potentials. Keratinocytes isolated from control littermates lacking the Cx26-G45E-IRES-eGFP cassette were used to gauge the basal membrane current contributed by other voltage-activated channels present in the primary cells (Figure 2-5a). Cx26-G45E keratinocytes were previously shown to have significantly increased cell size by histological examination (Mese *et al.*, 2011). To account for this, cell membrane capacitance was measured to estimate cell surface area and used to compute current density prior to plotting the aggregate data as a function of membrane potential (Figure 2-5f). Control keratinocytes possessed modest membrane currents for potentials ranging -110 to +110mV. Cx26-G45E keratinocytes passed substantially higher currents, particularly at depolarizing voltages. Re-recording in the presence of 100μM mefloquine reduced membrane currents to levels at or below control. The data indicate that 100μM

mefloquine is adequate to eliminate Cx26-G45E hemichannel activity in a mammalian system of higher complexity and physiological relevance. However, our results also highlight the imperfect specificity of mefloquine for connexin channels. Mefloquine has been observed to additionally inhibit voltage-gated L-type calcium channels, Kir6.2 and KvLQT1 potassium channels, volume-regulated and calcium activated chloride channels, and pannexins (Gribble *et al.*, 2000; Kang *et al.*, 2001; Maertens *et al.*, 2000; Suadicani *et al.*, 2006; Traebert *et al.*, 2004; Verselis and Srinivas, 2013). Optimization of the molecular structure to enrich sensitivity for Cx26 and/or decrease affinity for other targets may be possible through medicinal chemistry techniques (Wermuth, 2004). Nevertheless, mefloquine is confirmed to potently inhibit Cx26-G45E hemichannels. Minimally, this provides an agent to further structure-function analyses aimed at elucidating the molecular bases of errors in gating and permeation that accompany mutations. Importantly, mefloquine and related hemichannels inhibitors may also demonstrate therapeutic utility in KID syndrome.

Zinc modulated Cx26-G45E hemichannel activity in transgenic keratinocytes

Patch clamp analysis of freshly isolated transgenic Cx26-G45E keratinocytes was repeated with extracellularly applied Zn^{++}. Large macroscopic membrane currents associated with Cx26-G45E transgenic keratinocytes were reduced by 50μM Zn^{++}, with inhibitory effects most evident for inward currents at hyperpolarizing membrane potentials (Figure 2-6a). Tapering of Cx26-G45E hemichannel activity by 50μM Zn^{++} was observed across voltages -110 to +110mV by plotting current densities (Figure 2-6b).

In vitro expression of KID-associated mutant hemichannels causes cellular dysfunction and accelerated death, both in *Xenopus* oocytes and mammalian cell culture, that can be rescued by high extracellular calcium (Lee et al., 2009; Mhaske et

al.; Stong et al., 2006). Constitutively active or 'leaky' hemichannels may deplete the cells of important metabolites, such as ATP and cAMP, with deleterious consequences. Additionally, changes in hemichannel calcium permeability have been clearly demonstrated for two mutations, Cx26-A40V and -G45E, suggesting that dysregulated hemichannels may provide a route for excessive entry of calcium (Sanchez et al.). Resulting imbalances in intracellular-extracellular ionic gradients may disrupt paracrine signaling pathways or cause injurious osmotic pressures. Exogenous extracellular supply of a divalent cation, such as Zn^{++}, may reinforce an important mode of endogenous hemichannel regulation to prevent loss of cellular viability and tissue integrity.

In summary, we show two *in vitro* functional assays supporting the use of mefloquine and extracellular Zn^{++} as hemichannel inhibitors to study Cx26 mutants linked to KID syndrome. Extracellular Zn^{++} demonstrated marginally higher potency as well as fuller coverage of the Cx26 hemichannel mutant forms considered. Furthermore, Zn^{++} may represent a gap-junction-sparing inhibitor useful for isolating the explicit functions of hemichannels that relate to homeostatic maintaince. Unfortunately, the pervasive involvement of divalent cations in cellular processes would likely invite a plethora of off-target secondary effects that may preclude fruitful testing in animal models.

Mefloquine may provide a viable small molecule inhibitor for certain Cx26 mutant, including the lethal Cx26-G45E, particularly given the paucity of reagents with higher specificity/selectivity. Mefloquine has been reported to inhibit only one connexin isoform co-localizing with Cx26 in the epidermis, Cx43 (Cruikshank *et al.*, 2004). Loss of cellular coupling by Cx43 causes the developmental ectodermal disorder oculodentodigital dysplasia, which involves little disturbance of epidermal proliferation/differentiation (Jamsheer *et al.*, 2014). Moreover, a distinct set of connexin26 mutations causing palmoplantar keratoderma are thought to operate through *trans*-dominant inhibition of

wild-type Cx43 (Rouan *et al.*, 2001). These mutations cause hyperkeratosis that is confined to palmar/plantar skin, indicating that other connexin and non-connexin membrane channels may be capable of compensating for deficiencies in Cx43 function elsewhere (Richard *et al.*, 1998). An overlap in gap-junction and hemichannel blocking activity remains a primary drawback associated with mefloquine. However, defects in Cx26 gap-junctional communication do not appear to be causative of epidermal pathologies. Cx26 mutations causing KID syndrome have proven capricious with regard to their retention or deficiency of gap-junction functionality. For example, expression of Cx26-G45E and -N14K in cell pairs leaves gap junctional conductance unaffected relative to wild-type (gating is altered, however), where as active coupling is not detected for Cx26-G12R and the prevalent -D50N (Gerido *et al.*, 2007; Lee *et al.*, 2009). The clearest indication that the native function of Cx26 is not essential in the epidermal renewal process stems from the absence of cutaneous abnormalities in patients with autosomal recessive non-syndromic hearing loss, which is predominantly due to loss of Cx26 function (White, 2000; Zhao *et al.*, 2006). The apparent apathy of the epidermis to Cx26 gap junction functional status favors the use of mefloquine in exploring the pathological implications of excessive hemichannel currents.

Whether alterations in Cx26 hemichannel patency and/or permeability are sufficient to upset epidermal homeostasis in KID syndrome remains to be definitively shown. Hemichannels are speculated to participate in delicate paracrine signaling which may involve the extracellular release of ATP (Cotrina *et al.*, 1998; Kang *et al.*, 2008), glutamate (Ye *et al.*, 2003), NAD^+ (Bruzzone *et al.*, 2001), and prostaglandins (Jiang and Cherian, 2003). Connexin-specific inhibitors, with subtype-selectivity and high affinity for mutant forms causing human genetic diseases, are needed to evaluate hypotheses formulated from *in vitro* functional studies. The use of currently available inhibitors in animal models will help to clarify a physiological niche for unapposed hemichannels in numerous tissue systems and may offer novel therapeutic strategies for gain-of-function genetic disorders.

MATERIALS AND METHODS

Molecular cloning

Human wild-type and mutant Cx26 were cloned into the *Bam*HI restriction site of the pCS2+ expression vector (Turner and Weintraub, 1994) for functional assays in *Xenopus laevis* oocytes. Cx26-G45E, -D50N, -G12R, -N14K, -A88V, and -D50A were prepared from the wild-type template by site-directed mutagenesis using overlap extension PCR (Horton *et al.*, 1990) as previously described (Gerido *et al.*, 2007; Lee *et al.*, 2009; Mhaske *et al.*, 2013). Cx26-A40V was directly amplified from patient genomic DNA as previously described (Montgomery *et al.*, 2004).

In vitro transcription and oocyte microinjection

Human wild-type Cx26 and 7 mutant plasmid DNAs were linearized by NotI digestion and transcribed using the SP6 mMessage mMachine (Ambion, Austin, TX) to yield cRNAs. The Stony Brook University IACUC approved a protocol for oocyte removal from *Xenopus laevis*. Adult females were anesthetized with ethyl 3-aminobenzoate methanesulfonate and ovarian lobes were surgically excised. Oocyte lobes were digested in 7.5mg/mL collagenase B and 5.0mg/mL hyaluronidase in modified Barth's (MB) medium without Ca^{++} for 15 minutes at 37°C with constant shaking. Stage V-VI oocytes were separated and injected with 10ng of an antisense morpholino oligonucleotide to endogenous connexin38 (Barrio *et al.*, 1991; Bruzzone *et al.*, 1993), to eliminate endogenous connexin. Oocytes were next injected with wild-type Cx26, Cx26-G45E, -D50N, -A40V, -A88V, -G12R, -D50A, -N14K cRNA transcripts or H_2O as a negative control and cultured in MB media supplemented with 4mM $CaCl_2$ for 15-18 hours before electrophysiological assay.

Preparation of oocyte samples for Western blot analysis

Oocytes were collected and homogenized in 1mL of buffer containing 5mM Tris pH 8.0, 5mM EDTA, and protease inhibitors (Roche diagnostics, Indianapolis, IN by mechanical passage through a series of needles of diminishing size (White *et al.*, 1992). During cell lysis, samples were kept on ice and at 4°C during incubation or centrifugation. Yolk granules were separated from extracts by centrifugation at 1000g for 5 minutes. Membranes were pelleted by centrifugation at 100,000g for 30 minutes, resuspended in SDS sample buffer (2μL/oocyte), separated on 12% SDS gels, and transferred to nitrocellulose membranes. Blots were blocked with 5% milk in 1xTBS/0.1% tween20 for 1 hour at room temperature and probed with a polyclonal rabbit anti-Cx26 antibody (Invitrogen, Carlsbad, CA), at a 1:1000 dilution and subsequently incubated with a horseradish peroxidase-conjugated anti-rabbit secondary antibody (Jackson ImmunoResearch, West Grove, PA) at 1:5000 dilution. For loading control, blots were washed, re-probed with a monoclonal mouse β-actin antibody (Abcam, Cambridge, MA) and incubated with a horseradish peroxidase-conjugated anti-mouse secondary antibody (GE Healthcare Biosciences, Pittsburgh, PA).

Inhibitory drugs

Quinine family small molecules investigated, including mefloquine (([R*,S*]-[2,8-Bis-trifluoromethyl-quinolin-4-yl]-piperidin-2-yl-methanol hydrochloride), QU020 ([2,8-Bis-trifluoromethyl-quinolin-4-yl]-pyridin-2-yl-methanone, QU021 (2,8-Bis[trifluoromethyl]-4-quinolyl[1-oxypyrid-2-yl] methane), QU022 (4-Chloro-2-trichloromethyl-quinoline), and QU026 ([2,8-Bis-trifluoromethyl-quinolin-4-yl]-pyridin-2-yl-methanol), were acquired from Bioblocks, Inc. (San Diego, CA). All drugs were

solubilized in dimethyl sulfoxide (DMSO) at a stock concentration of 100mM and stored at -20°C.

Voltage clamp recording of hemichannel currents and small molecule inhibitor properties

Macroscopic recordings of hemichannel currents were acquired from single *Xenopus* oocytes using a GeneClamp 500 amplifier controlled by a PC-compatible computer through a Digidata 1440A interface (Axon instruments, Foster City, CA). Stimulus and data collection paradigms were programmed with pClamp 10.2 software (Axon Instruments). Current and voltage electrodes (1.5mm diameter glass, World Precision Instruments, Sarasota, FL) were pulled to a resistance of 1-2MΩ on a vertical puller (Narishige, Tokyo, Japan) and filled with a conducting solution containing 3M KCl, 10mM EGTA, and 10mM HEPES pH 7.4. Whole-cell current traces were obtained by initial clamping at -40mV and subsequent 5-8 second depolarizing pulses spanning -30 to +60mV in 10mV increments (Lee *et al.*, 2009). Pharmacologic inhibitor compounds were tested during a 50-sweep series of 5 seconds 100mV depolarizations from the -40mV holding potential over a 5 minute experimental duration. Recordings were initiated by active gravity-fed perfusion with MB medium lacking Ca^{++} for a 10-pulse period to ensure minimal clamp leakage and stability of the steady state membrane current. Small molecule inhibitors or ionic salts ($ZnSO_4$) were then introduced using a three-way valve to rapidly exchange bathing solutions in a custom 0.5mL chamber for 15 voltage pulses. During the final 25-pulse period, the inhibitor solution was flushed out with MB media lacking Ca^{++} to assess reversibility. Instantaneous whole-cell membrane current corresponding to each voltage pulse was extracted from raw data and normalized to the starting current for examination of the fractional change upon perfusion.

Isolation of primary transgenic Cx26-G45E keratinocytes

Primary murine keratinocytes with transgenic expression of human Cx26-G45E were isolated from epidermal tissue using a previously established mouse model of KID syndrome as previously described (Mese *et al.*, 2011). KID lesions were induced in animals between 4 and 8 weeks of age by two weeks of doxycycline supplemented diet (200mg/kg). Lesion severity was non-invasively assessed by *in vivo* fluorescence detection of eGFP by imaging under isoflurane anesthesia in a Maestro small animal imaging system (Cri, Woburn, MA). Following euthanasia of animals, 3-5mm dorsal skin lesions comprising the epidermis and dermis were resected and cells were isolated for short-term culture (Lichti *et al.*, 2008). Samples were floated in 0.25% trypsin at 37°C for 45 minutes, mechanically minced, passed through a 100μm cell strainer, and plated on 12mm glass coverslips coated with 40μM poly-D-lysine hydrobromide to facilitate rapid attachment. Primary cells were cultured in regular media supplemented with 0.2mM $CaCl_2$ for 2 hours at 37°C and 5% CO_2 before using for immunocytochemistry or patch clamp electrophysiology. GFP transgene expression was maintained without doxycycline supplementation for up to 6 hours. The Stony Brook University IACUC approved all procedures involving mice.

Immunocytochemistry

Primary epidermal keratinocytes were fixed with 1% paraformaldehyde in phosphate buffered saline (PBS) for 1 hour at room temperature and then blocked and permeabilized with 5% bovine serum albumin (BSA) in PBS plus 0.1% triton X-100 for 30 minutes at room temperature. Coverslips were mounted on slides using Vectashield with nuclear-staining 4',6'-diamidino-2-phenylindole (DAPI) (Vector Laboratories, Burlingame, CA). Slides were viewed on a BX51 microscope and photographed with a DP72 digital camera (Olympus, Lake Success, NY).

Patch clamp electrophysiology

Primary murine epidermal keratinocytes were used for whole-cell patch clamp at room temperature as previously described (Mese *et al.*, 2011). Cells on 12mm glass coverslips were immersed in a calcium-free bath (Tyrode's) solution containing 137.7mM NaCl, 5.4mM KCl, 2.3mM NaOH, 1mM $MgCl_2$, 2mM $CsCl_2$, 4mM $BaCl_2$, 10mM glucose, and 5mM HEPES (pH 7.4). Patch pipettes were pulled from glass capillaries with a horizontal puller (Sutter Instruments, Novato, CA) and filled with a conducting solution containing 120mmol/L K aspartate, 5mM HEPES, 10mM ethylene glycol tetraacetic acid, and 3mM NaATP (pH 7.2). To begin each experiment, cells were clamped at 0mV and subsequently stepped from -110 to +110mV in 20mV increments. Following the initial set of hemichannel current recordings, inhibitor effects were tested by perfusing dishes with small molecules (MFQ/QU0) diluted in Tyrode's solution, and re-recording within 30-90 seconds of media exchange.

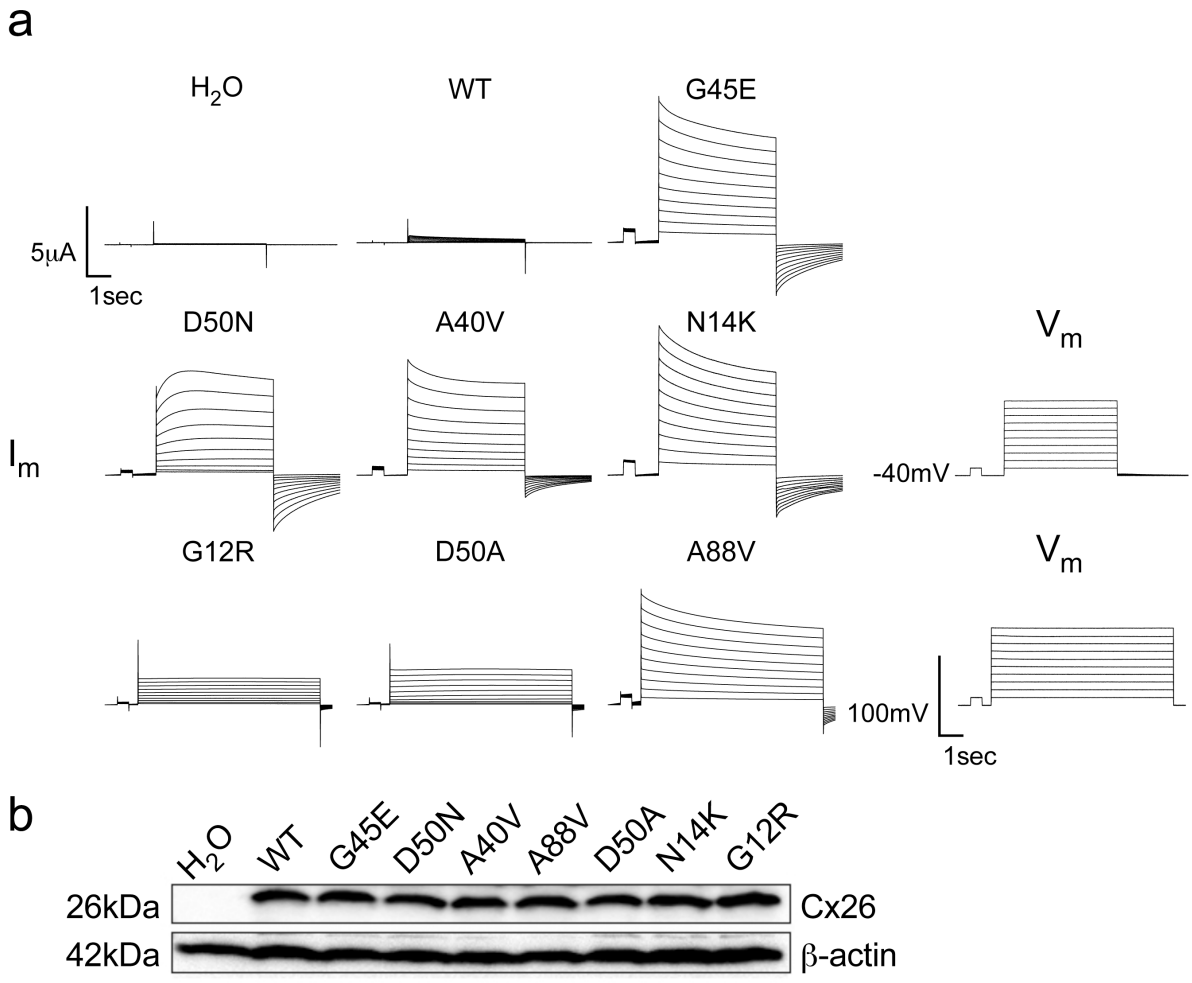

Figure 2-1. KID syndrome associated Cx26 mutations induced large hemichannel currents in *Xenopus* oocytes. (a) Cells were clamped at -40mV and subjected to voltage pulses spanning -30 to +60mV in 10mV steps (V_m). H_2O-injected cells displayed negligible whole-cell membrane currents (I_m). Cx26 expressing oocytes all exhibited hemichannel currents, however, KID syndrome mutations showed much larger currents than wild-type (WT). (b) WT and mutant connexins are equivalently translated in *Xenopus* oocytes. Membrane extracts were probed with an antibody against Cx26. H_2O-injected controls did not express Cx26, whereas WT, Cx26-G45E, -D50N, -A40V, -A88V, -D50A, -N14K, and -G12R were detected with similar band intensities. Blots were stripped and reprobed with an antibody against β-actin, which was present at comparable levels in all lanes.

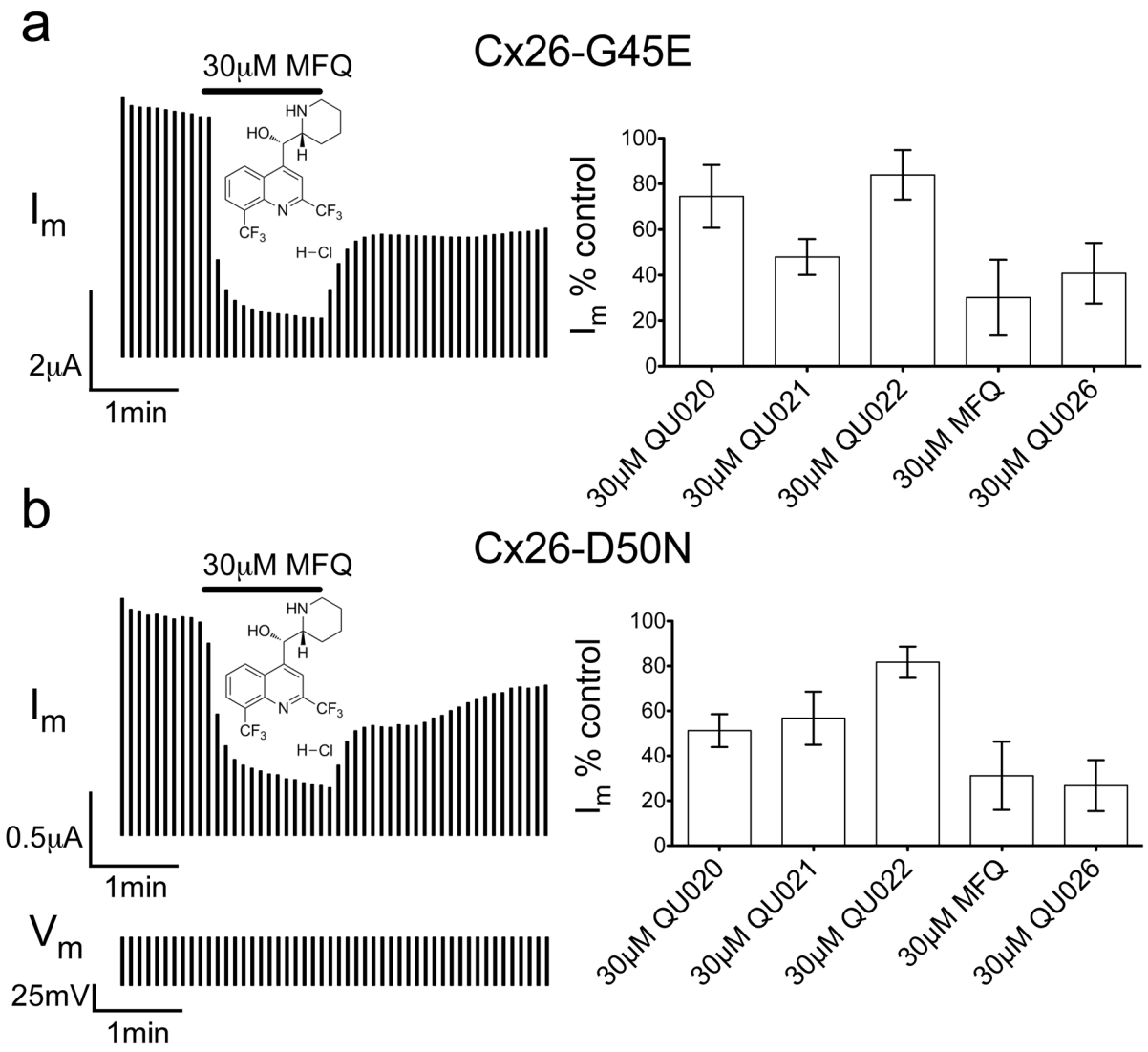

Figure 2-2. Mefloquine (MFQ) and quinine derivatives (QU0) suppressed (a) Cx26-G45E and (b) -D50N hemichannel currents in *Xenopus* oocytes. Single cells held at -40mV were repeatedly pulsed with +50mV depolarizations (V_m) and membrane current (I_m) was measured. Cells were exposed to 30μM inhibitor for 90 seconds by switching perfusion solutions after one minute (left, shown for mefloquine). Inhibitors were washed out for 2.5 minutes, showing partial reversibility at the concentration tested. Summary data for inhibitors QU020, QU021, QU022, MFQ, and QU026 are shown as the mean residual instantaneous membrane current during 30μM drug application as a percentage of the pre-drug value (right). MFQ and QU026 produced the greatest inhibition of Cx26-G45E and -D50N membrane currents. Data are the means ± SD.

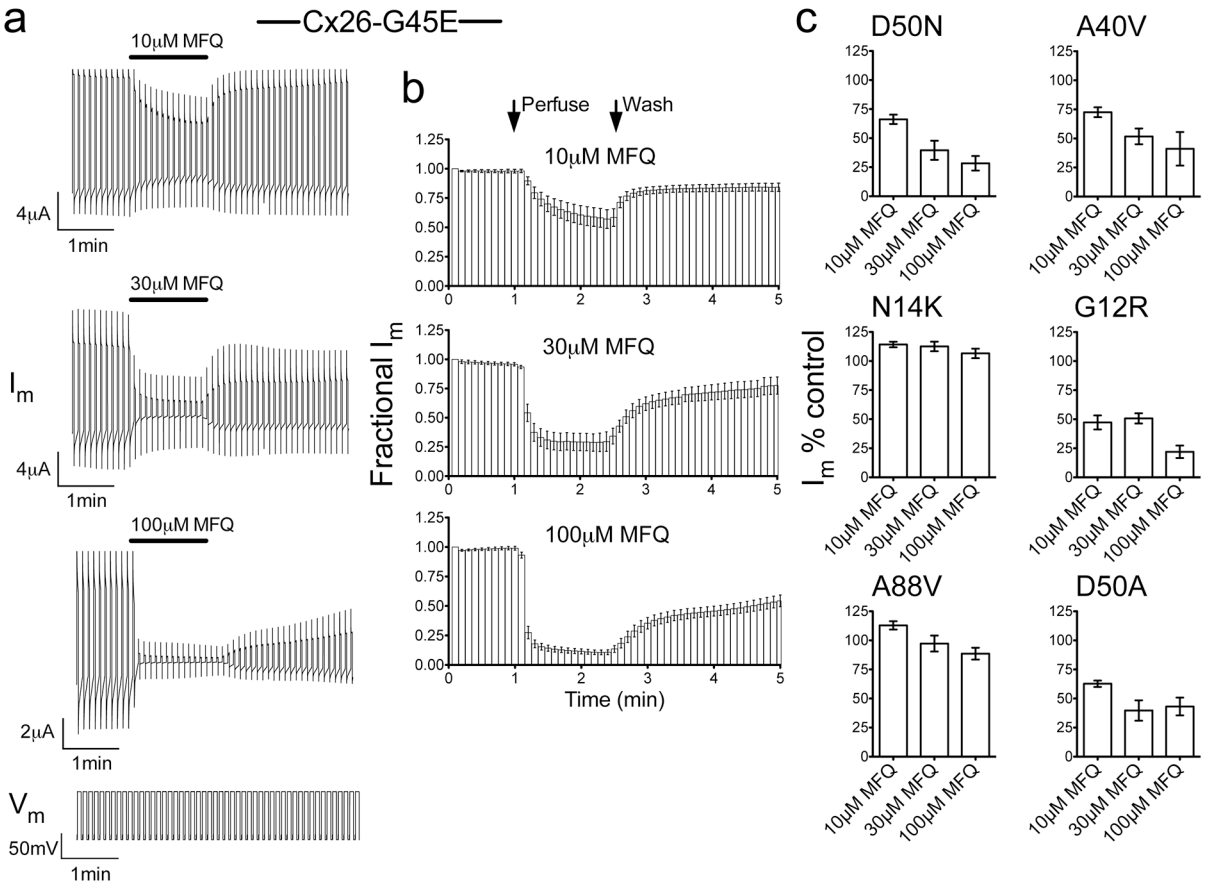

Figure 2-3. Mefloquine (MFQ) attenuated KID-associated Cx26 hemichannel currents in a concentration-dependent and mutant-selective manner. (a) Voltage clamp recordings for three *Xenopus* oocytes expressing Cx26-G45E showed an increasing magnitude of membrane current (I_m) block with 10, 30, and 100μM MFQ. (b) Mean MFQ response characteristics across Cx26-G45E-expressing cells showed that membrane current, plotted as a fraction of the starting value, fell by >25%, >50%, and >75% upon exposure to 10 (N=5), 30 (N=5), and 100μM (N=10) MFQ, respectively. (c) Effect of 10, 30, and 100μM MFQ perfusion on cells injected with Cx26-D50N, -A40V, -N14K, -G12R, -A88V, and -D50A. Bars represent the mean membrane current in the presence of the inhibitor as a percentage of the pre-drug value (N=5). Data are means ± SEM.

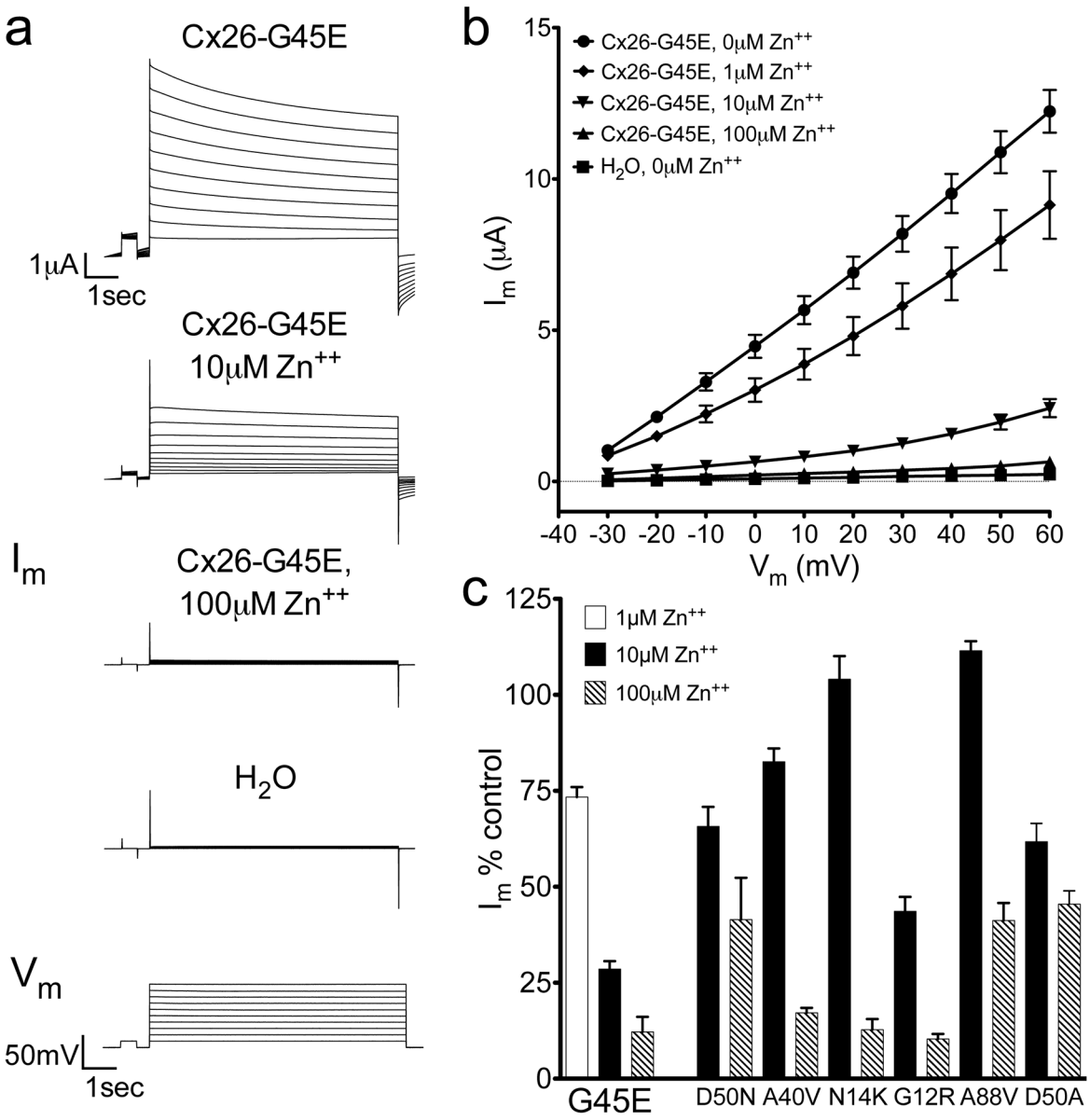

Figure 2-4. Extracellular zinc (Zn^{++}) reduced abnormal hemichannel activities associated with KID-causing Cx26 mutations in *Xenopus* oocytes. (a) Representative membrane current (I_m) traces corresponding to a single Cx26-G45E-expressing cell recorded in the presence of 0, 10, and 100μM Zn^{++}. An H_2O-injected control cell is shown for comparison. (b) Mean currents plotted against membrane potential (V_m) illustrated current-voltage relationships. Control cells showed negligible current (N=10). Whole-cell currents observed in Cx26-G45E oocytes (N=16) were inhibited by addition of 1 (N=5), 10 (N=5), and 100μM (N=5) Zn^{++} to the medium. (c) Concentration dependent effects of zinc perfusion in cells expressing Cx26-G45E, -D50N, -A40V, -N14K, -G12R, -A88V, and -D50A. Bars represent the mean current as a percentage of the pre-drug value for five cells. Data are means ± SEM.

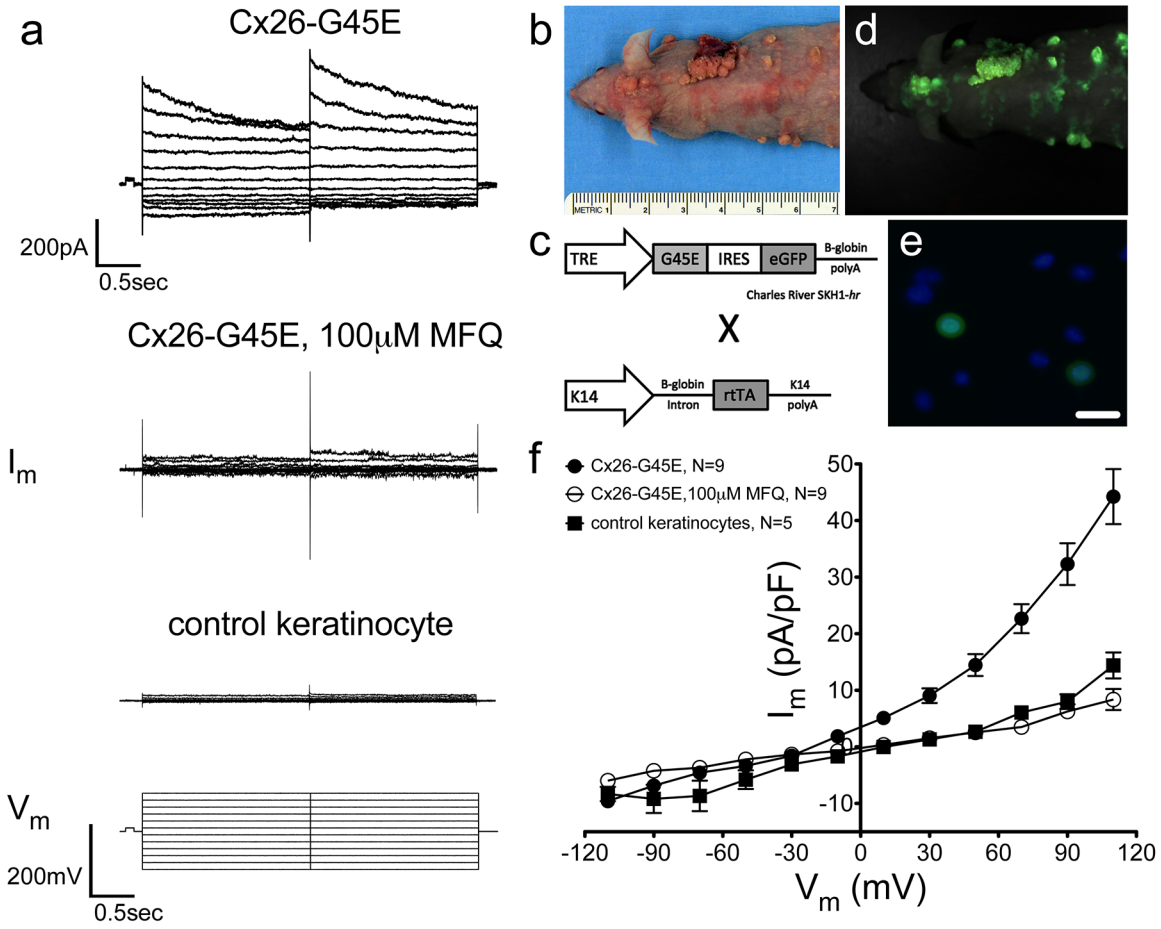

Figure 2-5. Mefloquine inhibited hemichannel activity in transgenic Cx26-G45E keratinocytes. (a) Whole-cell membrane currents (I_m) were recorded by patch clamp electrophysiology. Nominal currents were observed in control keratinocytes. Large macroscopic currents (I_m) were elicited from Cx26-G45E-expressing cells stepped to membrane potentials (V_m) between -110 and +110mV and were suppressed by 100μM mefloquine. (b-c) Cx26-G45E mice recapitulate the epidermal pathology of KID syndrome using inducible tissue-specific expression of Cx26-G45E and eGFP in a hairless background. (d) *In vivo* fluorescence imaging demonstrated spatial correlation of fluorescence with skin lesions. (e) Keratinocytes isolated from Cx26-G45E lesions retained eGFP expression, facilitating their identification for patch clamp electrophysiology (bar, 10μm). (f) Current density plotted against membrane potential (V_m) showed large macroscopic currents were elicited from Cx26-G45E cells (N=9) that were diminished by the addition of 100μM mefloquine (N=9) to levels resembling control cells (N=5). Data are means ± SEM.

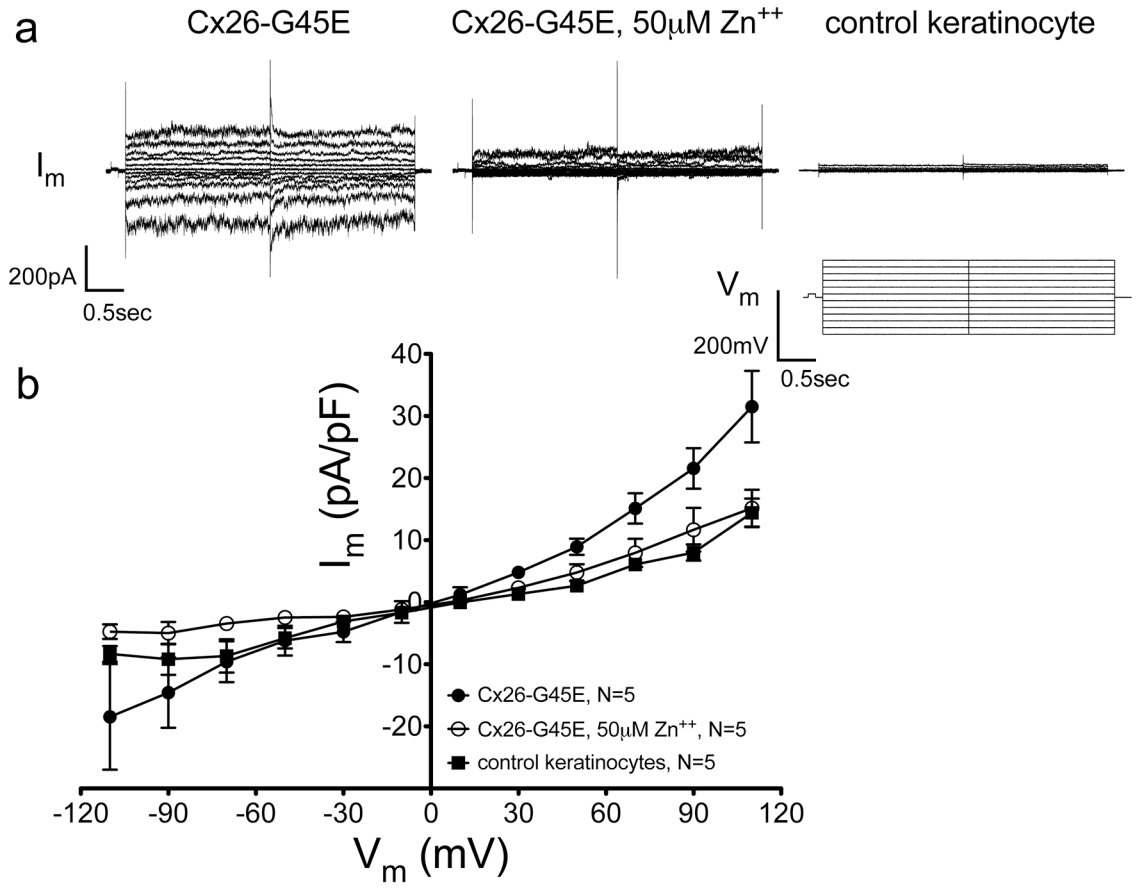

Figure 2-6. Zinc decreased hemichannel currents in transgenic Cx26-G45E keratinocytes. (a) Patch clamp recording of Cx26-G45E keratinocytes showed robust membrane currents (I_m) that were partially inhibited by supplementation of the bathing media with 50μM Zn^{++}. Keratinocytes isolated from control animals display modest whole-cell current flow for the same range in membrane potential (V_m). (b) Membrane current density was computed using cell capacitances to account for variations in cell sizes and plotted as a function of membrane potential. 50μM Zn^{++} effectively reduced hemichannel currents at both hyperpolarizing and depolarizing potentials. Data are means ± SEM for five single cells.

Chapter 3. Inhibition of lethal KID mutations Cx26-G45E and Cx26-A88V by broad-spectrum gap-junction inhibitors

ABSTRACT

Mutations in the human gene encoding connexin26 (Cx26 or *GJB2*) trigger a wide array of deafness and skin disease. The fact that disparate clinical disorders arise from mutations in the same gene implies that distinct channel activities influence homeostatic maintenance in the cochlea and epidermis. The majority of Cx26 mutations causing keratitis-ichthyosis-deafness (KID) syndrome display a functionally unifying increase in non-junctional hemichannel activation. This phenomenon has been particularly well defined for two mutations that are linked to a lethal form of KID syndrome, Cx26-G45E and Cx26-A88V. Recently, connexin modulators have drawn attention as research tools to complement knockout strategies in efforts to understand the functions of hemichannels in normal physiology as well as their alleged roles in disease. Furthermore, currently available connexin inhibitors may offer novel therapeutic prospects in cases of gain-of-function pathophysiology, as with KID syndrome. Here, we use two different electrophysiological assays to generate preliminary data showing that flufenamic acid (FFA) and carbenoxolone (CBX) effectively inhibit hemichannel currents induced by exogenous expression of human Cx26-G45E and Cx26-A88V.

INTRODUCTION

Connexins are ubiquitously expressed transmembrane proteins that organize into intercellular channel structures called gap junctions in vertebrate cells (Bruzzone *et al.*, 1996). Gap junctions electrically and metabolically couple cell networks and are important for the maintenance of tissue homeostasis as well as coordinated function. Certain connexin isoforms also function in a non-junctional configuration to mediate the diffusional exchange of ions and small metabolites with the extracellular compartment (Kar *et al.*, 2012). Mutations in connexin-encoding genes cause a wide variety of human hereditary diseases (Pfenniger *et al.*, 2011). Mutations in connexin26 (Cx26), an epidermal gap junction protein, lead to several clinically disparate disorders of keratinization including keratitis-ichthyosis-deafness syndrome (KID), palmoplantar keratoderma (PPK), bart pumphrey syndrome, and vohwinkel syndrome (Richard, 2005; Scott and Kelsell, 2011). Keratitis-ichthyosis-deafness (KID) syndrome is a rare form of syndromic deafness with heterogeneous cutaneous manifestations (de Zwart-Storm *et al.*, 2011; Skinner *et al.*, 1981).

At least 10 germline heterozygous missense mutations in Cx26 have been discovered following a clinical diagnosis of KID syndrome (Iossa *et al.*, 2011; Richard *et al.*, 2002). Cell-based assays have elucidated the influences of individual mutations on the functional status of the channels they form. KID-associated Cx26 mutations are entirely incongruent with regard to loss or retention of gap junctional conductance (Lee and White, 2009b). In contrast, of the tested KID-associated Cx26 mutations, a majority has been observed to form non-junctional hemichannels with abnormal activity (Donnelly *et al.*, 2012; Gerido *et al.*, 2007; Lee *et al.*, 2009; Levit *et al.*, 2012; Mhaske *et al.*, 2013; Montgomery *et al.*, 2004; Sanchez *et al.*, 2010; Stong *et al.*, 2006). Specifically, expression of Cx26-D50N, -G45E, -A88V, -D50A, -A40V, -N14K, and -G12R all induced excessive hemichannel fluxes that represent a significant departure from the wild-type channel behavior. Furthermore, several laboratories have now

demonstrated that unimpeded hemichannel openings and/or corruption of permeability properties result in cell damage and an increased rate of cell death (Berger *et al.*, 2014; Chi *et al.*, 2012; Donnelly *et al.*, 2012; Essenfelder *et al.*, 2004; Gerido *et al.*, 2007; Lee *et al.*, 2009; Stong *et al.*, 2006).

Fatal forms of KID syndrome have been described in patients with the Cx26-G45E and Cx26-A88V mutations (de Berker *et al.*, 1993; Haruna *et al.*, 2010; Janecke *et al.*, 2005; Jonard *et al.*, 2008; Koppelhus *et al.*, 2011; Sbidian *et al.*, 2010). Clinical findings include vascularizing corneal inflammation with compromised or absent visual acuity, profound bilateral sensorineural hearing loss, and progressive ichthyotic erythroderma with follicular hyperkeratosis and palmoplantar keratoderma. Variably present are dystrophic nails, photophobia, hypohidrosis, alopecia areata, and increased susceptibility to developing squamous cell carcinoma (Coggshall *et al.*, 2013; Grob *et al.*, 1987; Mazereeuw-Hautier *et al.*, 2007). The cutaneous disease expands throughout the neonatal period from discrete keratotic, psoriasiform and/or verrucous papules and plaques to diffuse, reticulated hyperkeratinization. Erosions and ulcerations undermine the barrier role of the skin, resulting in a primary immunodeficiency and recurrent mucocutanous infections with life threatening sequela (Coggshall *et al.*, 2013; Gilliam and Williams, 2002; Haruna *et al.*, 2010; Helm *et al.*, 1990; Jonard *et al.*, 2008; Koppelhus *et al.*, 2011; Sbidian *et al.*, 2010).

Cx26-G45E and Cx26-A88V display marked inflation of hemichannel activity for the range of voltages encompassing the physiological resting membrane potential of human keratinocytes (Gerido *et al.*, 2007; Mese *et al.*, 2011; Mhaske *et al.*, 2013; Sanchez *et al.*, 2010). Several mutations leading to milder clinical presentations, including the most commonly reported Cx26-D50N mutation (Wonkam *et al.*, 2013), are shown to induce hemichannel currents of substantially lower magnitudes (Lee *et al.*, 2009; Sanchez *et al.*, 2013). It has been proposed that individual amino acid substitutions alter the regulatory mechanisms of the Cx26 hemichannel voltage-gating

machinery in different ways (Sanchez *et al.*, 2010; Sanchez *et al.*, 2013). Moreoever, mutations that lead to severe disease phenotypes, such as Cx26-G45E and Cx26-A88V, are speculated to correlate with greater channel open probabilities and, consequently, higher membrane currents.

Cases of Cx26-G45E- and Cx26-A88V-related KID syndrome are infrequent. The few reported in the medical literature have invariably followed dismal clinical courses, leading to rapid decline and patient death in infancy (Haruna *et al.*, 2010; Jonard *et al.*, 2008; Koppelhus *et al.*, 2011; Sbidian *et al.*, 2010). Instances of KID syndrome presenting in conjunction with other mutations, such as Cx26-D50N, are generally regarded as having good prognosis for survival into adulthood (Kelly *et al.*, 2008; Titeux *et al.*, 2009; Wonkam *et al.*, 2013; Yotsumoto *et al.*, 2003). Pharmacological inhibitors with affinity for connexin26 hemichannels are needed to evaluate the putative relationship between the extent of aberrant membrane currents and the severity of epidermal pathology. Additionally, properly chosen hemichannel inhibitors may be considered for adjunct therapies in high-risk patients for whom early diagnosis is made and genetic analysis is available.

Efforts to develop novel connexin blockers with clinical value have been slow to progress. Identifying inhibitors with connexin-specific and isoform-selective action is labor-intensive in the absence of robust high-throughput screening technologies. Further challenges arise in isolating hemichannel-directed effects as well as testing disease-causing mutations individually. A few currently available broad-spectrum gap-junction inhibitor compounds have been safely administered to humans and tolerated for long-term therapy (Cao and Zheng, 2014; Garza, 2010; Mozsik *et al.*, 2011; Pinder *et al.*, 1976). Broad-acting agents are likely to have off-target activities on other proteins involved in membrane transport; however, adverse effects were in many cases minimal and/or manageable (Cao and Zheng, 2014; Garza, 2010; Mozsik *et al.*, 2011; Pinder *et al.*, 1976). Such compounds are desirable starting points for rational drug

discovery/design in connexin-associated gain-of-function disorders. We are pursuing preliminary functional studies with molecules for which a history of safety and pharmacokinetic data exist in the interest of reducing the time from bench to bedside. Here, we used two different electrophysiological assays to show that both flufenamic acid (FFA) and carbenoxolone disodium salt (CBX) are potent inhibitors of Cx26-G45E and Cx26-A88V hemichannels. These results suggest that these small molecules warrant consideration for local delivery to epidermal connexins in dire instances of KID syndrome where other treatment options fail.

RESULTS AND DISCUSSION

Flufenamic acid suppressed Cx26-G45E hemichannel activity

Flufenamic acid (FFA) is a non-steroidal anti-inflammatory drug (NSAID) with broad activities as a modulator of membrane channels (Guinamard *et al.*, 2013). To quickly determine whether Cx26-G45E hemichannels are sentitive to FFA application, we expressed the protein in *Xenopus* oocytes by microinjection of cRNAs and assayed membrane currents by voltage clamp electrophysiology. H_2O-injected cells showed negligible membrane currents (data not shown). Cx26-G45E-expressing cells exhibited large reproducible outward membrane currents that were squelched by the presence of 150μM FFA (Figure 3-1a). Overall, Cx26-G45E hemichannel currents were reduced by 81.7±6.54% (N=15) following 5 minutes of 150μM FFA perfusion (Figure 3-1b).

FFA is highly promiscuous with regard to its activity on ionic channels. It is known to inhibit numerous physiologically relevant non-selective cation channels, including connexin channels and most transient receptor potential (TRP) family channels, as well as calcium-activated chloride channels, and others (Guinamard *et al.*, 2013).

Additionally, it causes activation of two-pore outwardly rectifying potassium channels and sodium channels (Guinamard *et al.*, 2013). Effective concentrations are reported to be very variable across different channel types, stretching from low micromolar concentrations into the millimolar range (Guinamard *et al.*, 2013). FFA has been shown to uncouple Cx43 and Cx50 gap junctions in a pH-dependent manner by both dye measurement and electrophysiological techniques (Harks *et al.*, 2001; Skeberdis *et al.*, 2011; Srinivas and Spray, 2003). Half-maximal concentrations were determined to be between 20 and 60μM for both Cx43 and Cx50 (Harks *et al.*, 2001; Srinivas and Spray, 2003). Our data suggest that the half-maximal concentration corresponding to Cx26 would likely converge on this range as well. FFA is posited to act on connexins indirectly by binding to an adjacent modulatory site in the plasma membrane to influence channel conformation and, in turn, the open probability (Srinivas and Spray, 2003).

As with other NSAIDs, FFA possesses analgesic and anti-inflammatory properties through inhibition of cyclooxygenase-mediated prostaglandin synthesis. FFA has been used in clinical practice for local pain management in acute soft tissue injury and chronic musculoskeletal and joint disorders (Flower, 1974). The side effects associated with systemic distribution of NSAIDs, such as renal damage and gastrointestinal perturbations, are allayed by topical application and combination therapy (Moore *et al.*, 1998). Instances of allergic contact dermatitis have been reported in association with several currently favored topical NSAIDs such as diclofenac, etofenamate, and bufexamac, all of which are related to FFA through the fenamic acid parent structure (Barbaud, 2009). Interestingly, delayed contact hypersensitivity was found to be least common with FFA among 9 NSAIDs evaluated by patch testing in 371 patients with a previous diagnosis of contact allergy (Gniazdowska *et al.*, 1999). Moreover, fenamic acid derivatives have apparent cutaneous activity extending beyond immunologic involvement. Diclofenac is used to treat actinic keratosis as 3% diclofenac sodium gel and is tolerated for as long as 90 consecutive days (Dodds *et al.*, 2014). Bufexamac is formulated as a lotion or cream and used as an alternative to corticosteroids in subacute and chronic atopic dermatitis (Niedner and Iliev, 2001).

Our preliminary data support FFA as a molecule of interest in the context of fatal forms of KID syndrome. In fact, significant headway has been made with regard to incorporating FFA into efficient topical delivery vehicles for subgranular skin penetration (Rubio *et al.*, 2013; Wagner *et al.*, 2002). Given the plethora of connexins and other important membrane channels in the epidermis, a high degree of caution should be exercised if *in vivo* studies are attempted. Further cell-based work is needed to systematically detail the FFA dose-response characteristics for Cx26 hemichannels and to expound on the current appreciation of secondary effects. In theory, innocuously low doses of FFA may mitigate epidermal deterioration and improve chances of survival in aggressive forms of KID syndrome if capable of just modest reductions in Cx26-G45E hemichannel currents.

Carbenoxolone failed to inhibit Cx26-A88V hemichannels in *Xenopus* oocytes

Carbenoxolone is a synthetic derivative of the licorice root extract glycyrrhetinic acid recognized to widely inhibit membrane channels and receptors, including pannexin, innexin, and connexin hemichannels and gap junctions (Davidson *et al.*, 1986). CBX is not thought to differentiate between connexin subtypes although comprehensive studies are lacking (Verselis and Srinivas, 2013). We sought to examine the effects of CBX on Cx26-G45E and Cx26-A88V hemichannels, using *Xenopus* oocytes for convenience. As a readout of global hemichannel activity, whole-cell membrane current was recorded from single cells by voltage clamping at -40mV and applying a series of depolarizing transmembrane potentials (Figure 3-2, V_m). Negligible membrane currents were detectable in H_2O-injected oocytes for voltages spanning -30 to +60mV (Figure 3-2b). Cx26-A88V expression caused a 50-fold expansion of outward membrane current flow (Figure 3-2a). Recording in the presence of 50μM (Figure 3-2c) or 500μM (Figure 3-2d) CBX did not significantly alter Cx26-A88V hemichannel currents (<15% reduction), even when cells were exposed to drug for greater than 20 minutes (data not shown). As a

positive control, Cx26-A88V-expressing cells were recorded in media supplemented with 100μM Zn^{++}, which resulted in >90% suppression of membrane current (Figure 3-2e). Each cell was exposed to a single drug concentration.

The *Xenopus* oocyte expression system constitutes a convenient means of assaying macroscopic membrane currents in a communication deficient background. Additionally, an abundance of data in the literature enables comparative analysis of results. Previously, we demonstrated that oocyte electrophysiology lends itself to quick and quantitative screening of inhibitors with presumed mutant or wild-type channel affinity to qualify candidates for further testing. However, oocytes may not provide a meaningful experimental platform in cases of highly lipophilic molecules. This is because fatty yolk granules in stage V-VI oocytes may cytoplasmically corral drugs to obscure effects that would otherwise be apparent in mammalian cell systems.

Carbenoxolone reduced Cx26-A88V and Cx26-G45E hemichannel currents with differential kinetics in HeLa cells

Given the unanimity of previous findings supporting carbenoxolone as a universal inhibitor of connexins (Juszczak and Swiergiel, 2009), we chose to test the drug in another experimental system. We transiently transfected HeLa cells with either Cx26-A88V or Cx26-G45E and measured membrane currents and channel conductance by whole-cell patch clamp electrophysiology (Figure 3-3). Untransfected HeLa cells displayed minimal membrane currents (Figure 3-3h) when stepped to membrane potentials between -110 and +110mV (Figure 3-3i, V_m). Membrane currents recorded from HeLa cells transfected with either Cx26-A88V (Figure 3-3a) or Cx26-G45E (Figure 3-3d) were robust at both hyperpolarizing and depolarizing potentials. Large membrane currents in cells expressing Cx26-A88V were suppressed by 50μM CBX with slow inhibitory kinetics (Figure 3-3, a-c). Specifically, Cx26-A88V membrane current

magnitudes were reduced by roughly 50% and 90% after 3 minutes (Figure 3-3b) and 10 minutes (Figure 3-3c) of drug exposure respectively. Cx26-G45E-associated membrane currents were similarly inhibited but with accelerated response kinetics (Figure 3-3, d-f). 90 seconds of drug exposure (Figure 3-3e) were sufficient to reduce the starting Cx26-G45E membrane current (Figure 3-3d) by roughly half. Approximately 15% of the Cx26-G45E membrane current remained after 3 minutes of 50μM CBX application (Figure 3-3f). In some cells, the activity of single Cx26-G45E hemichannels could be resolved (Figure 3-3j). In our sample trace, hemichannels had a unitary conductance value of ~300pS at a membrane potential of +110mV measured in 120mM potassium aspartate. This finding is in fair agreement with other recently reported human Cx26 hemichannel data (Mese *et al.*, 2011; Sanchez *et al.*, 2010).

Though our data are admittedly preliminary, they are supported by published studies of carbenoxolone-mediated inhibition of Cx26 and Cx43 channels (Brokamp *et al.*, 2012; Donnelly *et al.*, 2012; Spray *et al.*, 2002; Wang *et al.*, 2012). As with our Cx26 hemichannel data, carbenoxolone was observed to inactivate Cx43 gap junctions with unusually slow kinetics, requiring up to 15 minutes for the steady-state effect (Spray *et al.*, 2002; Wang *et al.*, 2012). The sluggish response times cast doubt on the plausibility of direct inhibitor actions (Verselis and Srinivas, 2013). It is possible that CBX acts indirectly through cytoplasmic intermediate molecules and/or membrane-delimited pathways and/or by stimulating channel internalization and protein turnover. Also similar to our finding, connexin channel inhibition by carbenoxolone was previously documented to be incomplete, even at high concentrations (Verselis and Srinivas, 2013). This characteristic was particularly evident for Cx43 (Wang *et al.*, 2012), which is abundantly expressed in the epidermis and elsewhere. Retention of basal channel activity despite CBX application may minimize untoward effects when targeting complex tissues by preserving homeostatic functions.

Carbenoxolone has been branded a ‘dirty’ drug (Connors, 2012) due to its imprecise targeting of diverse ion channels, receptors, and transporters. CBX inhibits calcium channels and purinergic receptors at concentrations near or below those that affect connexin channels (Bruzzone *et al.*, 2005; Suadicani *et al.*, 2006; Verselis and Srinivas, 2013; Vessey *et al.*, 2004). Furthermore, CBX has been shown to have direct effects on GABA receptors, which are prominent in CNS tissue (Beaumont and Maccaferri, 2011). CBX activities are known to have significant neurophysiological upshots, including a reduction in excitatory and inhibitory synaptic currents, alteration of intrinsic membrane properties, and suppression of action potentials (Rekling *et al.*, 2000; Rouach *et al.*, 2003; Tovar *et al.*, 2009; Verselis and Srinivas, 2013). However, CBX was undetectable by high performance liquid chromatography in the cerebrospinal fluid of intraperitoneally injected rats, suggesting that it is unable to cross the blood-brain barrier (Leshchenko *et al.*, 2006).

Carbenoxolone is presently licensed in the United Kingdom to treat reflux esophagitis and gastric ulceration (Mozsik *et al.*, 2011; Paschon *et al.*, 2012; Pinder *et al.*, 1976). Anti-inflammatory and cytoprotective effects conferred to the gastrointestinal mucosa by CBX were discovered in the 1960s (Goodier *et al.*, 1967). Adverse effects associated with systemic CBX are described as mineralocorticoid-like and include increased insulin sensitivity, hypokalemia, fluid retention, and hypertension (Andrews *et al.*, 2003; Pinder *et al.*, 1976). Topical formulations are under development to circumvent undesirable multi-organ reactions (Hirata *et al.*, 2013; Puglia *et al.*, 2013). Remarkably, the parent molecule glycyrrhetinic acid has risen in popularity in dermatologic practice over the past decade for topical relief of chronic recurrent seborrheic dermatitis and pruritic symptoms accompanying atopic dermatitis (Boguniewicz *et al.*, 2008; Silverberg, 2014; Turlier *et al.*, 2014; Veraldi *et al.*, 2009).

Our data indicate that CBX merits further attention as a inhibitor of mutated Cx26 hemichannels implicated in KID syndrome. Aberrant hemichannel activity is a shared

feature among the majority of Cx26 mutations causing KID syndrome and is hypothesized to mechanistically account for the development of skin problems (Donnelly *et al.*, 2012; Gerido *et al.*, 2007; Lee *et al.*, 2009; Levit *et al.*, 2012; Mhaske *et al.*, 2013; Montgomery *et al.*, 2004; Sanchez *et al.*, 2010; Stong *et al.*, 2006). Mutations that cause greater current leakage through hemichannels are alleged to provoke more severe skin phenotypes, but this has been difficult to establish due to the very small number of reported cases. Cx26-G45E and Cx26-A88V form hemichannels that pass massive currents and both mutations have resulted in lethal forms of KID syndrome, without exception (de Berker *et al.*, 1993; Gerido *et al.*, 2007; Haruna *et al.*, 2010; Janecke *et al.*, 2005; Jonard *et al.*, 2008; Koppelhus *et al.*, 2011; Mhaske *et al.*, 2013; Sanchez *et al.*, 2010; Sbidian *et al.*, 2010). This idea is further supported by biophysical analysis showing high Cx26-G45E hemichannel activity in primary keratinocytes derived from transgenic mice expressing this mutation, and these animals also developed lethal epidermal pathology (Mese *et al.*, 2011). Still, the clinical heterogeneity of KID syndrome has precluded meaningful genotype-phenotype correlations. Recently, a lethal occurrence of KID syndrome with the Cx26-S17F mutation was reported (Mazereeuw-Hautier *et al.*, 2014). This was unexpected because cells expressing Cx26-S17F have been shown to be deficient of both gap-junction and hemichannel functionality (Lee *et al.*, 2009; Richard *et al.*, 2002) and a mouse model based on conditional expression of Cx26-S17F under control of the endogenous Cx26 promoter produced only mild focal skin abnormalities in surviving pups (Schutz *et al.*, 2011).

Increased hemichannel activity has similarly been proposed as a pathogenic nexus between connexin31 (Cx31, *GJB3*) and connexin30 (Cx30, *GJB6*) mutations and their corresponding skin disorders. For example, the Cx31-R42P mutations associated with erythrokeratoderma variabilis was shown to form constitutively active hemichannels. Expression of Cx31-R42P in HeLa cells facilitated enchanced dye uptake and caused necrotic cell death, both of which could be prevented by treatment with a connexin channel inhibitor or increased extracellular calcium (Chi *et al.*, 2012). Two Cx30 mutations, Cx30-G11R and Cx30-A88V, linked to hidrotic ectodermal

dyplasia (Clouston syndrome) were reported to induce large voltage-activated currents resulting in cell death when expressed in *Xenopus* oocytes (Common *et al.*, 2002; Essenfelder *et al.*, 2004). HeLa cells transfected with either Cx30-G11R or Cx30-A88V released ATP into the extracellular milieu, presumable through porous hemichannels. Complicating matters is a loss-of-function mutation, Cx30-V37E, which produces a clinical constellation mimicking that of mild KID syndrome (Jan *et al.*, 2004). Cx30-V37E did not appear on the plasma membrane when ectopically expressed in rat epidermal keratinocytes but remained confined to intracellular compartments associated with endoplasmic reticulum resident proteins (Berger *et al.*, 2014).

In summary, the extent to which increased connexin hemichannel currents contribute to keratinocyte apoptosis and epidermal pathologies is presently unclear. The appropriate experimental use of reagents such as flufenamic acid and carbenoxolone to temper excessive hemichannel currents in cell viability and animal studies will be informative. Here, we presented preliminary evidence supporting their use with lethal KID mutations Cx26-G45E and Cx26-A88V. As an added benefit, these molecules derive from classes of drugs familiar to dermatologic practice and have established records of safe use in human patients, perhaps facilitating their adaptation to clinical applications as last-resort therapies upon validation.

MATERIALS AND METHODS

Molecular cloning

Human mutant Cx26 coding sequences were cloned into the *Bam*HI restriction site of the pCS2+ expression vector (Turner and Weintraub, 1994) for functional assays in *Xenopus laevis* oocytes. Cx26-G45E and Cx26-A88V were prepared from the wild-type template by site-directed mutagenesis using overlap extension PCR (Horton *et al.*, 1990) as previously described (Gerido *et al.*, 2007; Mhaske *et al.*, 2013). Following amplification, Cx26-G45E and Cx26-A88V were first cloned into pBluescript II (Agilent Technologies, Santa Clara, CA) and sequenced on both strands before subcloning into the pCS2+ vector for *Xenopus* expression or the pIRES2-EGFP2 vector (Clontech Laboratories, Mountain View, CA) for mammalian cell transfection.

In vitro transcription and oocyte microinjection

Plasmid DNAs were linearized by NotI digestion and transcribed using the SP6 mMessage mMachine (Ambion, Austin, TX) to yield cRNAs. The Stony Brook University IACUC approved a protocol for oocyte removal from *Xenopus laevis*. Adult females were anesthetized with ethyl 3-aminobenzoate methanesulfonate and ovarian lobes were surgically excised. Oocyte lobes were digested in 7.5mg/mL collagenase B and 5.0mg/mL hyaluronidase in modified Barth's (MB) medium without Ca^{++} for 15 minutes at 37°C with constant shaking. Stage V-VI oocytes were separated and injected with 10ng of an antisense morpholino oligonucleotide to the endogenous connexin38 (Barrio *et al.*, 1991; Bruzzone *et al.*, 1993). Oocytes were next injected with wild-type Cx26, Cx26-G45E, -D50N, -A40V, -A88V, -G12R, -D50A, -N14K cRNA transcripts or H_2O as a

negative control and cultured in MB media supplemented with 4mM $CaCl_2$ for 15-18 hours before electrophysiological assay.

Inhibitory drugs

Flufenamic acid (FFA) and Carbenoxolone disodium salt (CBX) were acquired from Sigma-Aldrich (St. Louis, MO). FFA was solubilized in dimethyl sulfoxide (DMSO) at a stock concentration of 100mM and stored at -20°C. CBX was solubilized in water and stored at room temperature for up to 2 weeks.

Voltage clamp recording of hemichannel currents

Macroscopic recordings of hemichannel currents were acquired from single *Xenopus* oocytes using a GeneClamp 500 amplifier controlled by a PC-compatible computer through a Digidata 1440A interface (Axon instruments, Foster City, CA). Stimulus and data collection paradigms were programmed with pClamp 10.2 software (Axon Instruments). Current and voltage electrodes (1.5mm diameter glass, World Precision Instruments, Sarasota, FL) were pulled to a resistance of 1-2MΩ on a vertical puller (Narishige, Tokyo, Japan) and filled with a conducting solution containing 3M KCl, 10mM EGTA, and 10mM HEPES pH 7.4. Whole-cell current traces were obtained by clamping at -40mV and applying 8 second depolarizing pulses spanning -30mV to +60mV in 10mV increments (Lee *et al.*, 2009). To test inhibitor effects, dishes were perfused with Ca^{++}-free media supplemented with small molecules of interest after the initial series of current recordings. Re-recording of hemichannel currents was performed within 60 seconds of each media exchange. Inhibitor compounds were additionally tested during a 100-sweep series of 5 second +50mV depolarizations from the -40mV holding potential over a 10 minute experimental duration. Recordings were initiated by

active gravity-fed perfusion with MB medium lacking Ca^{++} for a 20-pulse period to ensure minimal clamp leakage and stability of the steady state membrane current. Small molecule inhibitors were then introduced using a three-way valve to rapidly exchange bathing solutions in a custom 0.5mL chamber. Instantaneous whole-cell membrane current corresponding to each voltage pulse was extracted from raw data and plotted as a function of time.

Human cell transfection

Communication deficient HeLa cells were plated on 22-mm^2 coverslips, grown to 50% confluence, and transiently transfected with Cx26-G45E or Cx26-A88V in pIRES2-EGFP2 using and 10µg DNA lipofectamine 2000 according to the manufacturer's protocol (Invitrogen, Carlsbad, CA) as previously described (Mese *et al.*, 2011; Mhaske *et al.*, 2013). Calcium concentrations in the tissue culture media were elevated to a final concentration of 4mM with supplemental $CaCl_2$ and 18-24 hours were allowed for protein expression before electrophysiological assay.

Patch clamp recording of hemichannel currents

Transiently transfected HeLa cells were used for whole-cell patch clamp at room temperature as previously described (Mese *et al.*, 2011; Mhaske *et al.*, 2013). Cells on 22mm2 glass coverslips were immersed in a calcium-free Tyrode's solution containing 137.7mM NaCl, 5.4mM KCl, 2.3mM NaOH, 1mM $MgCl_2$, 2mM $CsCl_2$, 4mM $BaCl_2$, 10mM glucose, and 5mM HEPES (pH 7.4). Patch pipettes were pulled from glass capillaries with a horizontal puller (Sutter Instruments, Novato, CA) and filled with a conducting solution containing 120mmol/L K aspartate, 5mM HEPES, 10mM ethylene glycol tetraacetic acid, and 3mM NaATP (pH 7.2). To begin each experiment, cells were

clamped at 0mV and subsequently stepped for 2 second intervals to voltages ranging from -110mV to +110mV in 20mV increments. To test small molecule inhibitor effects, dishes were perfused with media supplemented with 50μM CBX and re-recorded within 30-90 seconds of media exchange.

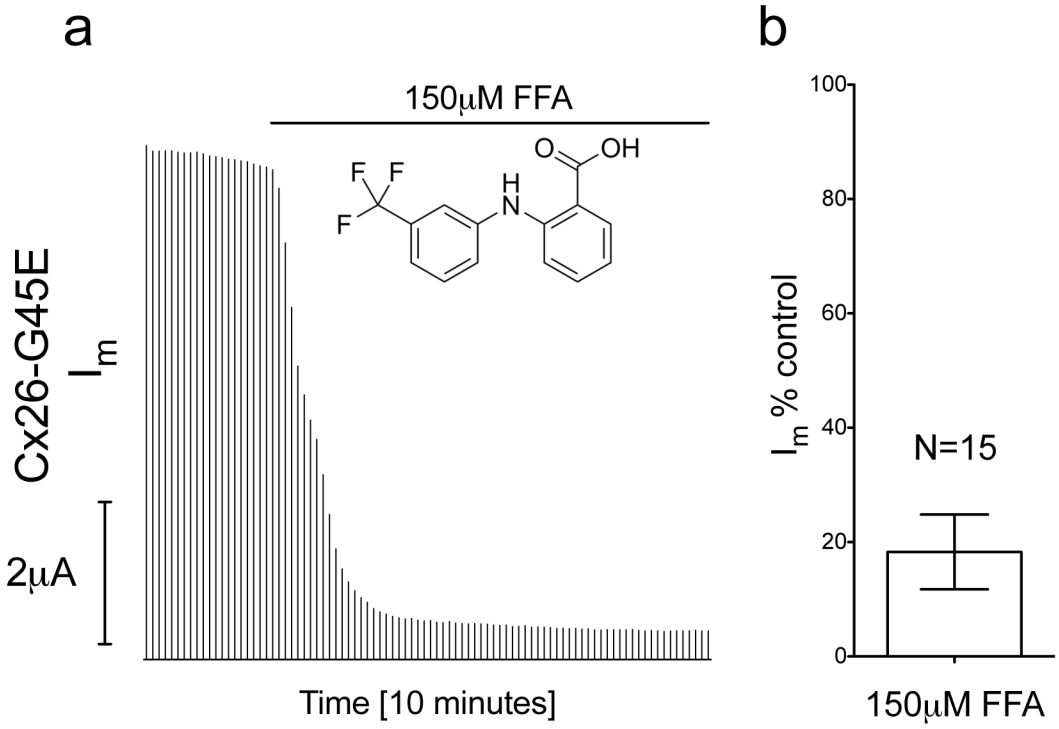

Figure 3-1. Flufenamic acid (FFA) inhibited Cx26-G45E hemichannels expressed in *Xenopus* oocytes. (a) Single cells at the -40mV holding potential were repeatedly pulsed with +50mV depolarizations and instantaneous membrane current (I_m) was measured. Cells were perfused with 150μM FFA after a 2 minute control period with modified barth's media lacking calcium. (b) Data is summarized as the mean residual instantaneous membrane current during drug application as a percentage of the control (pre-drug) magnitude, for 15 cells. 150μM FFA produced >80% reduction of Cx26-G45E membrane currents. Data are the means ± SD.

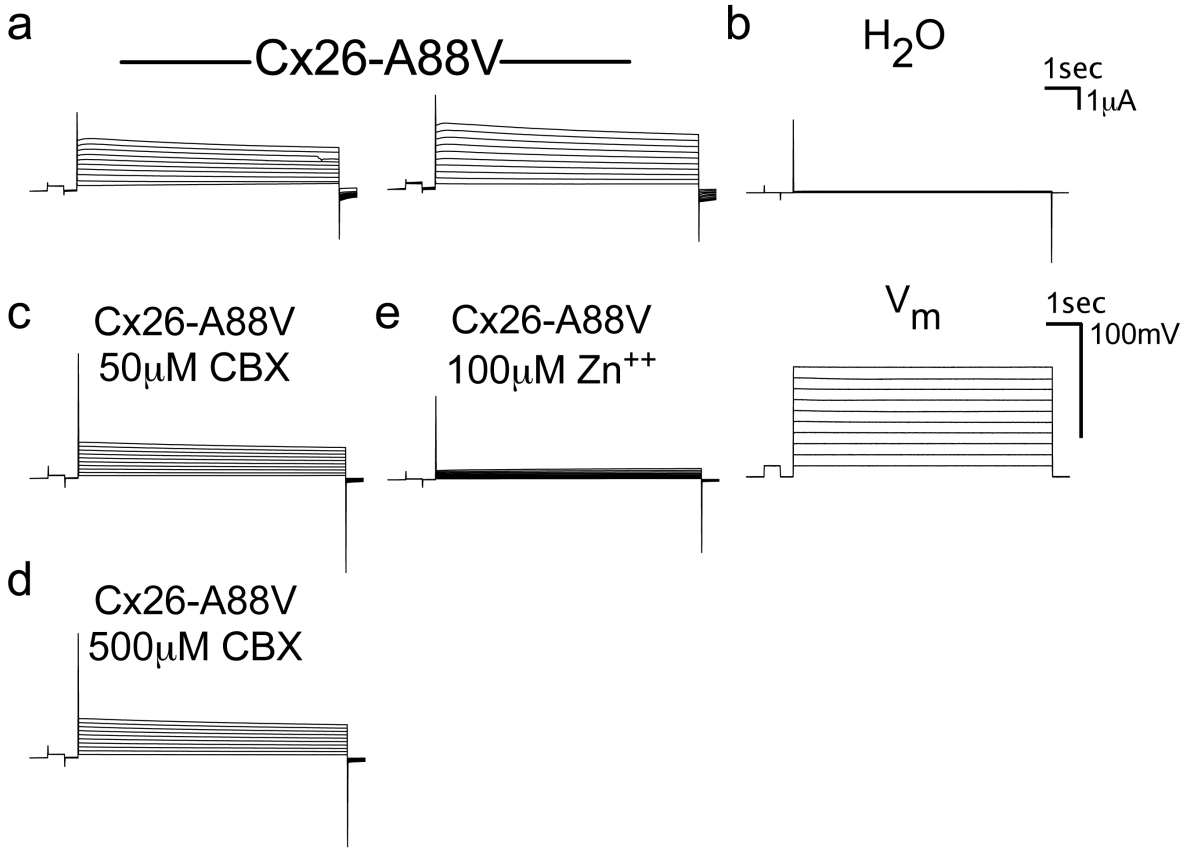

Figure 3-2. Carbenoxolone (CBX) failed to suppress Cx26-A88V hemichannel currents in *Xenopus* oocytes. Single cells were clamped at -40mV and subjected to voltage pulses spanning -30 to +60mV in 10mV steps (V_m). (a) Cx26-A88V-injected cells recorded in calcium-free media displayed large outward hemichannel currents whereas (b) whole-cell membrane currents were absent from H_2O-injected cells. Recording in the presence of either (c) 50 or (d) 500μM CBX did not significantly modulate Cx26-A88V hemichannel currents. (e) 100μM Zn^{++} produced sharp reduction of Cx26-A88V membrane currents when added to the bathing solution as a positive control.

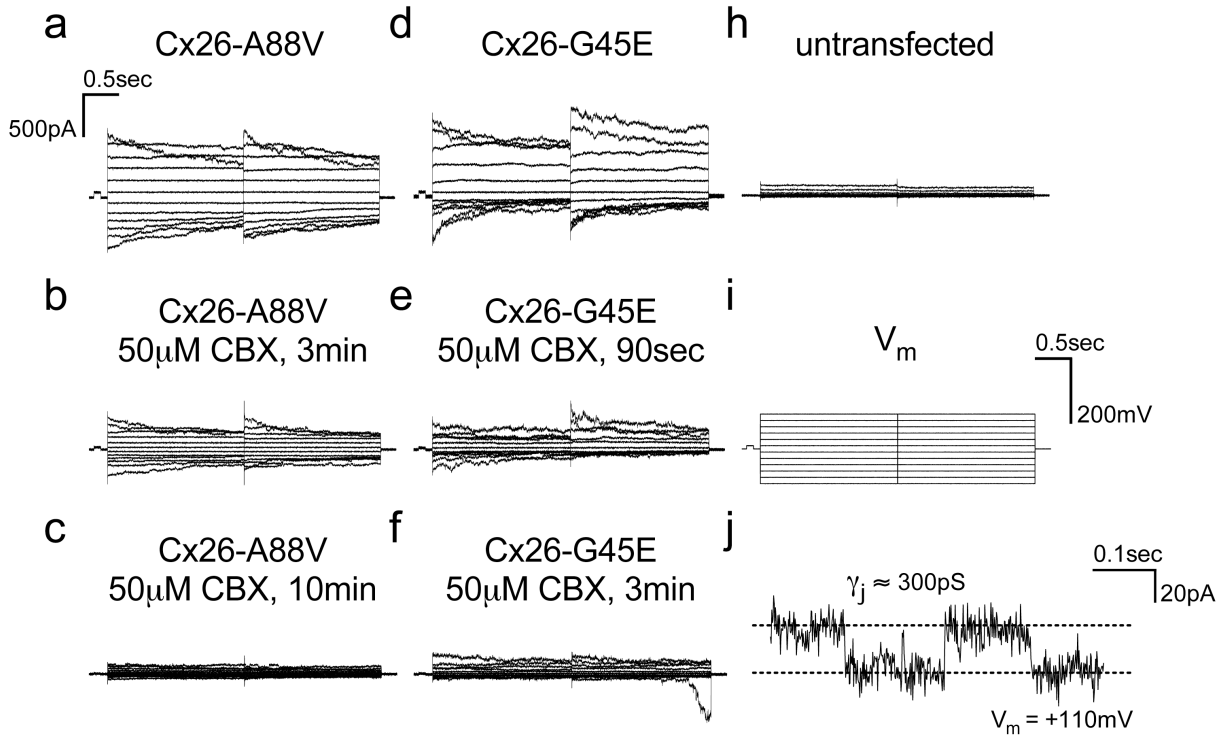

Figure 3-3. Carbenoxolone (CBX) inhibited large hemichannel currents induced by Cx26-A88V and Cx26-G45E expression in HeLa cells. Representative macroscopic membrane current traces obtained by patch clamp are shown for three cells (a-c, d-f, h) stepped to (i) membrane potentials (V_m) between -110 and +110mV. (h) Untransfected HeLa cells showed minimal membrane currents. HeLa cells transfected with (a) Cx26-A88V and (d) Cx26-G45E displayed large whole-cell membrane currents, both at hyperpolarizing and depolarizing membrane potentials. 50μM CBX caused >50% suppression of membrane currents after (b) 3 minutes of application for Cx26-A88V-expressing cells and (e) 90 seconds for Cx26-G45E-expressing cells. Membrane currents were diminished by >85% following extended bathing in the drug-containing media, (c) 10 minutes for Cx26-A88V and (f) 3 minutes for Cx26-G45E. (j) Single-channel activity was observed in Cx26-G45E-transfected HeLa cells with a unitary conductance (γ_j) value of ~300pS, consistent with the size expected for a Cx26 hemichannel.

Chapter 4. Concluding remarks and future directions: Initiating a paradigm for *in vivo* testing of hemichannel inhibitors in a mouse model of KID syndrome

The connexins are a multi-gene family of integral membrane proteins that are dynamically and pervasively expressed throughout the body. In vertebrate cells, connexin hexamers form large and highly specialized aqueous pores called hemichannels that become the structural constituents of gap junctions (Goodenough and Paul, 2009). Hemichannels on the surfaces of neighboring cells align in head-to-head fashion, producing a pathway for direct diffusional exchange of cytoplasmic molecules and ions (Jiang and Gu, 2005). Only recently were non-junctional hemichannels recognized to function (DeVries and Schwartz, 1992; Paul *et al.*, 1991) as physiologically relevant conduits enabling communication via the extracellular space (Chandrasekhar and Bera, 2012; Evans *et al.*, 2006; Goodenough and Paul, 2003; Stout *et al.*, 2004). Tissues express connexin subtypes in specific spatial and temporal patterns according to developmental and functional requirements for electrical and metabolic coupling (Sohl and Willecke, 2003). Different channel compositions show unique permeability and regulation (Bedner *et al.*, 2006; Goldberg *et al.*, 1999; Niessen *et al.*, 2000; Weber *et al.*, 2004). Mutations resulting in a loss or alteration of controlled connexin functions have the capacity to disturb cellular homeostasis and cause human disease (Wei *et al.*, 2004).

Connexin26 function is essential in the inner ear, where it promotes appropriate cochlear potassium recycling (Xu and Nicholson, 2013). Connexin26 additionally resides in the deeper layers of the epidermis, although its native role in the skin is ambiguous because loss of function mutations do not appreciably affect this organ (Di *et al.*, 2001b). Connexin26 mutations leading to skin disorders are thought to do so by producing functionally aberrant channels that dominate over the wild-type behavior (Lai-Cheong *et al.*, 2007; Richard, 2005). This dissertation focused on mutations leading to

keratitis-ichthyosis-deafness syndrome for which high conductance hemichannels appear to be a unifying pathological mechanism (Donnelly *et al.*, 2012; Gerido *et al.*, 2007; Lee *et al.*, 2009; Montgomery *et al.*, 2004; Sanchez *et al.*, 2010; Stong *et al.*, 2006). These distinct connexin26 missense mutations, the majority of which occur sporadically, result in varying degrees of skin barrier insufficiency (Mazereeuw-Hautier *et al.*, 2007). KID mutations are concentrated in the amino-terminus (NT), first transmembrane domain (TM1), and first extracellular loop (E1), with the exception of Cx26-A88V, which appears in the second transmembrane domain (TM2). It is likely that gains in hemichannel activity observed with individual mutations reflect different ways by which flow through the pore can become unrestricted. From the limited available structure-function data relating to connexin26, we are able to postulate three general modes of channel dysregulation in KID syndrome:

1. Amino acid substitutions in E1 may interfere with binding of factors that either regulate the activation of loop gating or stabilize the closed channel conformation (Tang *et al.*, 2009; Verselis and Srinivas, 2008; Verselis *et al.*, 2009).

2. Mutations of pore-lining residues (Kronengold *et al.*, 2003; Sanchez *et al.*, 2010) may modify bulk or charge of side chains to decrease resistance, particularly in narrowed regions of the channel funnel (Maeda *et al.*, 2009).

3. NT mutations may change the density or morphology of a ‘plug’ structure, which is predicted to fold into the cytomplasmic vestibule to line the channel mouth with charged α-helices as a participant in voltage-gating (Kronengold *et al.*, 2012; Oshima *et al.*, 2008; Purnick *et al.*, 2000). Additionally, NT mutations may prevent proper interactions between the protein N-terminus and cytoplasmic loop that appear to influence junctional currents (Oh *et al.*, 1999).

Nevertheless, leaky hemichannels are assumed to negatively impact cell viability irrespective of the precise details surrounding errors in regulation.

In this dissertation, we advocated for the use of pharmacological devices to clarify the consequences of expanded Cx26 hemichannel activity. We have experimentally substantiated the utility of select small molecule inhibitors for pursuing future phenotypic rescue studies in cellular and animal models of KID syndrome. Importantly, these compounds may be effective in probing for therapeutic targets or alternatively may distinguish bystander effects of mutations that are irrelevant to pathogenesis. The availability of an inducible transgenic mouse expressing human Cx26-G45E in a tissue-specific manner (Mese *et al.*, 2011) will enable powerful examination of mutant hemichannel activities during epidermal differentiation. Moreover, the topical accessibility of connexin-expressing keratinocytes facilitates *in vivo* testing of inhibitor effects in this system.

Transgenic expression of Cx26-G45E in basal keratinocytes perturbs the balance between proliferation and differentiation processes to undermine normal epidermal cornification and turnover (Blanpain and Fuchs, 2009; Mese *et al.*, 2011). We induced young doubly transgenic TRE-G45E plus K14-rtTA hairless (SKH1) mice for 8 weeks and found that epidermal lesions reflected a continuum of pathology including, as expected, erythrokeratoderma and scaling (Figure 4-1, top). Histological analysis showed changes consistent with epidermal acanthosis, papillomatosis, and hyperkeratosis (Figure 4-1, bottom) that are characteristic of the human disease (Sbidian *et al.*, 2010). The genetic design employed a bicistronic expression vector with eGFP downstream of the Cx26-G45E coding sequence and an intervening internal ribosome entry site (IRES) element. This allowed for tracking of epidermal thickening by whole-animal *in vivo* fluorescence imaging (Figure 4-2). eGFP signal intensity, easily detectable in superficially located cells, directly correlated with lesion severity because hyperplasia results in additive fluorescence along the z-axis. Skin abnormalities in these animals appeared within 5-7 days of induction and could be reversed by withdrawal of the induction agent, as evidenced by disappearance of eGFP and regression of skin pathology (Figure 4-2). Our preliminary characterization suggests that this model lends itself to pharmacological trials in either prevention or intervention paradigms.

Drug delivery to the epidermis requires proper formulation to balance cutaneous penetration and retention. In general, molecules of higher lipophilicity better penetrate the hydrophobic lipid envelope formed by lamellar bodies at the interface between the stratum corneum and stratum granulosum. In KID syndrome and other ichthyosiform disorders, this barrier is progressively lost and patients suffer accelerated trans-epidermal water loss that exacerbates scaling (Tomita *et al.*, 2005). More problematic is a vulnerability to infectious organisms that enter by way of the large body surface area, overburden the naïve infant immune system, and result in septic complications (Coggshall *et al.*, 2013; Gilliam and Williams, 2002; Haruna *et al.*, 2010; Jonard *et al.*, 2008; Koppelhus *et al.*, 2011; Sbidian *et al.*, 2010). Therapeutic strategies should aim to restore epidermal barrier integrity before such an extent of disease is reached.

Microemulsion vehicles accommodate delivery of either lipophilic or hydrophilic drugs and are shown to enhance topical penetration relative to single-phase solvents (Lawrence, 1994; Lawrence and Rees, 2000; Lopes, 2014; Pepe *et al.*, 2012). Microemulsions are clear, thermodynamically stable, liquid nanocarriers that spontaneously form upon appropriate mixing of oil, water, and surfactant(s). The incorporation of drugs with moderate water solubility into an aqueous phase and subsequent dispersal as small droplets (<150nm) into an easily absorbed oily package is a popular approach (Dogrul *et al.*, 2014; Sasivimolphan *et al.*, 2012; Tenjarla, 1999). We formulated a test water-in-oil microemulsion containing a fluorescent tracer, Lucifer yellow, and topically applied it liberally to the left dorsal flank of an individually caged control SKH1 mouse under inhalational anesthesia (Figure 4-3a). *In vivo* fluorescence imaging showed dye retention 24 hours post-application. Lower amounts of dye were apparent on the most caudal aspects of the back beginning 6 hours post-application and disordered contralateral spreading was visible at later time points. These changes presumably reflected animal grooming behaviors and highlight practical considerations in constructing treatment protocols for rodents. Frozen sections of the left shoulder skin showed typical healthy epidermal architecture for the hairless strain after application of

the microemulsion for two consecutive days (Figure 4-3b). Fluorescence microscopy localized the bulk of Lucifer yellow to the dermis and subcutaneous tissue with only trace amounts appearing in the epidermis (Figure 4-3c). This result suggests that proper adjustment of the microemulsion components and/or ratios is needed to curtail transdermal passage while maintaining penetration properties. Typically, small deposits of drug are well retained in the avascular epidermis with a slow rate of clearance. Enduring drug presence should enable less frequent and lower dosing to minimize secondary effects and exposures to surfactants that may be irritants.

The strategic use of inhibitors may be helpful in addressing outstanding questions related to the few KID mutations that appear to be functionally null, such as Cx26-S17F. Traditionally, constitutive hemichannel activation has been thought to derail keratinocyte differentiation by corrupting the trans-epidermal extracellular calcium gradient (Mauro *et al.*, 1993; Proksch *et al.*, 2008; Reiss *et al.*, 1991). It is now abundantly clear that connexin channels allow transport of a host of additional important primary signaling molecules and second messengers such as cyclic nucleotides (Kanaporis *et al.*, 2008), ATP (Cotrina *et al.*, 1998; Kang *et al.*, 2008), glutamate (Ye *et al.*, 2003), NAD^+ (Bruzzone *et al.*, 2001), and prostaglandins (Jiang and Cherian, 2003), not all of which are detected by standard electrophysiological methods. Cx26-S17F was observed to form typical punctate plaques at cell-cell contacts when expressed in HeLa cells (Richard *et al.*, 2002). Dye-based methods or the use of reporter genes with sensitivity for evaluating changes in the permselectivity profiles of these channels may bare yet unnoticed functional disturbances. Patch pipette techniques may be used for quantitation of hypothetical differential selectivity phenomena. We further hypothesize that mutations in other connexin-encoding genes, such as Cx30 and Cx43, may affect the permselectivity properties of heteromeric channels in instances of co-localization and co-oligomerization to partially explain the apparent genetic heterogeneity of KID-like phenotypes (Berger *et al.*, 2014; Jan *et al.*, 2004; Richard *et al.*, 2002).

The clinical approach to KID syndrome currently centers on aggressive management of persistent bacterial and mycotic infections with systemic antibiotics and bleach baths. Skincare is empirically adjusted and often includes a combination of barrier creams, emollients, and keratolytics with or without topical and/or systemic retinoids (Abdollahi *et al.*, 2007; Braun-Falco, 2009; Richard, 2005). Retinoic acid use is intended to advance the stalled desquamation process in hyperkeratotic skin but there is evidence to suggest that it may in fact aggravate the underlying pathophysiology in KID syndrome. Retinoic acid has been shown to induce dramatic upregulation of Cx26 in human epidermis, at both the transcript and protein level, to an extent that was not paralleled by other connexins (Masgrau-Peya *et al.*, 1997). Heightened expression of Cx26 in KID syndrome would be expected to amplify mutation-driven injurious effects. This example emphatically underscores the need for targeted therapies in genodermatoses.

Proof-of-principle *in vivo* studies are needed to validate the putative therapeutic value of targeting connexins. Broad-spectrum connexin inhibitors, such as flufenamic acid and carbenoxolone, may provide a reasonable stepping-stone toward molecularly directed therapies. Existing connexin-inhibitor compounds with a history of safe use and for which a rational, basic science evidence-based, justification of novel applicability can be made are of particular interest in urgent manifestations of KID syndrome. Along this vein, a handful of connexin modulators are currently in pharmaceutical development that may be worthwhile to test on disease-causing connexin26 mutants. For instance, Tonabersat is a benzopyran capable of impeding cortical spreading depression mediated by neuronal-glial gap-junctions and well tolerated for chronic prophylaxis of migraine and seizures (Cao and Zheng, 2014; Garza, 2010). Ideally, to minimize toxicity potential, high affinity inhibitors should also possess binding specificity properties capable of resolving both the connexin subtype as well as the non-junctional hemichannel configuration. Mefloquine has displayed dose-dependent selectivity for certain connexin isoforms (Cruikshank *et al.*, 2004). However, the concentration required to inhibit connexin26 is approximately 10-fold higher than what is required for

its anti-malarial action and ancillary activities are a legitimate worry. Alternatively, taurine has been identified as a benign endogenous modulatory ligand capable of directly and reversibly inhibiting Cx26 channels with complete preference over Cx32 (Locke *et al.*, 2011). Significantly, an unrelated study found taurine to promote stabilization of keratinocyte membrane integrity with favorable effects on keratinocyte viability and the epidermal barrier (Anderheggen *et al.*, 2006). Also of interest are connexin mimetic peptides, which are complementary to short connexin sequence motifs and constitute highly specific and reversible inhibitors (Evans and Boitano, 2001). Notably, Gap19 produced gap-junction-sparing Cx43 hemichannel inhibition (Wang *et al.*, 2013) and Gap26 and Gap27 showed differential inhibitory kinetics for junctional and non-junctional channel forms (Desplantez *et al.*, 2012; Wang *et al.*, 2012). Still, specificity remains a challenge as peptides have also been observed to inhibit pannexins with no overlap in the amino acid sequences (Dahl, 2007). With regard to long-range angles, nucleic acid-based technologies for *in situ* gene silencing stand out as a pinnacle in therapeutics (Gonzalez-Gonzalez *et al.*, 2011). Local delivery of oligonucleotides (Rogers *et al.*, 2013) or siRNAs (Lara *et al.*, 2012) would, in theory, be curative in gain-of-function disorders for which the wild-type protein function is redundant, as appears to be the case in KID syndrome. Multi-disciplinary collaboration among clinicians, physiologists, and medicinal chemists will be necessary to carry the ideas herein to translational endpoints. In the meanwhile, movement of the field will be predicated on the availability of research tools to etch out biological roles for connexin hemichannels in health and disease.

MATERIALS AND METHODS

Histology

Skin samples comprising the dermis and epidermis were dissected and fixed in a 4% paraformaldehyde in PBS for 24 hours at room temperature in the dark. Fixed tissue was washed with PBS, dehydrated through an ethanol series, and embedded in paraffin. Sections of 5μm thickness were cut with a diamond knife with assistance from the Stony Brook University Histology Research Core. Sections were directly mounted on glass slides or deparaffinized, rehydrated, and stained with haematoxylin and eosin before mounting with vectashield medium. Slides were viewed on a BX51 microscope and photographed with a DP72 digital camera (Olympus, Lake Success, NY).

Microemulsion formulation

Water-in-oil microemulsion for topical application in hairless mice was tested by incorporation of 0.2μg/μL lucifer yellow CH lithium salt into the water phase (Molecular Probes, Eugene, OR). Water phase was prepared as 1:3 dimethyl sulfoxide (DMSO):H_2O and comprised 25% of the final microemulsion volume. Oil phase constituents were neutral oil miglyol 812N (Cremer, Hamburg, Germany) with surfactants tween80 (Sigma-Aldrich, St. Louis, MO) and EtOH, comprising 35, 30, and 10% of the final microemulsion volume respectively. Microemulsion was spontaneously formed by slowly injecting the water phase into the oil phase in a 4mL screw-top glass vial under constant stirring with a 5mm magnetic stir-bar at room temperature.

Whole-animal *in vivo* fluorescence imaging

All animal work was done with approval from the Stony Brook University Institutional Animal Care and Use Committee. TRE-G45E-IRES-eGFP plus K14-rtTA SKH1 hairless transgenic mice were generated previously (Mese *et al.*, 2011). For *in vivo* fluorescence detection, mice were anesthetized with isoflurane and imaged using a Maestro small animal imaging system (Cambridge Research & Instrumentation, Woburn, MA). Grey scale images were obtained with a 250ms exposure. Fluorescence images were obtained with a 75ms exposure.

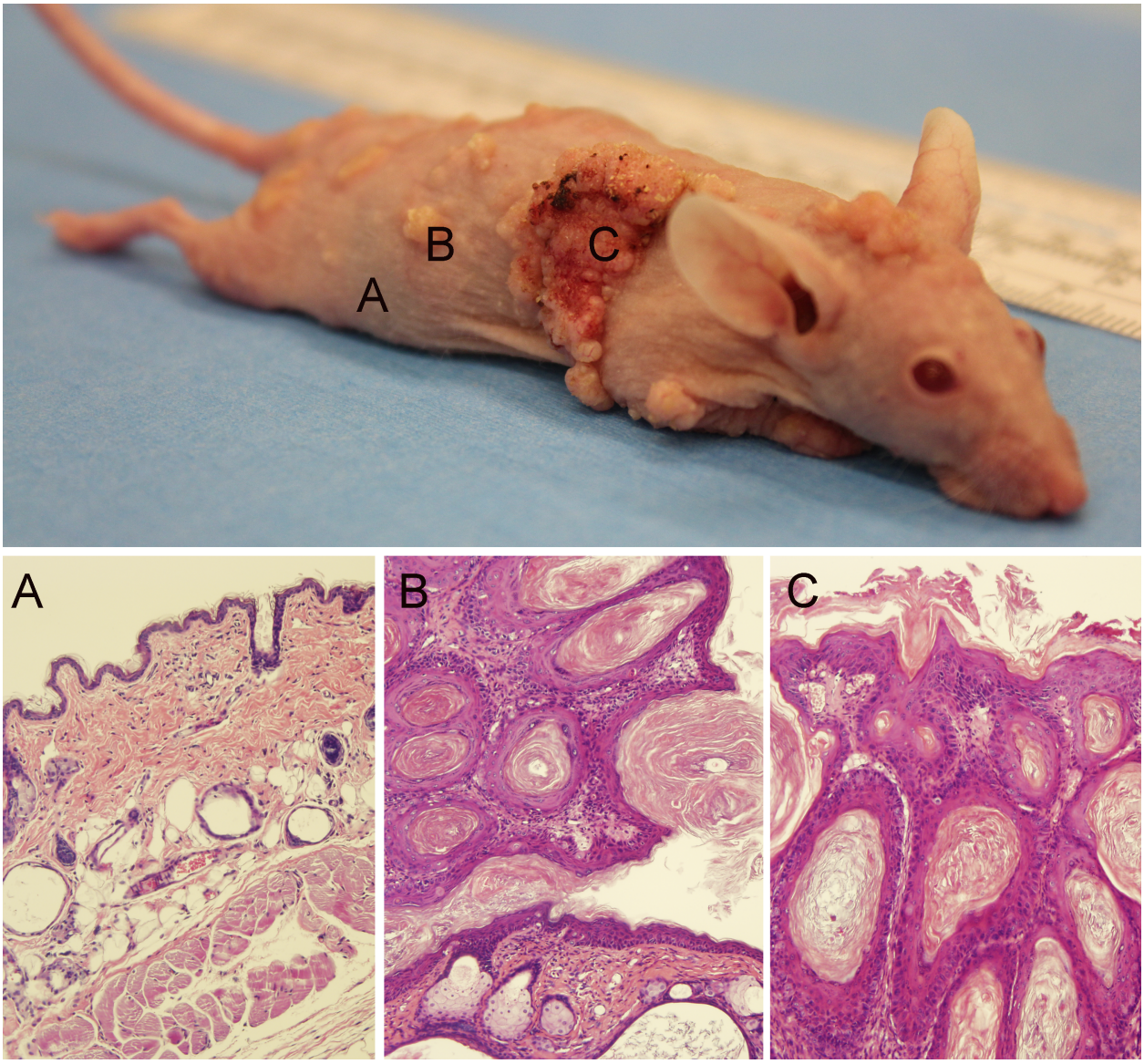

Figure 4-1. Histological analysis of dorsal skin lesions excised from a TRE-G45E plus K14-rtTA SKH1 transgenic mouse. Dermatopathology following 8 weeks of doxycycline supplemented diet (starting on post-natal day 30) ranged from regions of uninvolved tissue to massive epidermal hyperplasia (a) Grossly unaffected back skin samples from double transgenic animals displayed epidermal and dermal morphology consistent with normal for the SKH1 hairless strain. (b) Well-demarcated papillomatous exophytic growths were apparent in a scattered distribution with epidermal architecture resembling seborrheic keratosis with horny cysts. (c) Also present were impressively hyperkeratotic flat-topped plaques ± cutaneous ulceration. Micrographic features included acanthosis, frequent keratotic plugging, and sebaceous gland atrophy. Histology shown corresponds to 4% paraformaldehyde-fixed and paraffin-embedded tissue sectioned at 5μm, stained with haematoxylin and eosin, and photographed with a 20x objective.

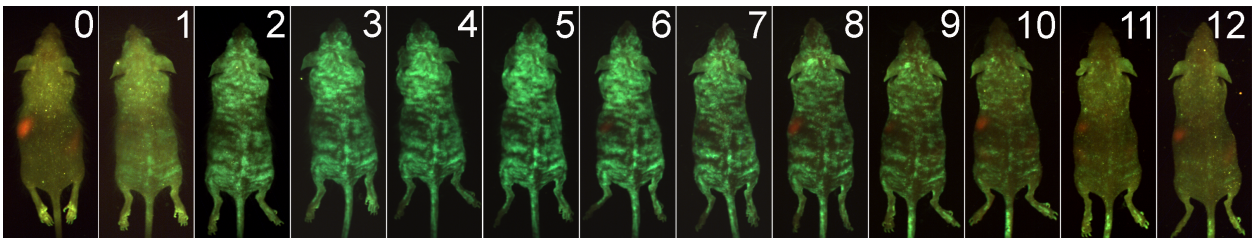

Figure 4-2. Kinetics of transgene induction in TRE-G45E-IRES-eGFP plus K14-rtTA SKH1 hairless mice tracked by *in vivo* fluorescence imaging. Doxycycline supplementation (200mg/kg) of animal chow caused rapid initiation of disease model progression with tight correlation between eGFP expression and lesion severity. Doxycycline was removed on day 5 to demonstrate regression of hyperkeratosis and eGFP signal disappearance corresponding to reduction in the epidermal thickness.

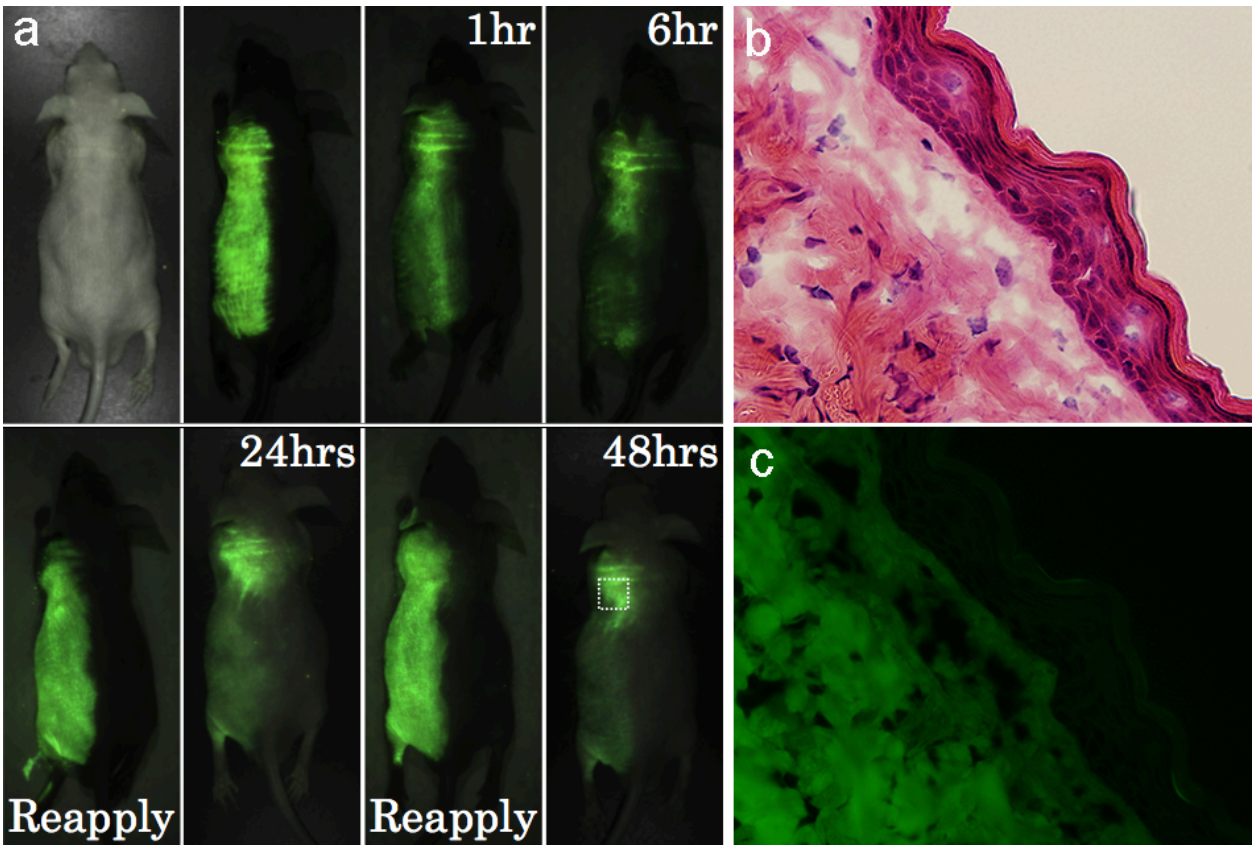

Figure 4-3. Delivery of Lucifer yellow CH to control SKH1 hairless mouse skin by water-in-oil microemulsion. (a) Topical application regimen with the dye-containing media was tested for 2 consecutive days on the left dorsal flank. Whole-animal *in vivo* fluorescence images were acquired at 1 hour and 6 hours post-drug application on day 1 and once/day thereafter. Dye retention was apparent at all time points, although less dye was visible on the most caudal aspects of the back beginning 6 hours post-application. Disordered contralateral spreading was apparent at later time points. (b) Histological analysis of frozen sections of left shoulder skin showed epidermal architecture normal to the SKH1 hairless strain. (c) Fluorescence microscopy localized dye absorption to the dermis and subcutaneous tissue with only trace amount present in the epidermis.

References

Abdollahi A, Hallaji Z, Esmaili N*, et al.* (2007) KID syndrome. *Dermatology online journal* 13:11.

Anand RJ, Hackam DJ (2005) The role of gap junctions in health and disease. *Crit Care Med* 33:S535-8.

Anderheggen B, Jassoy C, Waldmann-Laue M*, et al.* (2006) Taurine improves epidermal barrier properties stressed by surfactants-a role for osmolytes in barrier homeostasis. *Journal of cosmetic science* 57:1-10.

Andrews RC, Rooyackers O, Walker BR (2003) Effects of the 11 beta-hydroxysteroid dehydrogenase inhibitor carbenoxolone on insulin sensitivity in men with type 2 diabetes. *The Journal of clinical endocrinology and metabolism* 88:285-91.

Arita K, Akiyama M, Aizawa T*, et al.* (2006) A novel N14Y mutation in Connexin26 in keratitis-ichthyosis-deafness syndrome: analyses of altered gap junctional communication and molecular structure of N terminus of mutated Connexin26. *Am J Pathol* 169:416-23.

Bai D, del Corsso C, Srinivas M*, et al.* (2006) Block of specific gap junction channel subtypes by 2-aminoethoxydiphenyl borate (2-APB). *The Journal of pharmacology and experimental therapeutics* 319:1452-8.

Bakirtzis G, Choudhry R, Aasen T*, et al.* (2003) Targeted epidermal expression of mutant Connexin 26(D66H) mimics true Vohwinkel syndrome and provides a model for the pathogenesis of dominant connexin disorders. *Hum Mol Genet* 12:1737-44.

Barbaud A (2009) Contact dermatitis due to topical drugs. *Giornale italiano di dermatologia e venereologia : organo ufficiale, Societa italiana di dermatologia e sifilografia* 144:527-36.

Barrio LC, Suchyna T, Bargiello T*, et al.* (1991) Gap junctions formed by connexins 26 and 32 alone and in combination are differently affected by applied voltage. *Proc Natl Acad Sci U S A* 88:8410-4.

Beahm DL, Hall JE (2002) Hemichannel and junctional properties of connexin 50. *Biophysical journal* 82:2016-31.

Beaumont M, Maccaferri G (2011) Is connexin36 critical for GABAergic hypersynchronization in the hippocampus? *J Physiol* 589:1663-80.

Bedner P, Niessen H, Odermatt B*, et al.* (2006) Selective permeability of different connexin channels to the second messenger cyclic AMP. *J Biol Chem* 281:6673-81.

Beltramello M, Piazza V, Bukauskas FF*, et al.* (2005) Impaired permeability to Ins(1,4,5)P3 in a mutant connexin underlies recessive hereditary deafness. *Nature cell biology* 7:63-9.

Bennett MV, Contreras JE, Bukauskas FF*, et al.* (2003) New roles for astrocytes: gap junction hemichannels have something to communicate. *Trends Neurosci* 26:610-7.

Berger AC, Kelly JJ, Lajoie P*, et al.* (2014) Mutations in Cx30 that are linked to skin disease and non-syndromic hearing loss exhibit several distinct cellular pathologies. *J Cell Sci* 127:1751-64.

Bevans CG, Kordel M, Rhee SK*, et al.* (1998) Isoform composition of connexin channels determines selectivity among second messengers and uncharged molecules. *J Biol Chem* 273:2808-16.

Blanpain C, Fuchs E (2009) Epidermal homeostasis: a balancing act of stem cells in the skin. *Nat Rev Mol Cell Biol* 10:207-17.

Boguniewicz M, Zeichner JA, Eichenfield LF*, et al.* (2008) MAS063DP is effective monotherapy for mild to moderate atopic dermatitis in infants and children: a multicenter, randomized, vehicle-controlled study. *The Journal of pediatrics* 152:854-9.

Braun-Falco M (2009) Hereditary palmoplantar keratodermas. *Journal der Deutschen Dermatologischen Gesellschaft = Journal of the German Society of Dermatology : JDDG* 7:971-84; quiz 84-5.

Brokamp C, Todd J, Montemagno C*, et al.* (2012) Electrophysiology of single and aggregate Cx43 hemichannels. *PloS one* 7:e47775.

Bruzzone R, Barbe MT, Jakob NJ*, et al.* (2005) Pharmacological properties of homomeric and heteromeric pannexin hemichannels expressed in Xenopus oocytes. *Journal of neurochemistry* 92:1033-43.

Bruzzone R, Haefliger JA, Gimlich RL*, et al.* (1993) Connexin40, a component of gap junctions in vascular endothelium, is restricted in its ability to interact with other connexins. *Mol Biol Cell* 4:7-20.

Bruzzone R, Veronesi V, Gomes D*, et al.* (2003) Loss-of-function and residual channel activity of connexin26 mutations associated with non-syndromic deafness. *FEBS Lett* 533:79-88.

Bruzzone R, White TW, Paul DL (1996) Connections with connexins: the molecular basis of direct intercellular signaling. *Eur J Biochem* 238:1-27.

Bruzzone S, Guida L, Zocchi E*, et al.* (2001) Connexin 43 hemi channels mediate Ca2+-regulated transmembrane NAD+ fluxes in intact cells. *FASEB J* 15:10-2.

Bukauskas FF, Peracchia C (1997) Two distinct gating mechanisms in gap junction channels: CO2-sensitive and voltage-sensitive. *Biophys J* 72:2137-42.

Bukauskas FF, Verselis VK (2004) Gap junction channel gating. *Biochimica et biophysica acta* 1662:42-60.

Cao Y, Zheng OJ (2014) Tonabersat for migraine prophylaxis: a systematic review. *Pain physician* 17:1-8.

Chandrasekhar A, Bera AK (2012) Hemichannels: permeants and their effect on development, physiology and death. *Cell biochemistry and function* 30:89-100.

Chi J, Li L, Liu M*, et al.* (2012) Pathogenic connexin-31 forms constitutively active hemichannels to promote necrotic cell death. *PloS one* 7:e32531.

Coggshall K, Farsani T, Ruben B*, et al.* (2013) Keratitis, ichthyosis, and deafness syndrome: a review of infectious and neoplastic complications. *J Am Acad Dermatol* 69:127-34.

Common JE, Becker D, Di WL*, et al.* (2002) Functional studies of human skin disease- and deafness-associated connexin 30 mutations. *Biochemical and biophysical research communications* 298:651-6.

Connors BW (2012) Tales of a dirty drug: carbenoxolone, gap junctions, and seizures. *Epilepsy currents / American Epilepsy Society* 12:66-8.

Cotrina ML, Lin JH, Alves-Rodrigues A*, et al.* (1998) Connexins regulate calcium signaling by controlling ATP release. *Proc Natl Acad Sci U S A* 95:15735-40.

Cruikshank SJ, Hopperstad M, Younger M*, et al.* (2004) Potent block of Cx36 and Cx50 gap junction channels by mefloquine. *Proc Natl Acad Sci U S A* 101:12364-9.

D'Adamo P, Guerci VI, Fabretto A*, et al.* (2009) Does epidermal thickening explain GJB2 high carrier frequency and heterozygote advantage? *Eur J Hum Genet* 17:284-6.

Dahl G (2007) Gap junction-mimetic peptides do work, but in unexpected ways. *Cell Commun Adhes* 14:259-64.

Davidson JS, Baumgarten IM, Harley EH (1986) Reversible inhibition of intercellular junctional communication by glycyrrhetinic acid. *Biochemical and biophysical research communications* 134:29-36.

de Berker D, Branford WA, Soucek S*, et al.* (1993) Fatal keratitis ichthyosis and deafness syndrome (KIDS). Aural, ocular, and cutaneous histopathology. *The American Journal of dermatopathology* 15:64-9.

de Zwart-Storm EA, Rosa RF, Martin PE*, et al.* (2011) Molecular analysis of connexin26 asparagine14 mutations associated with syndromic skin phenotypes. *Exp Dermatol* 20:408-12.

Desplantez T, Verma V, Leybaert L*, et al.* (2012) Gap26, a connexin mimetic peptide, inhibits currents carried by connexin43 hemichannels and gap junction channels. *Pharmacological research : the official journal of the Italian Pharmacological Society* 65:546-52.

DeVries SH, Schwartz EA (1989) Modulation of an electrical synapse between solitary pairs of catfish horizontal cells by dopamine and second messengers. *The Journal of physiology* 414:351-75.

DeVries SH, Schwartz EA (1992) Hemi-gap-junction channels in solitary horizontal cells of the catfish retina. *J Physiol* 445:201-30.

Di WL, Common JE, Kelsell DP (2001a) Connexin 26 expression and mutation analysis in epidermal disease. *Cell Commun Adhes* 8:415-8.

Di WL, Rugg EL, Leigh IM*, et al.* (2001b) Multiple epidermal connexins are expressed in different keratinocyte subpopulations including connexin 31. *J Invest Dermatol* 117:958-64.

Dodds A, Chia A, Shumack S (2014) Actinic Keratosis: Rationale and Management. *Dermatology and therapy*.

Dogrul A, Arslan SA, Tirnaksiz F (2014) Water/oil type microemulsion systems containing lidocaine hydrochloride: in vitro and in vivo evaluation. *Journal of microencapsulation*.

Donnelly S, English G, de Zwart-Storm EA*, et al.* (2012) Differential susceptibility of Cx26 mutations associated with epidermal dysplasias to peptidoglycan derived from Staphylococcus aureus and Staphylococcus epidermidis. *Exp Dermatol* 21:592-8.

Ebihara L, Steiner E (1993) Properties of a nonjunctional current expressed from a rat connexin46 cDNA in Xenopus oocytes. *J Gen Physiol* 102:59-74.

Eskandari S, Zampighi GA, Leung DW*, et al.* (2002) Inhibition of gap junction hemichannels by chloride channel blockers. *The Journal of membrane biology* 185:93-102.

Essenfelder GM, Bruzzone R, Lamartine J*, et al.* (2004) Connexin30 mutations responsible for hidrotic ectodermal dysplasia cause abnormal hemichannel activity. *Hum Mol Genet* 13:1703-14.

Evans WH, Boitano S (2001) Connexin mimetic peptides: specific inhibitors of gap-junctional intercellular communication. *Biochemical Society transactions* 29:606-12.

Evans WH, De Vuyst E, Leybaert L (2006) The gap junction cellular internet: connexin hemichannels enter the signalling limelight. *Biochem J* 397:1-14.

Flower RJ (1974) Drugs which inhibit prostaglandin biosynthesis. *Pharmacological reviews* 26:33-67.

Garza I (2010) Tonabersat: a cortical spreading depression inhibitor as potential pharmacologic prophylaxis in migraine with aura. *Current neurology and neuroscience reports* 10:7-9.

Gerido DA, DeRosa AM, Richard G*, et al.* (2007) Aberrant hemichannel properties of Cx26 mutations causing skin disease and deafness. *Am J Physiol Cell Physiol* 293:C337-45.

Gerido DA, White TW (2004) Connexin disorders of the ear, skin, and lens. *Biochim Biophys Acta* 1662:159-70.

Giepmans BN, Hengeveld T, Postma FR*, et al.* (2001) Interaction of c-Src with gap junction protein connexin-43. Role in the regulation of cell-cell communication. *The Journal of biological chemistry* 276:8544-9.

Gilliam A, Williams ML (2002) Fatal septicemia in an infant with keratitis, ichthyosis, and deafness (KID) syndrome. *Pediatric dermatology* 19:232-6.

Gniazdowska B, Rueff F, Przybilla B (1999) Delayed contact hypersensitivity to non-steroidal anti-inflammatory drugs. *Contact dermatitis* 40:63-5.

Goldberg GS, Lampe PD, Nicholson BJ (1999) Selective transfer of endogenous metabolites through gap junctions composed of different connexins. *Nature cell biology* 1:457-9.

Goliger JA, Paul DL (1995) Wounding alters epidermal connexin expression and gap junction-mediated intercellular communication. *Mol Biol Cell* 6:1491-501.

Gonzalez D, Gomez-Hernandez JM, Barrio LC (2006) Species specificity of mammalian connexin-26 to form open voltage-gated hemichannels. *FASEB J* 20:2329-38.

Gonzalez-Gonzalez E, Kim YC, Speaker TJ*, et al.* (2011) Visualization of plasmid delivery to keratinocytes in mouse and human epidermis. *Scientific reports* 1:158.

Goodenough DA (1974) Bulk isolation of mouse hepatocyte gap junctions. Characterization of the principal protein, connexin. *J Cell Biol* 61:557-63.

Goodenough DA, Paul DL (2003) Beyond the gap: functions of unpaired connexon channels. *Nat Rev Mol Cell Biol* 4:285-94.

Goodenough DA, Paul DL (2009) Gap junctions. *Cold Spring Harb Perspect Biol* 1:a002576.

Goodier TE, Horwich L, Galloway RW (1967) Morphological observations on gastric ulcers treated with carbenoxolone sodium. *Gut* 8:544-7.

Gribble FM, Davis TM, Higham CE*, et al.* (2000) The antimalarial agent mefloquine inhibits ATP-sensitive K-channels. *Br J Pharmacol* 131:756-60.

Griffith AJ, Yang Y, Pryor SP*, et al.* (2006) Cochleosaccular dysplasia associated with a connexin 26 mutation in keratitis-ichthyosis-deafness syndrome. *Laryngoscope* 116:1404-8.

Grob JJ, Breton A, Bonafe JL*, et al.* (1987) Keratitis, ichthyosis, and deafness (KID) syndrome. Vertical transmission and death from multiple squamous cell carcinomas. *Arch Dermatol* 123:777-82.

Guinamard R, Simard C, Del Negro C (2013) Flufenamic acid as an ion channel modulator. *Pharmacology & therapeutics* 138:272-84.

Harks EG, de Roos AD, Peters PH*, et al.* (2001) Fenamates: a novel class of reversible gap junction blockers. *J Pharmacol Exp Ther* 298:1033-41.

Harris AL (2001) Emerging issues of connexin channels: biophysics fills the gap. *Quarterly reviews of biophysics* 34:325-472.

Haruna K, Suga Y, Oizumi A*, et al.* (2010) Severe form of keratitis-ichthyosis-deafness (KID) syndrome associated with septic complications. *J Dermatol* 37:680-2.

Helm K, Lane AT, Orosz J*, et al.* (1990) Systemic cytomegalovirus in a patient with the keratitis, ichthyosis, and deafness (KID) syndrome. *Pediatric dermatology* 7:54-6.

Hirata K, Helal F, Hadgraft J*, et al.* (2013) Formulation of carbenoxolone for delivery to the skin. *International journal of pharmaceutics* 448:360-5.

Horton RM, Cai ZL, Ho SN*, et al.* (1990) Gene splicing by overlap extension: tailor-made genes using the polymerase chain reaction. *Biotechniques* 8:528-35.

Iossa S, Marciano E, Franze A (2011) GJB2 Gene Mutations in Syndromic Skin Diseases with Sensorineural Hearing Loss. *Current genomics* 12:475-785.

Jamsheer A, Sowinska-Seidler A, Socha M*, et al.* (2014) Three novel GJA1 missense substitutions resulting in oculo-dento-digital dysplasia (ODDD) - Further extension of the mutational spectrum. *Gene* 539:157-61.

Jan AY, Amin S, Ratajczak P*, et al.* (2004) Genetic heterogeneity of KID syndrome: identification of a Cx30 gene (GJB6) mutation in a patient with KID syndrome and congenital atrichia. *J Invest Dermatol* 122:1108-13.

Janecke AR, Hennies HC, Gunther B*, et al.* (2005) GJB2 mutations in keratitis-ichthyosis-deafness syndrome including its fatal form. *Am J Med Genet A* 133A:128-31.

Jiang JX, Cherian PP (2003) Hemichannels formed by connexin 43 play an important role in the release of prostaglandin E(2) by osteocytes in response to mechanical strain. *Cell Commun Adhes* 10:259-64.

Jiang JX, Gu S (2005) Gap junction- and hemichannel-independent actions of connexins. *Biochim Biophys Acta* 1711:208-14.

Jonard L, Feldmann D, Parsy C*, et al.* (2008) A familial case of Keratitis-Ichthyosis-Deafness (KID) syndrome with the GJB2 mutation G45E. *Eur J Med Genet* 51:35-43.

Juszczak GR, Swiergiel AH (2009) Properties of gap junction blockers and their behavioural, cognitive and electrophysiological effects: animal and human studies. *Progress in neuro-psychopharmacology & biological psychiatry* 33:181-98.

Kam E, Melville L, Pitts JD (1986) Patterns of junctional communication in skin. *J Invest Dermatol* 87:748-53.

Kanaporis G, Mese G, Valiuniene L*, et al.* (2008) Gap junction channels exhibit connexin-specific permeability to cyclic nucleotides. *J Gen Physiol* 131:293-305.

Kang J, Chen XL, Wang L*, et al.* (2001) Interactions of the antimalarial drug mefloquine with the human cardiac potassium channels KvLQT1/minK and HERG. *J Pharmacol Exp Ther* 299:290-6.

Kang J, Kang N, Lovatt D*, et al.* (2008) Connexin 43 hemichannels are permeable to ATP. *J Neurosci* 28:4702-11.

Kanno Y, Loewenstein WR (1964) Low-Resistance Coupling between Gland Cells. Some Observations on Intercellular Contact Membranes and Intercellular Space. *Nature* 201:194-5.

Kar R, Batra N, Riquelme MA*, et al.* (2012) Biological role of connexin intercellular channels and hemichannels. *Archives of biochemistry and biophysics* 524:2-15.

Kelly B, Lozano A, Altenberg G*, et al.* (2008) Connexin 26 mutation in keratitis-ichthyosis-deafness (KID) syndrome in mother and daughter with combined conductive and sensorineural hearing loss. *International journal of dermatology* 47:443-7.

Kelsell DP, Wilgoss AL, Richard G*, et al.* (2000) Connexin mutations associated with palmoplantar keratoderma and profound deafness in a single family. *Eur J Hum Genet* 8:469-72.

Koppelhus U, Tranebjaerg L, Esberg G*, et al.* (2011) A novel mutation in the connexin 26 gene (GJB2) in a child with clinical and histological features of keratitis-ichthyosis-deafness (KID) syndrome. *Clin Exp Dermatol* 36:142-8.

Kronengold J, Srinivas M, Verselis VK (2012) The N-terminal half of the connexin protein contains the core elements of the pore and voltage gates. *J Membr Biol* 245:453-63.

Kronengold J, Trexler EB, Bukauskas FF*, et al.* (2003) Pore-lining residues identified by single channel SCAM studies in Cx46 hemichannels. *Cell Commun Adhes* 10:193-9.

Labarthe MP, Bosco D, Saurat JH*, et al.* (1998) Upregulation of connexin 26 between keratinocytes of psoriatic lesions. *J Invest Dermatol* 111:72-6.

Lai-Cheong JE, Arita K, McGrath JA (2007) Genetic diseases of junctions. *J Invest Dermatol* 127:2713-25.

Lara MF, Gonzalez-Gonzalez E, Speaker TJ*, et al.* (2012) Inhibition of CD44 gene expression in human skin models, using self-delivery short interfering RNA administered by dissolvable microneedle arrays. *Human gene therapy* 23:816-23.

Lawrence MJ (1994) Surfactant systems: microemulsions and vesicles as vehicles for drug delivery. *European journal of drug metabolism and pharmacokinetics* 19:257-69.

Lawrence MJ, Rees GD (2000) Microemulsion-based media as novel drug delivery systems. *Advanced drug delivery reviews* 45:89-121.

Lawrence TS, Beers WH, Gilula NB (1978) Transmission of hormonal stimulation by cell-to-cell communication. *Nature* 272:501-6.

Lee JR, Derosa AM, White TW (2009) Connexin mutations causing skin disease and deafness increase hemichannel activity and cell death when expressed in Xenopus oocytes. *J Invest Dermatol* 129:870-8.

Lee JR, White TW. Analysis of mutations in connexin26 associated with syndromic deafness. In: *Proceedings of the Conference Analysis of mutations in connexin26 associated with syndromic deafness;* 2009a; San Diego, CA, USA.

Lee JR, White TW (2009b) Connexin-26 mutations in deafness and skin disease. *Expert Rev Mol Med* 11:e35.

Lerer I, Sagi M, Malamud E*, et al.* (2000) Contribution of connexin 26 mutations to nonsyndromic deafness in Ashkenazi patients and the variable phenotypic effect of the mutation 167delT. *American journal of medical genetics* 95:53-6.

Leshchenko Y, Likhodii S, Yue W*, et al.* (2006) Carbenoxolone does not cross the blood brain barrier: an HPLC study. *BMC neuroscience* 7:3.

Levit NA, Mese G, Basaly MG*, et al.* (2012) Pathological hemichannels associated with human Cx26 mutations causing Keratitis-Ichthyosis-Deafness syndrome. *Biochim Biophys Acta* 1818:2014-9.

Li Z, Yan Y, Powers EA*, et al.* (2003) Identification of gap junction blockers using automated fluorescence microscopy imaging. *J Biomol Screen* 8:489-99.

Liang GS, de Miguel M, Gomez-Hernandez JM*, et al.* (2005) Severe neuropathy with leaky connexin32 hemichannels. *Ann Neurol* 57:749-54.

Lichti U, Anders J, Yuspa SH (2008) Isolation and short-term culture of primary keratinocytes, hair follicle populations and dermal cells from newborn mice and keratinocytes from adult mice for in vitro analysis and for grafting to immunodeficient mice. *Nat Protoc* 3:799-810.

Locke D, Kieken F, Tao L*, et al.* (2011) Mechanism for modulation of gating of connexin26-containing channels by taurine. *J Gen Physiol* 138:321-39.

Locke D, Koreen IV, Harris AL (2006) Isoelectric points and post-translational modifications of connexin26 and connexin32. *The FASEB journal : official publication of the Federation of American Societies for Experimental Biology* 20:1221-3.

Lopes LB (2014) Overcoming the cutaneous barrier with microemulsions. *Pharmaceutics* 6:52-77.

Lucke T, Choudhry R, Thom R*, et al.* (1999) Upregulation of connexin 26 is a feature of keratinocyte differentiation in hyperproliferative epidermis, vaginal epithelium, and buccal epithelium. *J Invest Dermatol* 112:354-61.

Maeda S, Nakagawa S, Suga M*, et al.* (2009) Structure of the connexin 26 gap junction channel at 3.5 A resolution. *Nature* 458:597-602.

Maertens C, Wei L, Droogmans G*, et al.* (2000) Inhibition of volume-regulated and calcium-activated chloride channels by the antimalarial mefloquine. *J Pharmacol Exp Ther* 295:29-36.

Malchow RP, Qian H, Ripps H (1993) Evidence for hemi-gap junctional channels in isolated horizontal cells of the skate retina. *J Neurosci Res* 35:237-45.

Martinez AD, Acuna R, Figueroa V*, et al.* (2009) Gap-junction channels dysfunction in deafness and hearing loss. *Antioxidants & redox signaling* 11:309-22.

Masgrau-Peya E, Salomon D, Saurat JH*, et al.* (1997) In vivo modulation of connexins 43 and 26 of human epidermis by topical retinoic acid treatment. *The journal of*

histochemistry and cytochemistry : official journal of the Histochemistry Society 45:1207-15.

Mauro TM, Isseroff RR, Lasarow R*, et al.* (1993) Ion channels are linked to differentiation in keratinocytes. *J Membr Biol* 132:201-9.

Mazereeuw-Hautier J, Bitoun E, Chevrant-Breton J*, et al.* (2007) Keratitis-ichthyosis-deafness syndrome: disease expression and spectrum of connexin 26 (GJB2) mutations in 14 patients. *Br J Dermatol* 156:1015-9.

Mazereeuw-Hautier J, Chiaverini C, Jonca N*, et al.* (2014) Lethal Form of Keratitis-Ichthyosis-Deafness Syndrome Caused by the GJB2 Mutation p.Ser17Phe. *Acta dermato-venereologica*.

Mese G, Richard G, White TW (2007) Gap junctions: basic structure and function. *J Invest Dermatol* 127:2516-24.

Mese G, Sellitto C, Li L*, et al.* (2011) The Cx26-G45E mutation displays increased hemichannel activity in a mouse model of the lethal form of keratitis-ichthyosis-deafness syndrome. *Mol Biol Cell* 22:4776-86.

Mese G, Valiunas V, Brink PR*, et al.* (2008) Connexin26 deafness associated mutations show altered permeability to large cationic molecules. *Am J Physiol Cell Physiol* 295:C966-74.

Meyer CG, Amedofu GK, Brandner JM*, et al.* (2002) Selection for deafness? *Nature medicine* 8:1332-3.

Mhaske PV, Levit NA, Li L*, et al.* (2013) The human Cx26-D50A and Cx26-A88V mutations causing keratitis-ichthyosis-deafness syndrome display increased hemichannel activity. *Am J Physiol Cell Physiol* 304:C1150-8.

Montgomery JR, White TW, Martin BL*, et al.* (2004) A novel connexin 26 gene mutation associated with features of the keratitis-ichthyosis-deafness syndrome and the follicular occlusion triad. *J Am Acad Dermatol* 51:377-82.

Moore RA, Tramer MR, Carroll D*, et al.* (1998) Quantitative systematic review of topically applied non-steroidal anti-inflammatory drugs. *Bmj* 316:333-8.

Mozsik G, Szabo IL, Czimmer J (2011) Approaches to gastrointestinal cytoprotection: from isolated cells, via animal experiments to healthy human subjects and patients with different gastrointestinal disorders. *Current pharmaceutical design* 17:1556-72.

Niedner R, Iliev D (2001) [Dermatological local therapy. How to control eczema]. *MMW Fortschritte der Medizin* 143:33-8.

Niessen H, Harz H, Bedner P*, et al.* (2000) Selective permeability of different connexin channels to the second messenger inositol 1,4,5-trisphosphate. *J Cell Sci* 113 (Pt 8):1365-72.

Oh S, Rubin JB, Bennett MV*, et al.* (1999) Molecular determinants of electrical rectification of single channel conductance in gap junctions formed by connexins 26 and 32. *J Gen Physiol* 114:339-64.

Oshima A, Tani K, Hiroaki Y*, et al.* (2008) Projection structure of a N-terminal deletion mutant of connexin 26 channel with decreased central pore density. *Cell Commun Adhes* 15:85-93.

Paschon V, Higa GS, Resende RR*, et al.* (2012) Blocking of connexin-mediated communication promotes neuroprotection during acute degeneration induced by mechanical trauma. *PloS one* 7:e45449.

Paul DL, Ebihara L, Takemoto LJ*, et al.* (1991) Connexin46, a novel lens gap junction protein, induces voltage-gated currents in nonjunctional plasma membrane of Xenopus oocytes. *The Journal of cell biology* 115:1077-89.

Pepe D, Phelps J, Lewis K*, et al.* (2012) Decylglucoside-based microemulsions for cutaneous localization of lycopene and ascorbic acid. *International journal of pharmaceutics* 434:420-8.

Petit C (2006) From deafness genes to hearing mechanisms: harmony and counterpoint. *Trends Mol Med* 12:57-64.

Petit C, Levilliers J, Hardelin JP (2001) Molecular genetics of hearing loss. *Annu Rev Genet* 35:589-646.

Pfenniger A, Wohlwend A, Kwak BR (2011) Mutations in connexin genes and disease. *Eur J Clin Invest* 41:103-16.

Picoli C, Nouvel V, Aubry F*, et al.* (2012) Human connexin channel specificity of classical and new gap junction inhibitors. *J Biomol Screen* 17:1339-47.

Pinder RM, Brogden RN, Sawyer PR*, et al.* (1976) Carbenoxolone: a review of its pharmacological properties and therapeutic efficacy in peptic ulcer disease. *Drugs* 11:245-307.

Proksch E, Brandner JM, Jensen JM (2008) The skin: an indispensable barrier. *Exp Dermatol* 17:1063-72.

Puglia C, Rizza L, Offerta A*, et al.* (2013) Formulation strategies to modulate the topical delivery of anti-inflammatory compounds. *Journal of cosmetic science* 64:341-53.

Purnick PE, Oh S, Abrams CK*, et al.* (2000) Reversal of the gating polarity of gap junctions by negative charge substitutions in the N-terminus of connexin 32. *Biophys J* 79:2403-15.

Reiss M, Lipsey LR, Zhou ZL (1991) Extracellular calcium-dependent regulation of transmembrane calcium fluxes in murine keratinocytes. *Journal of cellular physiology* 147:281-91.

Rekling JC, Shao XM, Feldman JL (2000) Electrical coupling and excitatory synaptic transmission between rhythmogenic respiratory neurons in the preBotzinger complex. *J Neurosci* 20:RC113.

Retamal MA, Cortes CJ, Reuss L*, et al.* (2006) S-nitrosylation and permeation through connexin 43 hemichannels in astrocytes: induction by oxidant stress and reversal by reducing agents. *Proceedings of the National Academy of Sciences of the United States of America* 103:4475-80.

Revel JP, Karnovsky MJ (1967) Hexagonal array of subunits in intercellular junctions of the mouse heart and liver. *J Cell Biol* 33:C7-C12.

Richard G (2005) Connexin disorders of the skin. *Clin Dermatol* 23:23-32.

Richard G, Rouan F, Willoughby CE*, et al.* (2002) Missense mutations in GJB2 encoding connexin-26 cause the ectodermal dysplasia keratitis-ichthyosis-deafness syndrome. *Am J Hum Genet* 70:1341-8.

Richard G, White TW, Smith LE*, et al.* (1998) Functional defects of Cx26 resulting from a heterozygous missense mutation in a family with dominant deaf-mutism and palmoplantar keratoderma. *Hum Genet* 103:393-9.

Ripps H, Qian H, Zakevicius J (2004) Properties of connexin26 hemichannels expressed in Xenopus oocytes. *Cell Mol Neurobiol* 24:647-65.

Rivas MV, Jarvis ED, Morisaki S*, et al.* (1997) Identification of aberrantly regulated genes in diseased skin using the cDNA differential display technique. *J Invest Dermatol* 108:188-94.

Robertson JD (1963) The Occurrence of a Subunit Pattern in the Unit Membranes of Club Endings in Mauthner Cell Synapses in Goldfish Brains. *J Cell Biol* 19:201-21.

Rogers FA, Hu RH, Milstone LM (2013) Local delivery of gene-modifying triplex-forming molecules to the epidermis. *J Invest Dermatol* 133:685-91.

Rouach N, Segal M, Koulakoff A*, et al.* (2003) Carbenoxolone blockade of neuronal network activity in culture is not mediated by an action on gap junctions. *J Physiol* 553:729-45.

Rouan F, White TW, Brown N*, et al.* (2001) trans-dominant inhibition of connexin-43 by mutant connexin-26: implications for dominant connexin disorders affecting epidermal differentiation. *J Cell Sci* 114:2105-13.

Rubinos C, Sanchez HA, Verselis VK*, et al.* (2012) Mechanism of inhibition of connexin channels by the quinine derivative N-benzylquininium. *J Gen Physiol* 139:69-82.

Rubio L, Alonso C, Rodriguez G*, et al.* (2013) Bicellar systems as new delivery strategy for topical application of flufenamic acid. *International journal of pharmaceutics* 444:60-9.

Saez JC, Retamal MA, Basilio D*, et al.* (2005) Connexin-based gap junction hemichannels: gating mechanisms. *Biochim Biophys Acta* 1711:215-24.

Saez JC, Schalper KA, Retamal MA*, et al.* (2010) Cell membrane permeabilization via connexin hemichannels in living and dying cells. *Exp Cell Res* 316:2377-89.

Salomon D, Saurat JH, Meda P (1988) Cell-to-cell communication within intact human skin. *J Clin Invest* 82:248-54.

Sanchez HA, Mese G, Srinivas M*, et al.* (2010) Differentially altered Ca2+ regulation and Ca2+ permeability in Cx26 hemichannels formed by the A40V and G45E mutations that cause keratitis ichthyosis deafness syndrome. *J Gen Physiol* 136:47-62.

Sanchez HA, Villone K, Srinivas M*, et al.* (2013) The D50N mutation and syndromic deafness: altered Cx26 hemichannel properties caused by effects on the pore and intersubunit interactions. *J Gen Physiol* 142:3-22.

Sasivimolphan P, Lipipun V, Ritthidej G*, et al.* (2012) Microemulsion-based oxyresveratrol for topical treatment of herpes simplex virus (HSV) infection: physicochemical properties and efficacy in cutaneous HSV-1 infection in mice. *AAPS PharmSciTech* 13:1266-75.

Sawey MJ, Goldschmidt MH, Risek B*, et al.* (1996) Perturbation in connexin 43 and connexin 26 gap-junction expression in mouse skin hyperplasia and neoplasia. *Mol Carcinog* 17:49-61.

Sbidian E, Feldmann D, Bengoa J*, et al.* (2010) Germline mosaicism in keratitis-ichthyosis-deafness syndrome: pre-natal diagnosis in a familial lethal form. *Clin Genet* 77:587-92.

Schalper KA, Orellana JA, Berthoud VM*, et al.* (2009) Dysfunctions of the diffusional membrane pathways mediated by hemichannels in inherited and acquired human diseases. *Curr Vasc Pharmacol* 7:486-505.

Schlagenhauf P, Adamcova M, Regep L*, et al.* (2011) Use of mefloquine in children - a review of dosage, pharmacokinetics and tolerability data. *Malaria journal* 10:292.

Schutz M, Auth T, Gehrt A*, et al.* (2011) The connexin26 S17F mouse mutant represents a model for the human hereditary keratitis-ichthyosis-deafness syndrome. *Hum Mol Genet* 20:28-39.

Scott CA, Kelsell DP (2011) Key functions for gap junctions in skin and hearing. *Biochem J* 438:245-54.

Silverberg JI (2014) Atopic Dermatitis: An Evidence-Based Treatment Update. *American journal of clinical dermatology*.

Skeberdis VA, Rimkute L, Skeberdyte A*, et al.* (2011) pH-dependent modulation of connexin-based gap junctional uncouplers. *J Physiol* 589:3495-506.

Skinner BA, Greist MC, Norins AL (1981) The keratitis, ichthyosis, and deafness (KID) syndrome. *Arch Dermatol* 117:285-9.

Sohl G, Willecke K (2003) An update on connexin genes and their nomenclature in mouse and man. *Cell Commun Adhes* 10:173-80.

Solan JL, Lampe PD (2009) Connexin43 phosphorylation: structural changes and biological effects. *The Biochemical journal* 419:261-72.

Spray DC, Rozental R, Srinivas M (2002) Prospects for rational development of pharmacological gap junction channel blockers. *Curr Drug Targets* 3:455-64.

Srinivas M, Hopperstad MG, Spray DC (2001) Quinine blocks specific gap junction channel subtypes. *Proc Natl Acad Sci U S A* 98:10942-7.

Srinivas M, Spray DC (2003) Closure of gap junction channels by arylaminobenzoates. *Mol Pharmacol* 63:1389-97.

Stong BC, Chang Q, Ahmad S*, et al.* (2006) A novel mechanism for connexin 26 mutation linked deafness: cell death caused by leaky gap junction hemichannels. *Laryngoscope* 116:2205-10.

Stout C, Goodenough DA, Paul DL (2004) Connexins: functions without junctions. *Current opinion in cell biology* 16:507-12.

Stout CE, Costantin JL, Naus CC*, et al.* (2002) Intercellular calcium signaling in astrocytes via ATP release through connexin hemichannels. *The Journal of biological chemistry* 277:10482-8.

Suadicani SO, Brosnan CF, Scemes E (2006) P2X7 receptors mediate ATP release and amplification of astrocytic intercellular Ca2+ signaling. *J Neurosci* 26:1378-85.

Sun J, Ahmad S, Chen S*, et al.* (2005) Cochlear gap junctions coassembled from Cx26 and 30 show faster intercellular Ca2+ signaling than homomeric counterparts. *Am J Physiol Cell Physiol* 288:C613-23.

Tang Q, Dowd TL, Verselis VK*, et al.* (2009) Conformational changes in a pore-forming region underlie voltage-dependent "loop gating" of an unapposed connexin hemichannel. *J Gen Physiol* 133:555-70.

Tao L, Harris AL (2007) 2-aminoethoxydiphenyl borate directly inhibits channels composed of connexin26 and/or connexin32. *Molecular pharmacology* 71:570-9.

Tenjarla S (1999) Microemulsions: an overview and pharmaceutical applications. *Critical reviews in therapeutic drug carrier systems* 16:461-521.

Titeux M, Mendonca V, Decha A*, et al.* (2009) Keratitis-ichthyosis-deafness syndrome caused by GJB2 maternal mosaicism. *J Invest Dermatol* 129:776-9.

Tomita Y, Akiyama M, Shimizu H (2005) Stratum corneum hydration and flexibility are useful parameters to indicate clinical severity of congenital ichthyosis. *Exp Dermatol* 14:619-24.

Tovar KR, Maher BJ, Westbrook GL (2009) Direct actions of carbenoxolone on synaptic transmission and neuronal membrane properties. *Journal of neurophysiology* 102:974-8.

Traebert M, Dumotier B, Meister L*, et al.* (2004) Inhibition of hERG K+ currents by antimalarial drugs in stably transfected HEK293 cells. *Eur J Pharmacol* 484:41-8.

Turlier V, Viode C, Durbise E*, et al.* (2014) Clinical and Biochemical Assessment of Maintenance Treatment in Chronic Recurrent Seborrheic Dermatitis: Randomized Controlled Study. *Dermatology and therapy*.

Turner DL, Weintraub H (1994) Expression of achaete-scute homolog 3 in Xenopus embryos converts ectodermal cells to a neural fate. *Genes Dev* 8:1434-47.

Valiunas V (2002) Biophysical properties of connexin-45 gap junction hemichannels studied in vertebrate cells. *The Journal of general physiology* 119:147-64.

Veenstra RD (1996) Size and selectivity of gap junction channels formed from different connexins. *J Bioenerg Biomembr* 28:327-37.

Veraldi S, De Micheli P, Schianchi R*, et al.* (2009) Treatment of pruritus in mild-to-moderate atopic dermatitis with a topical non-steroidal agent. *Journal of drugs in dermatology : JDD* 8:537-9.

Verselis VK, Ginter CS, Bargiello TA (1994) Opposite voltage gating polarities of two closely related connexins. *Nature* 368:348-51.

Verselis VK, Srinivas M (2008) Divalent cations regulate connexin hemichannels by modulating intrinsic voltage-dependent gating. *J Gen Physiol* 132:315-27.

Verselis VK, Srinivas M (2013) Connexin channel modulators and their mechanisms of action. *Neuropharmacology* 75:517-24.

Verselis VK, Trelles MP, Rubinos C*, et al.* (2009) Loop gating of connexin hemichannels involves movement of pore-lining residues in the first extracellular loop domain. *J Biol Chem* 284:4484-93.

Vessey JP, Lalonde MR, Mizan HA*, et al.* (2004) Carbenoxolone inhibition of voltage-gated Ca channels and synaptic transmission in the retina. *Journal of neurophysiology* 92:1252-6.

Wagner H, Kostka KH, Lehr CM*, et al.* (2002) Human skin penetration of flufenamic acid: in vivo/in vitro correlation (deeper skin layers) for skin samples from the same subject. *J Invest Dermatol* 118:540-4.

Wang HL, Chang WT, Li AH*, et al.* (2003) Functional analysis of connexin-26 mutants associated with hereditary recessive deafness. *Journal of neurochemistry* 84:735-42.

Wang N, De Bock M, Antoons G*, et al.* (2012) Connexin mimetic peptides inhibit Cx43 hemichannel opening triggered by voltage and intracellular Ca2+ elevation. *Basic research in cardiology* 107:304.

Wang N, De Vuyst E, Ponsaerts R*, et al.* (2013) Selective inhibition of Cx43 hemichannels by Gap19 and its impact on myocardial ischemia/reperfusion injury. *Basic research in cardiology* 108:309.

Weber PA, Chang HC, Spaeth KE*, et al.* (2004) The permeability of gap junction channels to probes of different size is dependent on connexin composition and permeant-pore affinities. *Biophys J* 87:958-73.

Wei CJ, Xu X, Lo CW (2004) Connexins and cell signaling in development and disease. *Annu Rev Cell Dev Biol* 20:811-38.

Weingart R, Bukauskas FF (1998) Long-chain n-alkanols and arachidonic acid interfere with the Vm-sensitive gating mechanism of gap junction channels. *Pflugers Arch* 435:310-9.

Wermuth CG (2004) Selective optimization of side activities: another way for drug discovery. *J Med Chem* 47:1303-14.

White TW (2000) Functional analysis of human Cx26 mutations associated with deafness. *Brain Res Brain Res Rev* 32:181-3.

White TW, Bruzzone R, Goodenough DA*, et al.* (1992) Mouse Cx50, a functional member of the connexin family of gap junction proteins, is the lens fiber protein MP70. *Mol Biol Cell* 3:711-20.

White TW, Deans MR, O'Brien J*, et al.* (1999) Functional characteristics of skate connexin35, a member of the gamma subfamily of connexins expressed in the vertebrate retina. *Eur J Neurosci* 11:1883-90.

White TW, Paul DL (1999) Genetic diseases and gene knockouts reveal diverse connexin functions. *Annu Rev Physiol* 61:283-310.

Wonkam A, Noubiap JJ, Bosch J*, et al.* (2013) Heterozygous p.Asp50Asn mutation in the GJB2 gene in two Cameroonian patients with keratitis-ichthyosis-deafness (KID) syndrome. *BMC medical genetics* 14:81.

Xu J, Nicholson BJ (2013) The role of connexins in ear and skin physiology - functional insights from disease-associated mutations. *Biochim Biophys Acta* 1828:167-78.

Ye ZC, Wyeth MS, Baltan-Tekkok S*, et al.* (2003) Functional hemichannels in astrocytes: a novel mechanism of glutamate release. *J Neurosci* 23:3588-96.

Yotsumoto S, Hashiguchi T, Chen X*, et al.* (2003) Novel mutations in GJB2 encoding connexin-26 in Japanese patients with keratitis-ichthyosis-deafness syndrome. *Br J Dermatol* 148:649-53.

Zhang Y, Tang W, Ahmad S*, et al.* (2005) Gap junction-mediated intercellular biochemical coupling in cochlear supporting cells is required for normal cochlear functions. *Proc Natl Acad Sci U S A* 102:15201-6.

Zhao HB, Kikuchi T, Ngezahayo A*, et al.* (2006) Gap junctions and cochlear homeostasis. *J Membr Biol* 209:177-86.

Appendix A. MATLAB code for hemichannel data analysis

```
%% Noah Levit 11/04/10

close all; clear all; clc

%H2O control
filename1 = input('Negative control filename: ', 's');
number1 = input('Number of control recordings: ');

H2O(:,1) = [-30 -20 -10 0 10 20 30 40 50 60];
ControlData(:, 1) = [-30 -20 -10 0 10 20 30 40 50 60];

for i=0:(number1-1)
    num = num2str(i,'%04i');
    filename = sprintf('%s_%s%s',filename1, num,'.abf');
    ABF = abfload2(filename);
    X = size(ABF(:,:,:));
    Y = X(1,3);
    for j=1:Y
        contDATA(:, j) = ABF(:,2,j);
        H2O(j, i+2) = [contDATA(275, j)-contDATA(25, j)];
    end
    figure;
    plot(contDATA);
    title('H2O hemichannel current')
    xlabel('Time (msec)')
    ylabel('nA')
    csvwrite(filename, contDATA, 1, 1);
end
figure; plot(H2O(:,1), H2O(:, 2:i+2));
title('H2O controls')
xlabel('Voltage (mV)')
ylabel('nA')
csvwrite('H2O', H2O, 1, 1);

for k=1:Y
    ControlData(k, 2) = mean(H2O(k,2:i+2));
    ControlData(k, 3) = std(H2O(k,2:i+2));
end
csvwrite('ControlData', ControlData, 1, 1);

clear all;

%Cx26 mutants
filename2 = input('Experimental filename: ', 's');
number2 = input('Number of experimental recordings: ');

mutant(:,1) = [-30 -20 -10 0 10 20 30 40 50 60];
ExpData(:, 1) = [-30 -20 -10 0 10 20 30 40 50 60];

for i=0:(number2-1)
    num = num2str(i,'%04i');
```

```
    filename = sprintf('%s_%s%s',filename2, num,'.abf');
    ABF = abfload2(filename);
    X = size(ABF(:,:,:));
    Y = X(1,3);
    for j=1:Y
        expDATA(:, j) = ABF(:,2,j);
        mutant(j, i+2) = [expDATA(275, j)-expDATA(25, j)];
    end
    csvwrite(filename, expDATA, 1, 1);
    figure;
    plot(expDATA);
    title('Cx26 mutant hemichannel current')
    xlabel('Time (msec)')
    ylabel('nA')
end

figure; plot(mutant(:,1), mutant(:, 2:i+2));
title('Cx26 hemichannel currents')
xlabel('Voltage (mV)')
ylabel('An')
csvwrite('Cx26 mutant', mutant, 1, 1);

for k=1:Y
    ExpData(k, 2) = mean(mutant(k,2:i+2));
    ExpData(k, 3) = std(mutant(k,2:i+2));
end
csvwrite('ExpData', ExpData, 1, 1);

load ControlData;
figure; errorbar(ControlData(:,1), ControlData(:,2), ControlData(:,3)); hold
on;
title('Cx26 hemichannel currents')
xlabel('Voltage (mV)')
ylabel('nA')
errorbar(ExpData(:,1), ExpData(:,2), ExpData(:,3));
hold off;

clear all;

%Perfusion
filename3 = input('Perfusion filename: ', 's');
number3 = input('Number of drug trials: ');

Perf(:,1) = [-30 -20 -10 0 10 20 30 40 50 60];

for i=0:(number3-1)
    num = num2str(i,'%04i');
    filename = sprintf('%s_%s%s',filename3, num,'.abf');
    ABF = abfload2(filename);
    X = size(ABF(:,:,:));
    Y = X(1,3);
    for j=1:Y
        PerfDATA(:, j) = ABF(:,2,j);
        Perf(j, i+1) = [PerfDATA(250, j)-PerfDATA(25, j)];
    end
    csvwrite(filename, PerfDATA, 1, 1);
    figure;
```

```
    plot(PerfDATA);
    title('Hemichannel current elicited by 100mV sweeps')
    xlabel('Time (msec)')
    ylabel('An')
end

figure; plot(Perf);
title('Perfusion')
xlabel('Sweep #')
ylabel('An')
csvwrite('Perf', Perf, 1, 1);

clear all;
```

Appendix B. Modulation of Cx26-G45E hemichannel currents by co-expression with constitutively active PI3K

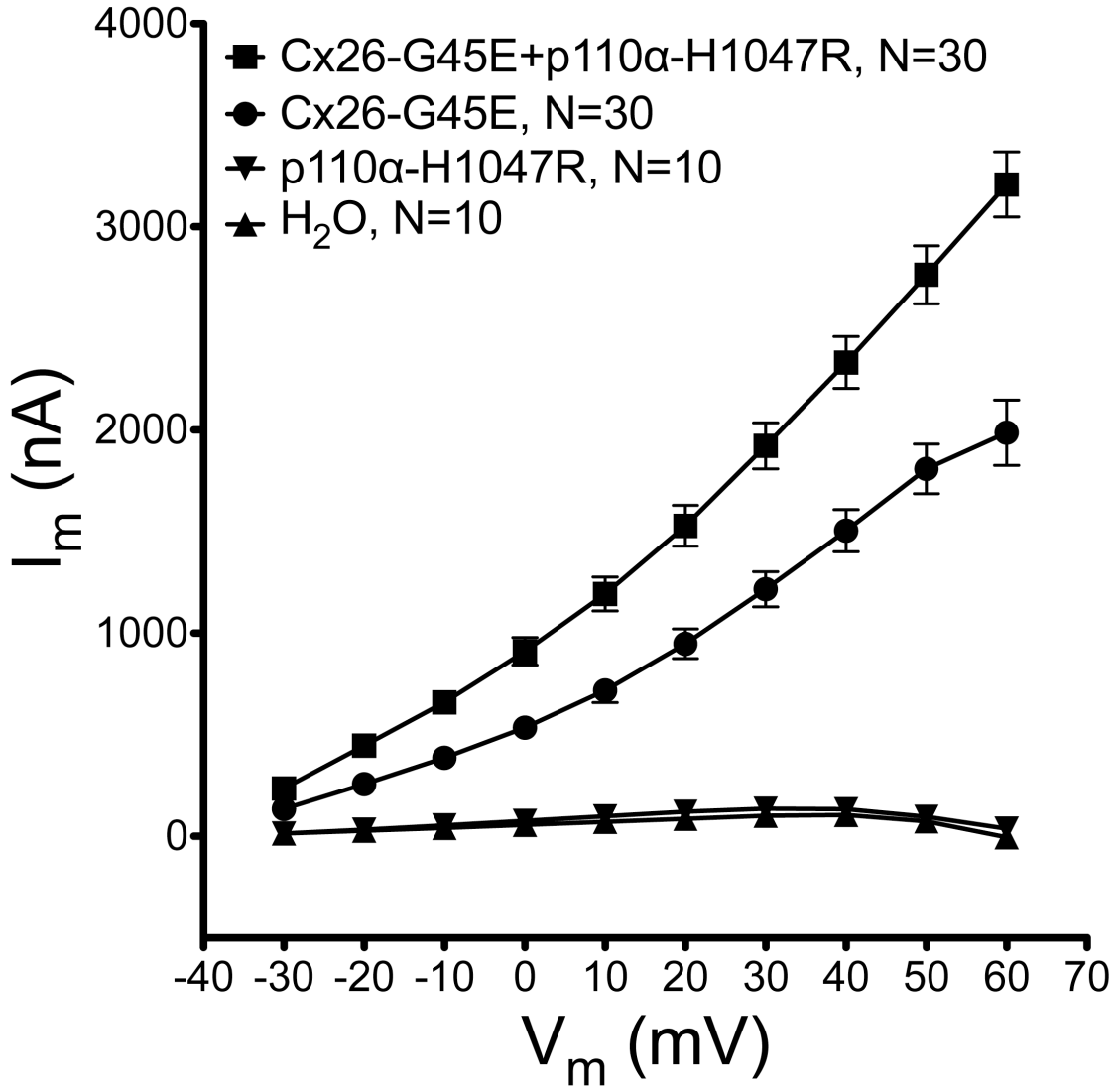

Co-expression of Cx26-G45E and a constitutively active p110α phosphatidylinositol-4,5-bisphosphate 3-kinase (PI3K) mutant (H1047R) in *Xenopus* ooyctes potentiated whole-cell membrane currents. Single cells were clamped at a -40mV holding potential and subjected to voltage pulses spanning -30 to +60mV in 10mV steps. Mean instantaneous currents (I_m) plotted against membrane potential (V_m) illustrated current-voltage relationships. H_2O- (N=10) and p110α-H1047R- (N=10) injected cells displayed negligible membrane currents for the tested range of stimuli. Oocytes expressing Cx26-G45E (N=30) showed large outward membrane fluxes that were most impressive at depolarizing membrane potentials and were significantly elevated by the presence of p110α-H1047R (N=30). Data are the means ± SEM. *** p110α-H1047R plasmid DNA courtesy of the Lin Lab, Stony Brook University, Stony Brook, NY